



March 30, 2005

U. S. Nuclear Regulatory Commission  
Attention: Document Control Desk  
Washington, D.C. 20555

Serial No. 05-194  
ESP/JDH  
Docket No. 52-008

**DOMINION NUCLEAR NORTH ANNA, LLC**  
**NORTH ANNA EARLY SITE PERMIT APPLICATION**  
**RESPONSES TO DRAFT SAFETY EVALUATION REPORT OPEN ITEMS**

On December 20, 2004, the NRC issued its Draft Safety Evaluation Report (DSER) for Dominion Nuclear North Anna, LLC's North Anna Early Site Permit application. The DSER contained several open items for which the NRC requested a response.

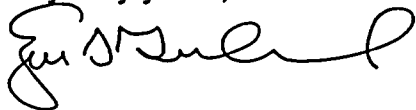
This letter contains responses to the following open items:

- Open Item 2.5-1. A response to DSER Open Item 2.5-1 was provided in Dominion's January 25, 2005 letter, Serial No. 04-785. During telephone conversations on March 9 and 15, 2005, the NRC Staff requested additional information related to this open item. A supplemental response to Open Item 2.5-1 is enclosed.
- Open Item 2.5-2. A planned approach for responding to Open Item 2.5-2 was submitted in Dominion's February 18, 2005 letter, Serial No. 04-785A. A partial response to this open item was provided in Dominion's March 3, 2005 letter, Serial No. 05-785B. The remaining response to Open Item 2.5-2 is enclosed.

It is our intent to update the North Anna ESP application to reflect our responses to the DSER open items. Planned changes to the application are identified following the response to each open item.

If you have any questions or require additional information, please contact Mr. Joseph Hegner at 804-273-2770.

Very truly yours,



Eugene S. Grecheck  
Vice President-Nuclear Support Services

D074

Enclosures:

1. Responses to Draft Safety Evaluation Report Open Items 2.5-1 and 2.5-2
2. "EPRI Response Pertaining to the Dominion Nuclear North Anna, LLC (Dominion) North Anna Early Site Permit Application DSER Open Item 2.5-1," Letter from Edmund T. Rumble, Electric Power Research Institute, March 25, 2005

Commitments made in this letter:

1. Update the North Anna ESP application to reflect responses to DSER Open Items.

cc: (with enclosures)

U. S. Nuclear Regulatory Commission, Region II  
Sam Nunn Atlanta Federal Center  
61 Forsyth Street, SW  
Suite 23T85  
Atlanta, Georgia 30303

Mr. Jack Cushing  
U. S. Nuclear Regulatory Commission  
Washington, D.C. 20555

Mr. M. S. King  
NRC Senior Resident Inspector  
North Anna Power Station

Ms. Belkys Sosa  
U. S. Nuclear Regulatory Commission  
Washington, D.C. 20555

COMMONWEALTH OF VIRGINIA

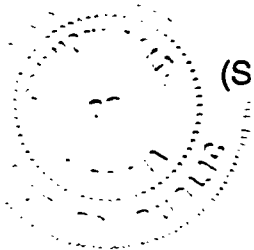
COUNTY OF HENRICO

The foregoing document was acknowledged before me, in and for the County and Commonwealth aforesaid, today by Eugene S. Grecheck, who is Vice President, Nuclear Support Services, of Dominion Nuclear North Anna, LLC. He has affirmed before me that he is duly authorized to execute and file the foregoing document on behalf of Dominion Nuclear North Anna, LLC, and that the statements in the document are true to the best of his knowledge and belief.

Acknowledged before me this 30<sup>TH</sup> day of March, 2005.

My Commission expires: May 31, 2006

Vicki L. Huel  
Notary Public



(SEAL)

**Enclosure 1**

**Responses to Draft Safety Evaluation Report  
Open Items 2.5-1 and 2.5-2**

**DSER Open Item 2.5-1 (DSER pages 2-165 and 2-166)**

On DSER pages 2-165 and 2-166, the NRC staff posed three distinct questions related to Dominion's ground motion evaluation. The three questions were collectively identified as Open Item 2.5-1.

**Part 1 of DSER Open Item 2.5-1**

In RAI 2.5.2-2, the staff asked the applicant to provide additional details on the 2003 EPRI ground motion evaluation that it used for the ESP PSHA. To update PSHAs in the CEUS, EPRI sponsored a Senior Seismic Hazard Advisory Committee Level 3 analysis. NUREG/CR-6372 provides the guidelines for performing this analysis. The EPRI ground motion study used 13 different ground motion attenuation relationships grouped into four clusters. In RAI 2.5.2-2(c), the staff asked the applicant to provide the weight assigned to each of the 13 ground-motion relationships within their respective cluster. For cluster 1, EPRI gave the highest weight (0.90) to the three attenuation relationships reported by Silva et al. The staff inferred from this higher weight that these relationships must have fit the data much better than other relationships. However, the applicant did not provide plots or tables of the residuals as a function of attenuation relation, magnitude, distance, and frequency. Therefore, the staff was unable to evaluate the weighting EPRI selected for cluster 1. Similarly, for clusters 2 and 3, the ground motion experts applied higher weights to different attenuation relationships within each cluster. Neither the EPRI 2003 ground motion report or the applicant's response to RAI 2.5.2-2 provided the rationale for these weights.

During telephone conversations on March 9 and 15, 2005, the NRC requested additional information related to this part of the open item to supplement Dominion's January 25, 2005 response [Dominion (2005)]. On March 17, 2005, the NRC sent a facsimile to Dominion [NRC (2005)] clarifying the additional information needed:

Provide residual plots (similar to Figure A-13 in the EPRI 2004 report) for each cluster 1 attenuation relationship for a range of frequencies (1 Hz to PGA) along with statistics for misfits (similar to Table A-4 in the EPRI 2004 report) for each frequency value. Show the calculation of the variance ( $\beta^2$ ) and final weight for each of the models.

**Supplemental Response to Part 1 of DSER Open Item 2.5-1**

1. Determination of Intracluster Weights

A description of the determination of intracluster weights for the EPRI (2004) ground motion model is provided in this section of the response. Please refer to Sections A.3 and A.4 of EPRI (2004).

As part of the EPRI CEUS Ground Motion Project, direct statistical comparisons were made with each of the median ground motion models and the strong-motion database. For each model, the deviation between the median prediction and the recorded motion was determined. The deviations were determined by:

$$\Delta_{ijk}(f) = a_{jk}(f) - z(m, r, f)_{ijk} \quad \text{(Equation A-1)}$$

where,

$\Delta_{ijk}(f) =$  deviation for frequency  $f$  between the recorded motion for earthquake  $j$  and station  $k$  and ground motion model  $i$  [*Note: This is the deviation of the natural log values which is not identified in EPRI (2004)*]

$a_{jk}(f) =$  recorded ground motion for frequency  $f$  obtained during earthquake  $j$  at station  $k$  (*Note: EPRI (2004) contains a typographical error showing  $a_{j\bar{i}}$ . Note also that this is the natural log of the recorded ground motion*)

$z(m, r, f)_{ijk} =$  median ground motion estimate for frequency  $f$  and model  $i$  and for event  $j$  with magnitude,  $m$ , and distance to the strong-motion recording station  $k$ ,  $r$ . (*Note that this is the natural log of the median ground motion from the model*)

For each model and frequency, the mean and variance of the model deviations were determined. In the CEUS database, there is considerable variation in the number of recordings that were obtained for each event. For example, there were a large number of recordings obtained from the 1988 Saguenay earthquake as compared to other events for which there may have only been 1 or 2 recorded motions. In order that estimates of the mean and variance not be skewed by events with a large number of recordings, a weighted approach was used. The data were weighted such that each event was given equal weight in the parameter estimation. The mean of the model deviations is:

$$\delta_i(f) = \frac{1}{n_e} \sum_j \frac{1}{n_{e,j}} \sum_k \Delta_{ijk}(f) \quad \text{(Equation A-2)}$$

where  $n_e$  is the number of events and  $n_{e,j}$  is the number of recordings for event j.

(Note: for Equation A-3, below, it is helpful to note that

$$\delta_{i,j}(f) = \frac{1}{n_{e,j}} \sum_k \Delta_{ijk}(f) )$$

The total variance

$$s_i^2(f) = \frac{1}{n_e} \sum_j \frac{1}{(n_{e,j}-1)} \sum_k (\Delta_{ijk}(f) - \delta_{i,j}(f))^2 + \frac{1}{n_e-1} \sum_j (\delta_{i,j}(f) - \delta_i(f))^2 \quad \text{(Equation A-3)}$$

where  $\delta_{i,j}(f)$  is the mean deviation for model i and event j and frequency f. [Note: EPRI (2004) contains 2 typographical errors in Equation A-3: 1) EPRI (2004) has this equation equal to  $s_k^2(f)$ , but this is the total variance for a given model i; 2) for the second term in the summation over k, EPRI (2004) incorrectly has this typed as  $\delta_k(f)$ . (Note: first term is 0 for events with only one recording,  $n_{e,j} = 1$ .) The total variance is a function of the intra-event and inter-event variability. The standard error of the estimated mean deviation (bias) for a model is,

$$s_{\delta,i}(f) = \left\{ \frac{1}{n} s_i^2(f) \right\}^{\frac{1}{2}} \quad \text{(Equation A-4)}$$

where n is the total number of recordings.

In the following example tables, the “Mean ( $\delta$ )” is “mean of the model deviations” [“bias”] from Equation A-2,  $\delta_i(f)$ , and “Standard error on the mean ( $\sigma_\delta$ )” is the “standard error of the estimated mean deviation (bias) for the model” from Equation A-4,  $s_{\delta,i}(f)$ .

Given a group of models (e.g., the models within a cluster, the set of cluster median models), relative weight for each model can be determined as a function of its consistency with recorded strong-motion data. A model’s consistency is a function of its mean deviation (bias) and the variability in mean. Relative weights are determined in inverse proportion to this variance with the data. For model i and frequency f, this variance is:

$$\beta_i^2(f) = \delta_i^2(f) + s_{\delta,i}^2(f) \quad \text{(Equation A-5)}$$

In order to determine a single weight for a median ground motion model, the model variance for frequencies of 1 Hz, 2.5 Hz, 5 Hz, and 10Hz were combined. (Note, since model results were not available for 2.5Hz, the results for 1Hz were included twice.) These frequencies are consistent with those used in Regulatory Guide 1.165 [NRC (1997)] to determine the controlling earthquakes and correspond to the frequency range of interest for commercial nuclear power plants. Combining the variances for these frequencies produced a single, frequency independent model variance,  $\beta_i^2$ .

For a group of models, relative weights were determined in inverse proportion to the model variance with the data as given by the following expression:

$$w_i = \frac{1}{\beta_i^2} \bigg/ \sum_i^m \frac{1}{\beta_i^2} \quad \text{(Equation A-6)}$$

The summation in the denominator normalizes the weights and is carried out over the number of models, m.

Tables 1 through 6 are the statistics tables for frequencies 1 Hz, 5 Hz, and 10 Hz for all six ground motion models of Cluster 1:

- Hwang & Huo (1997)
- Silva et al. (2002) - Single Corner Model with Constant Stress Drop
- Silva et al. (2002) - Single Corner Model with Constant Stress Drop and Saturation
- Silva et al. (2002) - Single Corner Model with Variable Stress Drop
- Toro et al. (1997) - Midcontinent Region
- Youngs fit to Frankel et al. (1996)

The Excel files that were used to calculate the statistics in Tables 1 through 6 were part of the data provided to the ground motion expert panel on January 27, 2003. In Tables 1 through 6, the values corresponding to Equations A-2 and A-4 are highlighted in bold.

Figures 1 through 6 provide plots of residuals [Mean ( $\delta$ ), Equation A-2] and the 90% confidence range. Corresponding to the tables, the residuals are plotted in five groups of differing distance bins. The 0 – 1000 km residuals are plotted at the left side of the plots, for plotting purposes around 12 km. Note that the residuals plots for 20 Hz, 25 Hz, and PGA are shown for illustration only, as they were not used in the intracluster weighting methodology, which focused on the frequencies of particular interest in Regulatory Guide 1.165 – that is, frequencies of 1 to 10 Hz.

**Table 1. Hwang & Huo (1997)**

<b>Frequency (Hz): 1</b>					
Distance Bins (km)	0	75	150	500	0
	75	150	500	1000	1000
Geometric Mean Distance (km)	26.3	115.3	287.1	733.3	154.3
Number of Data Points	17	26	56	52	151
Number of Earthquakes	11	8	11	10	20
<b>Mean (<math>\delta</math>) [Equation A-2]</b>	-1.49	-1.74	-1.05	0.34	-0.75
Factor = $\exp(\delta)$	0.23	0.18	0.35	1.41	0.47
Standard Deviation ( $\sigma_\Delta$ )	0.87	1.25	0.95	1.44	1.43
<b>Standard Error on the Mean (<math>\sigma_\delta</math>) [Equation A-4]</b>	0.21	0.24	0.13	0.20	0.12
90% Confidence Range	0.35	0.40	0.21	0.33	0.19
Mean + Std.Dev. ( $\delta + \sigma_\Delta$ )	-0.62	-0.49	-0.10	1.78	0.67
Mean - Std.Dev. ( $\delta - \sigma_\Delta$ )	-2.35	-2.99	-2.00	-1.10	-2.18
Mean Magnitude	4.9	4.8	5.0	5.3	5.0
<b>Frequency (Hz): 5</b>					
Distance Bins (km)	0	75	150	500	0
	75	150	500	1000	1000
Geometric Mean Distance (km)	26.3	115.3	265.5	718.2	118.2
Number of Data Points	17	26	54	44	141
Number of Earthquakes	11	8	9	7	17
<b>Mean (<math>\delta</math>) [Equation A-2]</b>	-0.45	-0.64	-0.33	0.04	-0.42
Factor = $\exp(\delta)$	0.64	0.53	0.72	1.05	0.66
Standard Deviation ( $\sigma_\Delta$ )	0.82	1.00	0.99	0.92	0.96
<b>Standard Error on the Mean (<math>\sigma_\delta</math>) [Equation A-4]</b>	0.20	0.20	0.14	0.14	0.08
90% Confidence Range	0.32	0.32	0.22	0.23	0.13
Mean + Std.Dev. ( $\delta + \sigma_\Delta$ )	0.36	0.36	0.67	0.97	0.54
Mean - Std.Dev. ( $\delta - \sigma_\Delta$ )	-1.27	-1.64	-1.32	-0.88	-1.38
Mean Magnitude	4.9	4.8	4.8	4.9	4.8

<b>Table 1. Hwang &amp; Huo (1997)</b>					
<b>Frequency (Hz): 10</b>					
Distance Bins (km)	0 75	75 150	150 500	500 1000	0 1000
Geometric Mean Distance (km)	26.3	115.3	265.5	716.4	117.8
Number of Data Points	17	25	54	43	139
Number of Earthquakes	11	8	9	7	17
<b>Mean (<math>\delta</math>) [Equation A-2]</b>	-0.11	-0.13	-0.26	-0.21	<b>-0.16</b>
Factor = $\exp(\delta)$	0.89	0.88	0.77	0.81	0.85
Standard Deviation ( $\sigma_\Delta$ )	0.54	0.91	0.91	0.96	0.74
<b>Standard Error on the Mean (<math>\sigma_\delta</math>) [Equation A-4]</b>	0.13	0.18	0.12	0.15	<b>0.06</b>
90% Confidence Range	0.22	0.30	0.20	0.24	0.10
Mean + Std.Dev. ( $\delta + \sigma_\Delta$ )	0.43	0.79	0.65	0.75	0.58
Mean - Std.Dev. ( $\delta - \sigma_\Delta$ )	-0.66	-1.04	-1.16	-1.17	-0.90
Mean Magnitude	4.9	4.8	4.8	4.9	4.8

**Table 2. Silva et al. (2002) – Single Corner Model with Constant Stress Drop**

<b>Frequency (Hz): 1</b>					
Distance Bins (km)	0	75	150	500	0
	75	150	500	1000	1000
Geometric Mean Distance (km)	26.3	115.3	287.1	733.3	154.3
Number of Data Points	17	26	56	52	151
Number of Earthquakes	11	8	11	10	20
<b>Mean (<math>\delta</math>) [Equation A-2]</b>	-0.29	-0.24	0.13	0.63	<b>0.21</b>
Factor = $\exp(\delta)$	0.75	0.79	1.14	1.88	1.23
Standard Deviation ( $\sigma_{\Delta}$ )	0.86	1.15	0.87	1.21	1.09
<b>Standard Error on the Mean (<math>\sigma_{\delta}</math>) [Equation A-4]</b>	0.21	0.23	0.12	0.17	<b>0.09</b>
90% Confidence Range	0.34	0.37	0.19	0.28	0.14
Mean + Std.Dev. ( $\delta + \sigma_{\Delta}$ )	0.58	8.91	1.00	1.84	1.29
Mean - Std.Dev. ( $\delta - \sigma_{\Delta}$ )	-1.15	-1.39	-0.74	-0.58	-0.88
Mean Magnitude	4.9	4.8	5.0	5.3	5.0
<b>Frequency (Hz): 5</b>					
Distance Bins (km)	0	75	150	500	0
	75	150	500	1000	1000
Geometric Mean Distance (km)	26.3	115.3	265.5	718.2	118.2
Number of Data Points	17	26	54	44	141
Number of Earthquakes	11	8	9	7	17
<b>Mean (<math>\delta</math>) [Equation A-2]</b>	0.05	0.22	0.55	0.35	<b>0.19</b>
Factor = $\exp(\delta)$	1.05	1.25	1.73	1.42	1.21
Standard Deviation ( $\sigma_{\Delta}$ )	0.69	0.89	0.87	0.71	0.85
<b>Standard Error on the Mean (<math>\sigma_{\delta}</math>) [Equation A-4]</b>	0.17	0.17	0.12	0.11	<b>0.07</b>
90% Confidence Range	0.27	0.29	0.19	0.18	0.12
Mean + Std.Dev. ( $\delta + \sigma_{\Delta}$ )	0.74	1.11	1.42	1.06	1.04
Mean - Std.Dev. ( $\delta - \sigma_{\Delta}$ )	-0.64	-0.67	-0.32	-0.37	-0.66
Mean Magnitude	4.9	4.8	4.8	4.9	4.8

<b>Table 2. Silva et al. (2002) – Single Corner Model with Constant Stress Drop</b>					
<b>Frequency (Hz): 10</b>					
Distance Bins (km)	0	75	150	500	0
	75	150	500	1000	1000
Geometric Mean Distance (km)	26.3	115.3	265.5	716.4	117.8
Number of Data Points	17	25	54	43	139
Number of Earthquakes	11	8	9	7	17
<b>Mean (<math>\delta</math>) [Equation A-2]</b>	0.36	0.71	0.53	-0.23	<b>0.34</b>
Factor = $\exp(\delta)$	1.44	2.03	1.70	0.79	1.40
Standard Deviation ( $\sigma_{\Delta}$ )	0.48	0.88	0.89	0.71	0.83
<b>Standard Error on the Mean (<math>\sigma_{\delta}</math>) [Equation A-4]</b>	0.12	0.18	0.12	0.11	<b>0.07</b>
90% Confidence Range	0.19	0.29	0.20	0.18	0.12
Mean + Std.Dev. ( $\delta + \sigma_{\Delta}$ )	0.85	1.59	1.42	0.47	1.17
Mean - Std.Dev. ( $\delta - \sigma_{\Delta}$ )	-0.12	-0.18	-0.36	-0.94	-0.49
Mean Magnitude	4.9	4.8	4.8	4.9	4.8

<b>Table 3. Silva et al. (2002) – Single Corner Model with Constant Stress Drop and Saturation</b>					
<b>Frequency (Hz): 1</b>					
Distance Bins (km)	0	75	150	500	0
	75	150	500	1000	1000
Geometric Mean Distance (km)	26.3	115.3	287.1	733.3	154.3
Number of Data Points	17	26	56	52	151
Number of Earthquakes	11	8	11	10	20
<b>Mean (<math>\delta</math>) [Equation A-2]</b>	-0.31	-0.26	0.16	0.71	<b>0.24</b>
Factor = $\exp(\delta)$	0.73	0.77	1.17	2.03	1.27
Standard Deviation ( $\sigma_\Delta$ )	0.87	1.15	0.88	1.23	1.11
<b>Standard Error on the Mean (<math>\sigma_\delta</math>) [Equation A-4]</b>	0.21	0.22	0.12	0.17	<b>0.09</b>
90% Confidence Range	0.35	0.37	0.19	0.28	0.15
Mean + Std.Dev. ( $\delta + \sigma_\Delta$ )	0.56	0.89	1.03	1.94	1.35
Mean - Std.Dev. ( $\delta - \sigma_\Delta$ )	-1.18	-1.40	-0.72	-0.52	-0.87
Mean Magnitude	4.9	4.8	5.0	5.3	5.0
<b>Frequency (Hz): 5</b>					
Distance Bins (km)	0	75	150	500	0
	75	150	500	1000	1000
Geometric Mean Distance (km)	26.3	115.3	265.5	718.2	118.2
Number of Data Points	17	26	54	44	141
Number of Earthquakes	11	8	9	7	17
<b>Mean (<math>\delta</math>) [Equation A-2]</b>	0.02	0.20	0.59	0.48	<b>0.23</b>
Factor = $\exp(\delta)$	1.02	1.22	1.81	1.62	1.26
Standard Deviation ( $\sigma_\Delta$ )	0.70	0.89	0.87	0.70	0.87
<b>Standard Error on the Mean (<math>\sigma_\delta</math>) [Equation A-4]</b>	0.17	0.17	0.12	0.11	<b>0.07</b>
90% Confidence Range	0.28	0.29	0.19	0.17	0.12
Mean + Std.Dev. ( $\delta + \sigma_\Delta$ )	0.72	1.09	1.46	1.18	1.10
Mean - Std.Dev. ( $\delta - \sigma_\Delta$ )	-0.68	-0.68	-0.27	-0.22	-0.63
Mean Magnitude	4.9	4.8	4.8	4.9	4.8

<b>Table 3. Silva et al. (2002) – Single Corner Model with Constant Stress Drop and Saturation</b>					
<b>Frequency (Hz): 10</b>					
Distance Bins (km)	0	75	150	500	0
	75	150	500	1000	1000
Geometric Mean Distance (km)	26.3	115.3	265.5	716.4	117.8
Number of Data Points	17	25	54	43	139
Number of Earthquakes	11	8	9	7	17
<b>Mean (<math>\delta</math>) [Equation A-2]</b>	0.34	0.69	0.58	-0.09	<b>0.38</b>
Factor = $\exp(\delta)$	1.40	1.99	1.78	0.91	1.47
Standard Deviation ( $\sigma_\Delta$ )	0.47	0.88	0.87	0.67	0.79
<b>Standard Error on the Mean (<math>\sigma_\delta</math>) [Equation A-4]</b>	0.12	0.18	0.12	0.10	<b>0.07</b>
90% Confidence Range	0.19	0.29	0.19	0.17	0.11
Mean + Std.Dev. ( $\delta + \sigma_\Delta$ )	0.81	1.57	1.45	0.58	1.17
Mean - Std.Dev. ( $\delta - \sigma_\Delta$ )	-0.13	-0.20	-0.29	-0.76	-0.40
Mean Magnitude	4.9	4.8	4.8	4.9	4.8

**Table 4. Silva et al. (2002) – Single Corner Model with Variable Stress Drop**

<b>Frequency (Hz): 1</b>					
Distance Bins (km)	0	75	150	500	0
	75	150	500	1000	1000
Geometric Mean Distance (km)	26.3	115.3	287.1	733.3	154.3
Number of Data Points	17	26	56	52	151
Number of Earthquakes	11	8	11	10	20
<b>Mean (<math>\delta</math>) [Equation A-2]</b>	-0.36	-0.32	0.05	0.56	<b>0.14</b>
Factor = $\exp(\delta)$	0.70	0.73	1.05	1.76	1.15
Standard Deviation ( $\sigma_\Delta$ )	0.87	1.16	0.86	1.20	1.08
<b>Standard Error on the Mean (<math>\sigma_\delta</math>) [Equation A-4]</b>	0.21	0.23	0.11	0.17	<b>0.09</b>
90% Confidence Range	0.35	0.37	0.19	0.27	0.14
Mean + Std.Dev. ( $\delta + \sigma_\Delta$ )	0.51	0.84	0.91	1.77	1.22
Mean - Std.Dev. ( $\delta - \sigma_\Delta$ )	-1.23	-1.48	-0.81	-0.64	-0.94
Mean Magnitude	4.9	4.8	5.0	5.3	5.0
<b>Frequency (Hz): 5</b>					
Distance Bins (km)	0	75	150	500	0
	75	150	500	1000	1000
Geometric Mean Distance (km)	26.3	115.3	265.5	718.2	118.2
Number of Data Points	17	26	54	44	141
Number of Earthquakes	11	8	9	7	17
<b>Mean (<math>\delta</math>) [Equation A-2]</b>	-0.11	0.05	0.38	0.19	<b>0.03</b>
Factor = $\exp(\delta)$	0.89	1.05	1.46	1.21	1.03
Standard Deviation ( $\sigma_\Delta$ )	0.70	0.91	0.88	0.72	0.86
<b>Standard Error on the Mean (<math>\sigma_\delta</math>) [Equation A-4]</b>	0.17	0.18	0.12	0.11	<b>0.07</b>
90% Confidence Range	0.28	0.29	0.20	0.18	0.12
Mean + Std.Dev. ( $\delta + \sigma_\Delta$ )	0.58	0.96	1.26	0.91	0.88
Mean - Std.Dev. ( $\delta - \sigma_\Delta$ )	-0.81	-0.86	-0.50	-0.53	-0.83
Mean Magnitude	4.9	4.8	4.8	4.9	4.8

<b>Table 4. Silva et al. (2002) – Single Corner Model with Variable Stress Drop</b>					
<b>Frequency (Hz): 10</b>					
<b>Distance Bins (km)</b>	<b>0</b>	<b>75</b>	<b>150</b>	<b>500</b>	<b>0</b>
	<b>75</b>	<b>150</b>	<b>500</b>	<b>1000</b>	<b>1000</b>
<b>Geometric Mean Distance (km)</b>	26.3	115.3	265.5	716.4	117.8
<b>Number of Data Points</b>	17	25	54	43	139
<b>Number of Earthquakes</b>	11	8	9	7	17
<b>Mean (<math>\delta</math>) [Equation A-2]</b>	0.19	0.52	0.35	-0.40	<b>0.16</b>
<b>Factor = exp(<math>\delta</math>)</b>	1.21	1.68	1.42	0.67	1.17
<b>Standard Deviation (<math>\sigma_{\Delta}</math>)</b>	0.48	0.89	0.89	0.72	0.83
<b>Standard Error on the Mean (<math>\sigma_{\delta}</math>) [Equation A-4]</b>	0.12	0.18	0.12	0.11	<b>0.07</b>
<b>90% Confidence Range</b>	0.19	0.29	0.20	0.18	0.11
<b>Mean + Std.Dev. (<math>\delta + \sigma_{\Delta}</math>)</b>	0.66	1.41	1.24	0.32	0.99
<b>Mean - Std.Dev. (<math>\delta - \sigma_{\Delta}</math>)</b>	-0.29	-0.37	-0.54	-1.13	-0.67
<b>Mean Magnitude</b>	4.9	4.8	4.8	4.9	4.8

<b>Table 5. Toro et al. (1997) - Midcontinent Region</b>					
<b>Frequency (Hz): 1</b>					
Distance Bins (km)	0	75	150	500	0
	75	150	500	1000	1000
Geometric Mean Distance (km)	26.3	115.3	287.1	733.3	154.3
Number of Data Points	17	26	56	52	151
Number of Earthquakes	11	8	11	10	20
<b>Mean (<math>\delta</math>) [Equation A-2]</b>	-0.87	-1.30	-1.28	-0.61	-0.85
Factor = $\exp(\delta)$	0.42	0.27	0.28	0.54	0.43
Standard Deviation ( $\sigma_{\Delta}$ )	0.86	1.22	0.88	1.26	1.10
<b>Standard Error on the Mean (<math>\sigma_{\delta}</math>) [Equation A-4]</b>	0.21	0.24	0.12	0.18	0.09
90% Confidence Range	0.34	0.39	0.19	0.29	0.15
Mean + Std.Dev. ( $\delta + \sigma_{\Delta}$ )	-0.02	-0.08	-0.40	0.65	0.25
Mean - Std.Dev. ( $\delta - \sigma_{\Delta}$ )	-1.73	-2.52	-2.16	-1.87	-1.95
Mean Magnitude	4.9	4.8	5.0	5.3	5.0
<b>Frequency (Hz): 5</b>					
Distance Bins (km)	0	75	150	500	0
	75	150	500	1000	1000
Geometric Mean Distance (km)	26.3	115.3	265.5	718.2	118.2
Number of Data Points	17	26	54	44	141
Number of Earthquakes	11	8	9	7	17
<b>Mean (<math>\delta</math>) [Equation A-2]</b>	-0.47	-0.76	-0.59	0.05	-0.53
Factor = $\exp(\delta)$	0.62	0.47	0.56	1.05	0.59
Standard Deviation ( $\sigma_{\Delta}$ )	0.81	1.04	1.03	1.00	0.98
<b>Standard Error on the Mean (<math>\sigma_{\delta}</math>) [Equation A-4]</b>	0.20	0.20	0.14	0.15	0.08
90% Confidence Range	0.32	0.33	0.23	0.25	0.14
Mean + Std.Dev. ( $\delta + \sigma_{\Delta}$ )	0.33	0.27	0.44	1.05	0.45
Mean - Std.Dev. ( $\delta - \sigma_{\Delta}$ )	-1.28	-1.80	-1.61	-0.95	-1.51
Mean Magnitude	4.9	4.8	4.8	4.9	4.8

<b>Table 5. Toro et al. (1997) - Midcontinent Region</b>					
<b>Frequency (Hz): 10</b>					
Distance Bins (km)	0	75	150	500	0
	75	150	500	1000	1000
Geometric Mean Distance (km)	26.3	115.3	265.5	716.4	117.8
Number of Data Points	17	25	54	43	139
Number of Earthquakes	11	8	9	7	17
<b>Mean (<math>\delta</math>) [Equation A-2]</b>	0.05	0.03	-0.12	0.10	<b>0.00</b>
Factor = $\exp(\delta)$	1.05	1.03	0.88	1.10	1.00
Standard Deviation ( $\sigma_\Delta$ )	0.54	0.93	0.93	1.02	0.74
<b>Standard Error on the Mean (<math>\sigma_\delta</math>) [Equation A-4]</b>	0.13	0.19	0.13	0.16	<b>0.06</b>
90% Confidence Range	0.22	0.30	0.21	0.25	0.10
Mean + Std.Dev. ( $\delta + \sigma_\Delta$ )	0.59	0.96	0.80	1.12	0.75
Mean - Std.Dev. ( $\delta - \sigma_\Delta$ )	-0.50	-0.90	-1.05	-0.92	-0.74
Mean Magnitude	4.9	4.8	4.8	4.9	4.8

**Table 6. Youngs fit to Frankel et al. (1996)**

<b>Frequency (Hz): 1</b>					
Distance Bins (km)	0	75	150	500	0
	75	150	500	1000	1000
Geometric Mean Distance (km)	26.3	115.3	287.1	733.3	154.3
Number of Data Points	17	26	56	52	151
Number of Earthquakes	11	8	11	10	20
<b>Mean (<math>\delta</math>) [Equation A-2]</b>	-0.49	-1.15	-1.28	-0.85	<b>-0.78</b>
Factor = $\exp(\delta)$	0.61	0.32	0.28	0.43	0.46
Standard Deviation ( $\sigma_\Delta$ )	0.97	1.28	0.90	1.21	1.12
<b>Standard Error on the Mean (<math>\sigma_\delta</math>) [Equation A-4]</b>	0.24	0.25	0.12	0.17	<b>0.09</b>
90% Confidence Range	0.39	0.41	0.20	0.27	0.15
Mean + Std.Dev. ( $\delta + \sigma_\Delta$ )	0.48	0.13	-0.38	0.36	0.34
Mean - Std.Dev. ( $\delta - \sigma_\Delta$ )	-1.46	-2.44	-2.18	-2.06	-1.91
Mean Magnitude	4.9	4.8	5.0	5.3	5.0
<b>Frequency (Hz): 5</b>					
Distance Bins (km)	0	75	150	500	0
	75	150	500	1000	1000
Geometric Mean Distance (km)	26.3	115.3	265.5	718.2	118.2
Number of Data Points	17	26	54	44	141
Number of Earthquakes	11	8	9	7	17
<b>Mean (<math>\delta</math>) [Equation A-2]</b>	-0.29	-0.70	-0.52	-0.11	<b>-0.47</b>
Factor = $\exp(\delta)$	0.75	0.49	0.60	0.90	0.63
Standard Deviation ( $\sigma_\Delta$ )	0.87	1.01	0.92	0.81	0.97
<b>Standard Error on the Mean (<math>\sigma_\delta</math>) [Equation A-4]</b>	0.21	0.20	0.12	0.12	<b>0.08</b>
90% Confidence Range	0.34	0.33	0.20	0.20	0.13
Mean + Std.Dev. ( $\delta + \sigma_\Delta$ )	0.57	0.31	0.40	0.70	0.50
Mean - Std.Dev. ( $\delta - \sigma_\Delta$ )	-1.16	-1.72	-1.43	-0.92	-1.43
Mean Magnitude	4.9	4.8	4.8	4.9	4.8

<b>Table 6. Youngs fit to Frankel et al. (1996)</b>					
<b>Frequency (Hz): 10</b>					
Distance Bins (km)	0	75	150	500	0
	75	150	500	1000	1000
Geometric Mean Distance (km)	26.3	115.3	265.5	716.4	117.8
Number of Data Points	17	25	54	43	139
Number of Earthquakes	11	8	9	7	17
<b>Mean (<math>\delta</math>) [Equation A-2]</b>	0.05	-0.11	-0.12	-0.03	<b>-0.04</b>
Factor = $\exp(\delta)$	1.05	0.90	0.89	0.97	0.96
Standard Deviation ( $\sigma_\Delta$ )	0.67	0.98	0.81	0.76	0.76
<b>Standard Error on the Mean (<math>\sigma_\delta</math>) [Equation A-4]</b>	0.16	0.20	0.11	0.12	<b>0.06</b>
90% Confidence Range	0.27	0.32	0.18	0.19	0.11
Mean + Std.Dev. ( $\delta + \sigma_\Delta$ )	0.72	0.87	0.69	0.73	0.72
Mean - Std.Dev. ( $\delta - \sigma_\Delta$ )	-0.63	-1.08	-0.93	-0.79	-0.80
Mean Magnitude	4.9	4.8	4.8	4.9	4.8

Figure 1

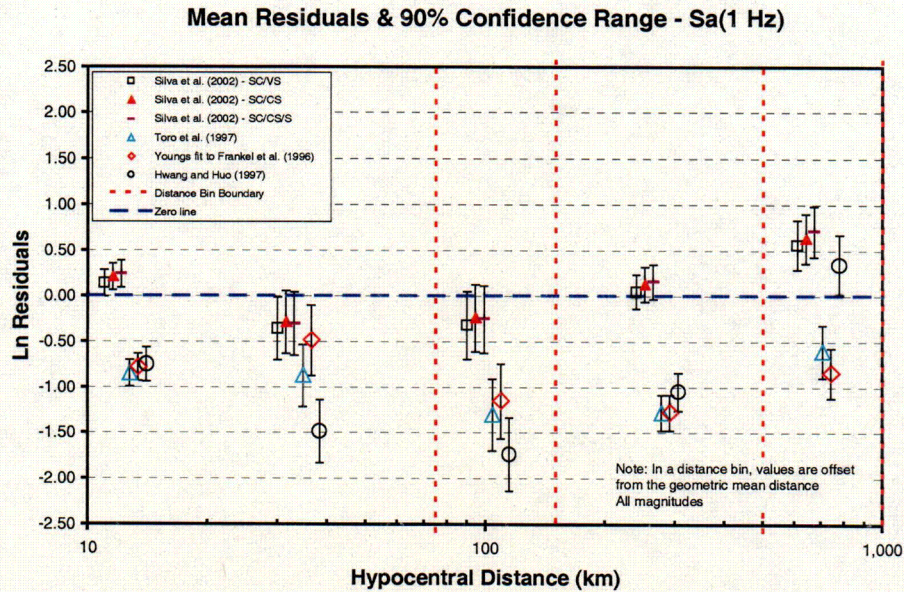
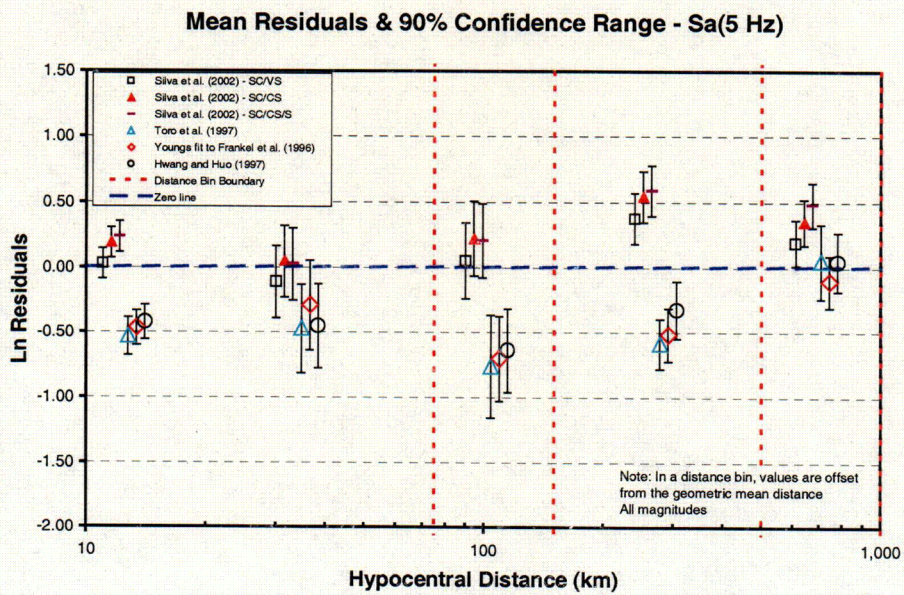


Figure 2



col

Figure 3

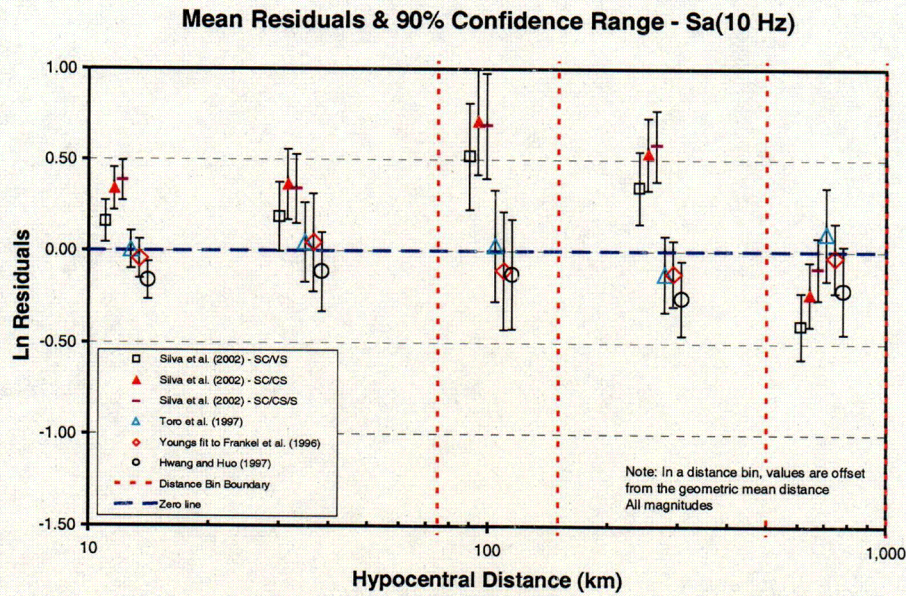
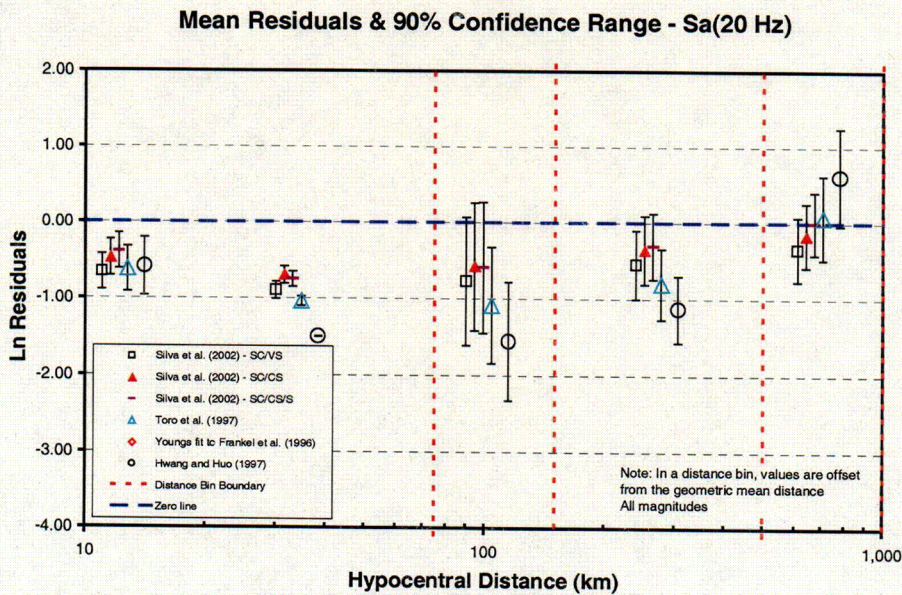


Figure 4



CO2

Figure 5

Mean Residuals & 90% Confidence Range - Sa(25 Hz)

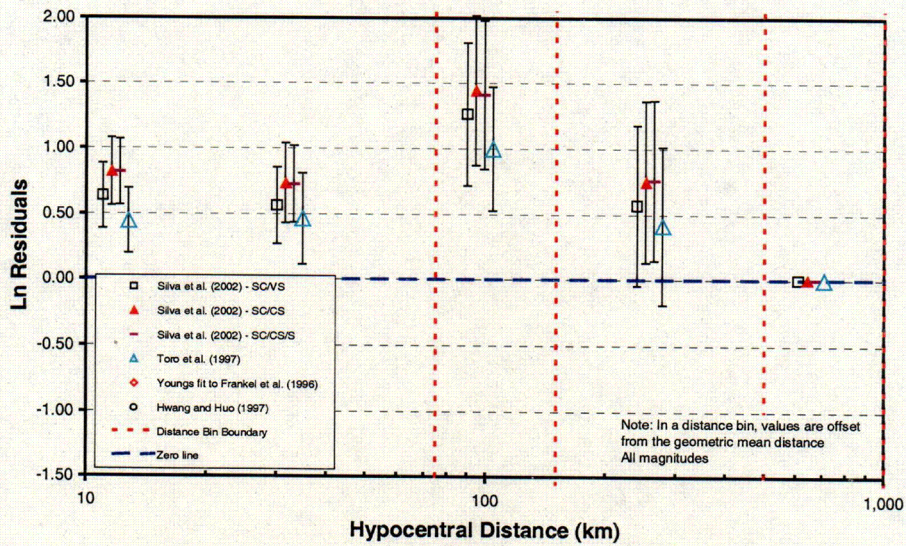
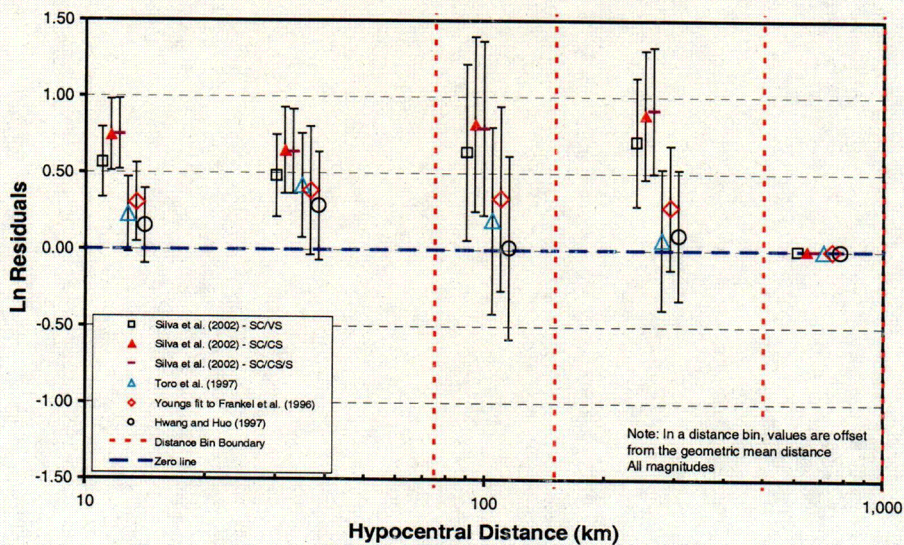


Figure 6

Mean Residuals & 90% Confidence Range - PGA



Given the tabulated statistics and the equations presented earlier, the intracluster weights for Cluster 1 models were determined, as presented in Table 7.

<b>Table 7. Intracluster Weights for Cluster 1 Models</b>			
	$\delta_i(\phi)$	$\sigma_{\delta_i}(\phi)$	$\beta_i^2(\phi)$
	<i>Eqn A-2</i>	<i>Eqn A-4</i>	<i>Eqn A-5</i>
<b>1 Hz</b>			
Hwang & Huo (1997)	-0.752	0.116	0.579
Silva et al. (2002) -- SC-CS	0.209	0.088	0.051
Silva et al. (2002) -- SC-CS-S	0.239	0.090	0.065
Silva et al. (2002) -- SC-VS	0.139	0.088	0.027
Toro et al. (1997)	-0.850	0.089	0.731
Frankel et al. (1996)	-0.784	0.091	0.622
<b>5 Hz</b>			
Hwang & Huo (1997)	-0.423	0.081	0.185
Silva et al. (2002) -- SC-CS	0.190	0.072	0.041
Silva et al. (2002) -- SC-CS-S	0.233	0.073	0.059
Silva et al. (2002) -- SC-VS	0.026	0.072	0.006
Toro et al. (1997)	-0.531	0.083	0.289
Frankel et al. (1996)	-0.467	0.081	0.225
<b>10 Hz</b>			
Hwang & Huo (1997)	-0.163	0.063	0.030
Silva et al. (2002) -- SC-CS	0.339	0.071	0.120
Silva et al. (2002) -- SC-CS-S	0.384	0.067	0.152
Silva et al. (2002) -- SC-VS	0.159	0.070	0.030
Toro et al. (1997)	0.005	0.063	0.004
Frankel et al. (1996)	-0.042	0.065	0.006

For each model, the  $\beta_i^2(f)$  values for the three frequencies are summed. Note that the values for 1 Hz is counted twice, as discussed previously. Following Equation A-6, the weight for each model is provided in Table 8. The Table 8 weights are those identified in Table 3-5 of EPRI (2004).

<b>Table 8. Model Weights</b>			
<b>Models</b>	$\Sigma\beta_i^2(\phi) = \beta_i^2$	$1/\beta_i^2$	<b>Weight</b>
Hwang & Huo (1997)	1.374	0.728	0.037
Silva et al. (2002) -- SC-CS	0.264	3.788	0.192
Silva et al. (2002) -- SC-CS-S	0.342	2.923	0.148
Silva et al. (2002) -- SC-VS	0.090	11.052	0.560
Toro et al. (1997)	1.755	0.570	0.029
Frankel et al. (1996)	1.475	0.678	0.034

2. Comparison Plots of Data Versus Cluster 1 Ground Motion Models

Figure 7 is a plot of the available CEUS rock data used during the EPRI (2004) development. In Figures 8 through 15, the 6 models of Cluster 1 are plotted in comparison to the data. Note that the data has been grouped into two magnitude ranges (two plots for each frequency) and that the models use an average magnitude, as indicated.

In the development of intracluster weights based on fitting the data, the weights were developed using the explicit magnitudes of the earthquakes and the weights considered only frequencies of 1 Hz [counted twice to compensate for 2.5 Hz relations not consistently available across models], 5 Hz, and 10 Hz. PGA is shown only for comparison and was not used in the developments of the weights.



Figure 8

Data Comparison Cluster 1: 1 Hz

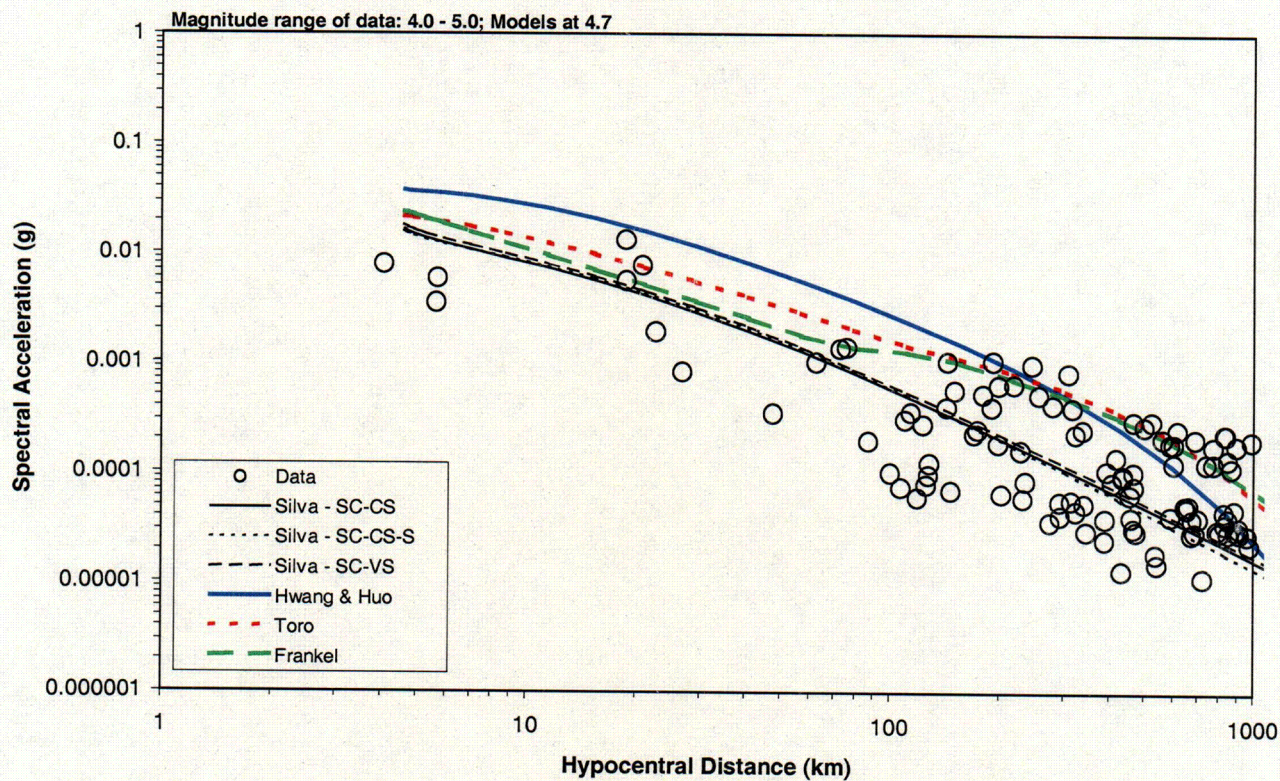


Figure 9

Data Comparison Cluster 1: 1 Hz

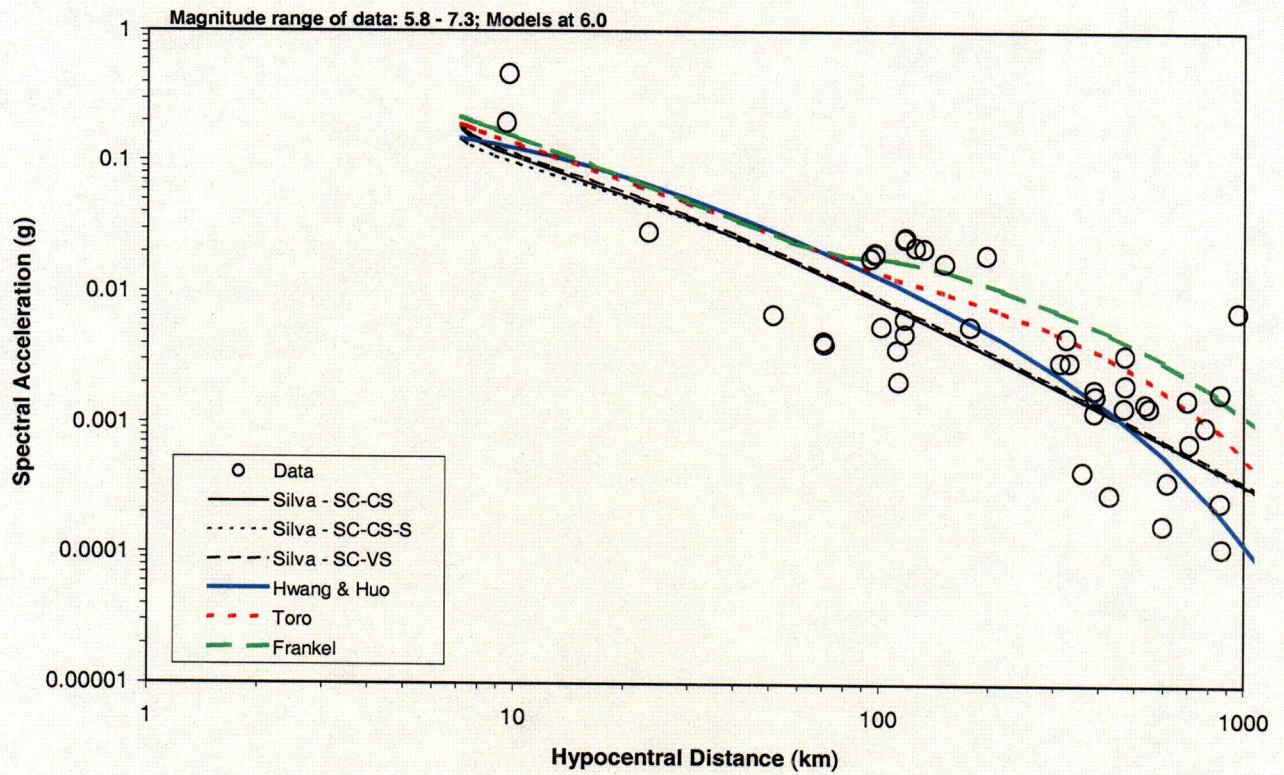
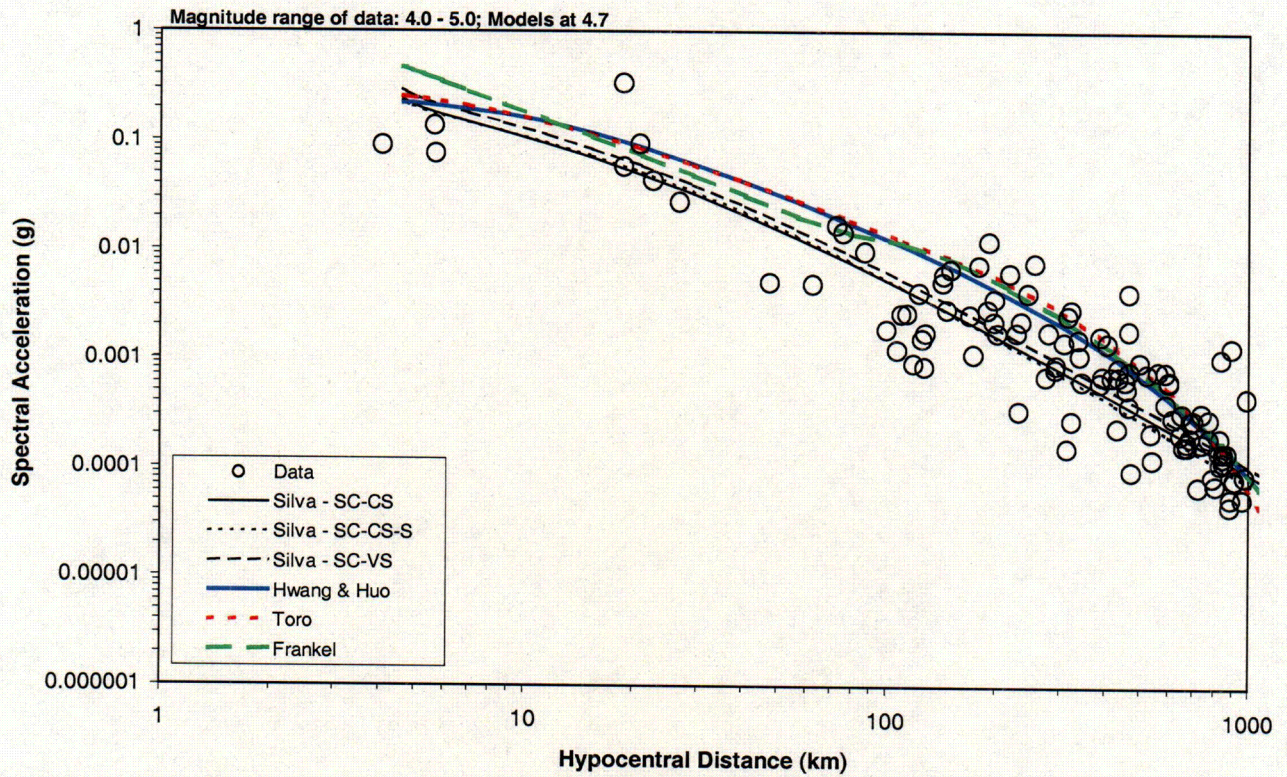


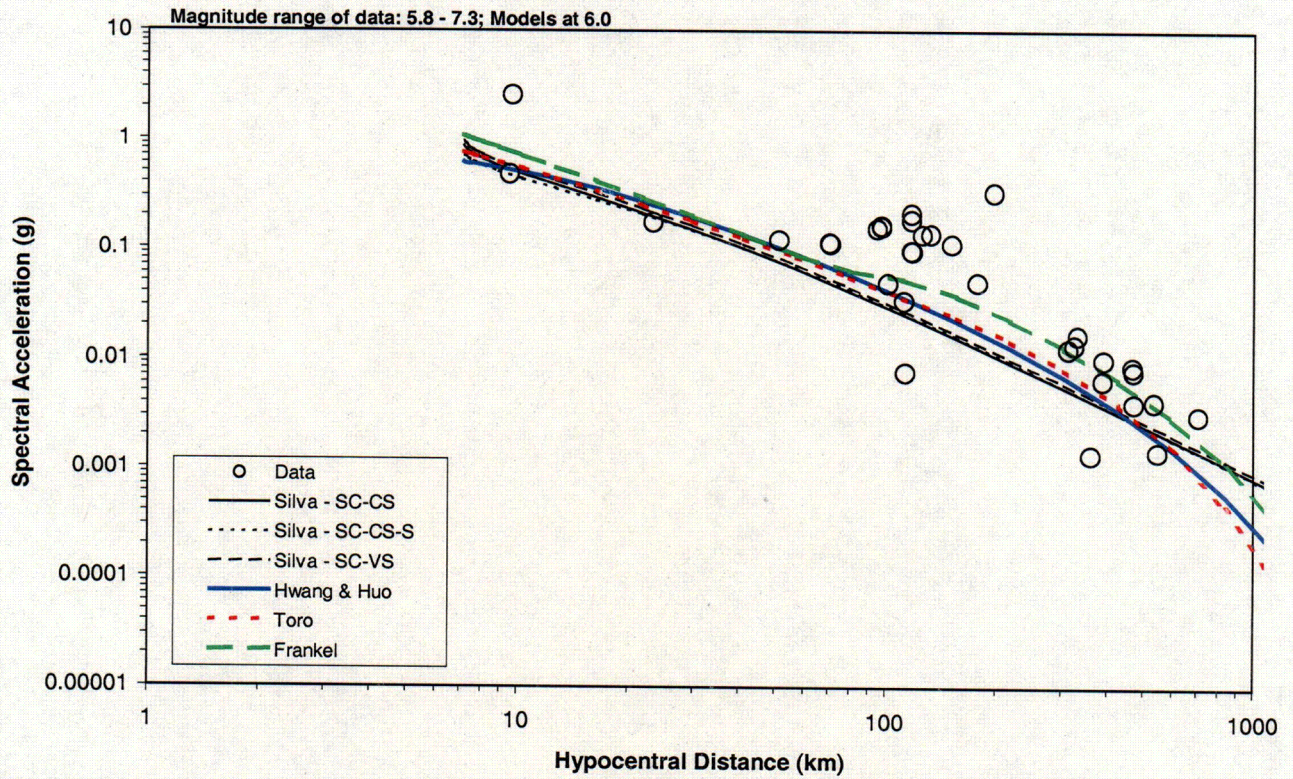
Figure 10

Data Comparison Cluster 1: 5 Hz



COG

Figure 11  
Data Comparison Cluster 1: 5 Hz



CO7

Figure 12

Data Comparison Cluster 1: 10 Hz

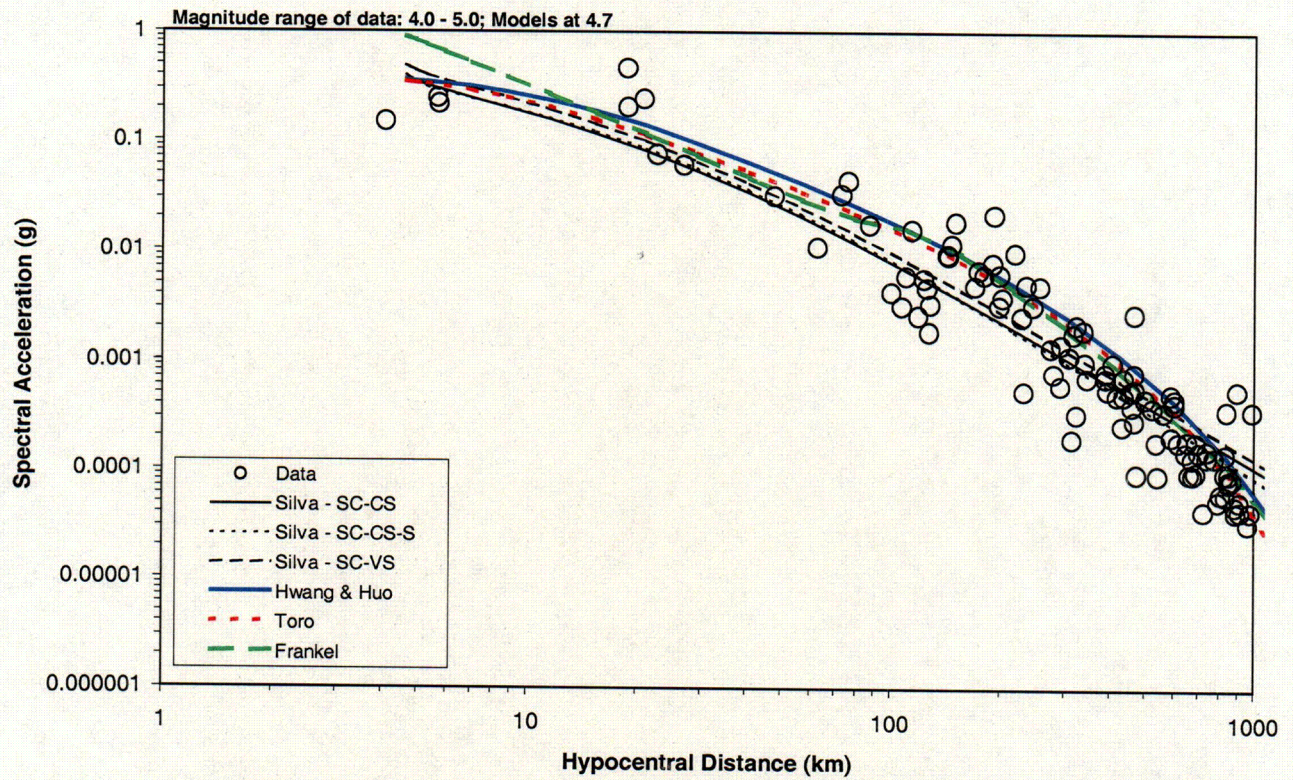


Figure 13

Data Comparison Cluster 1: 10 Hz

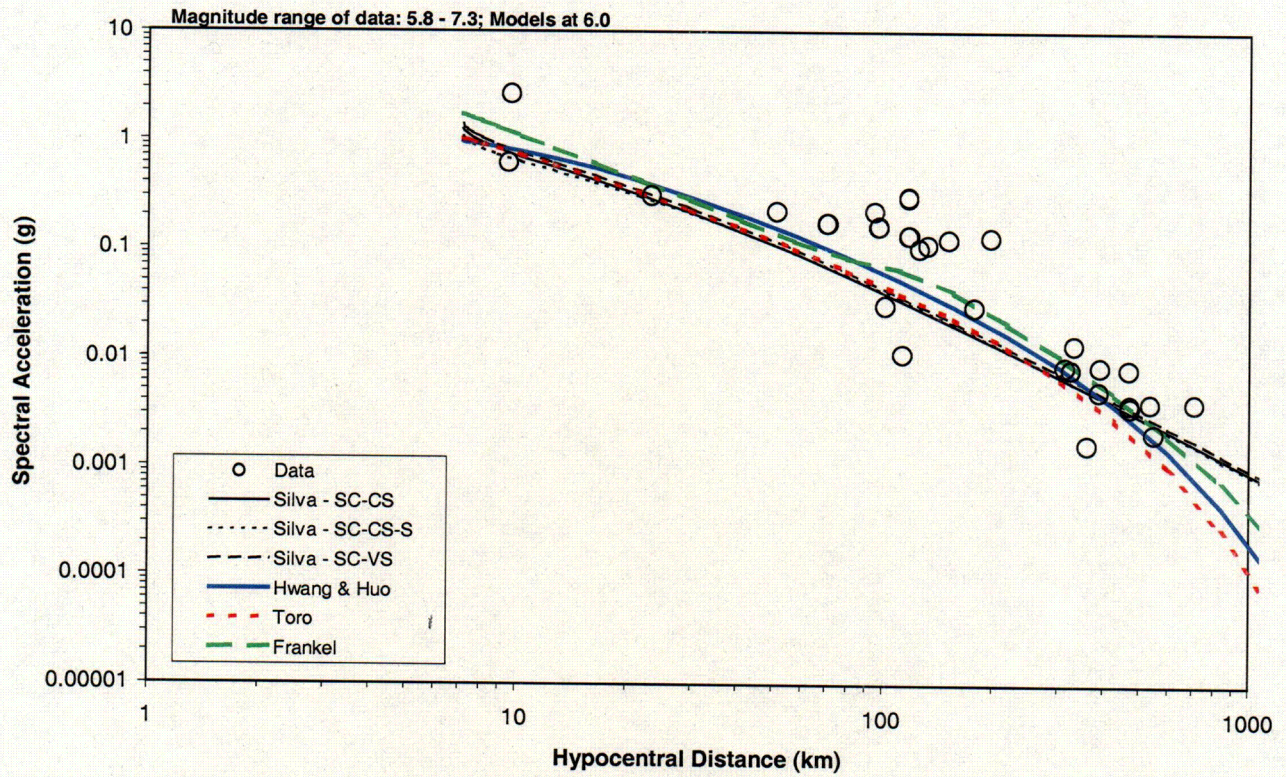


Figure 14  
Data Comparison Cluster 1: PGA

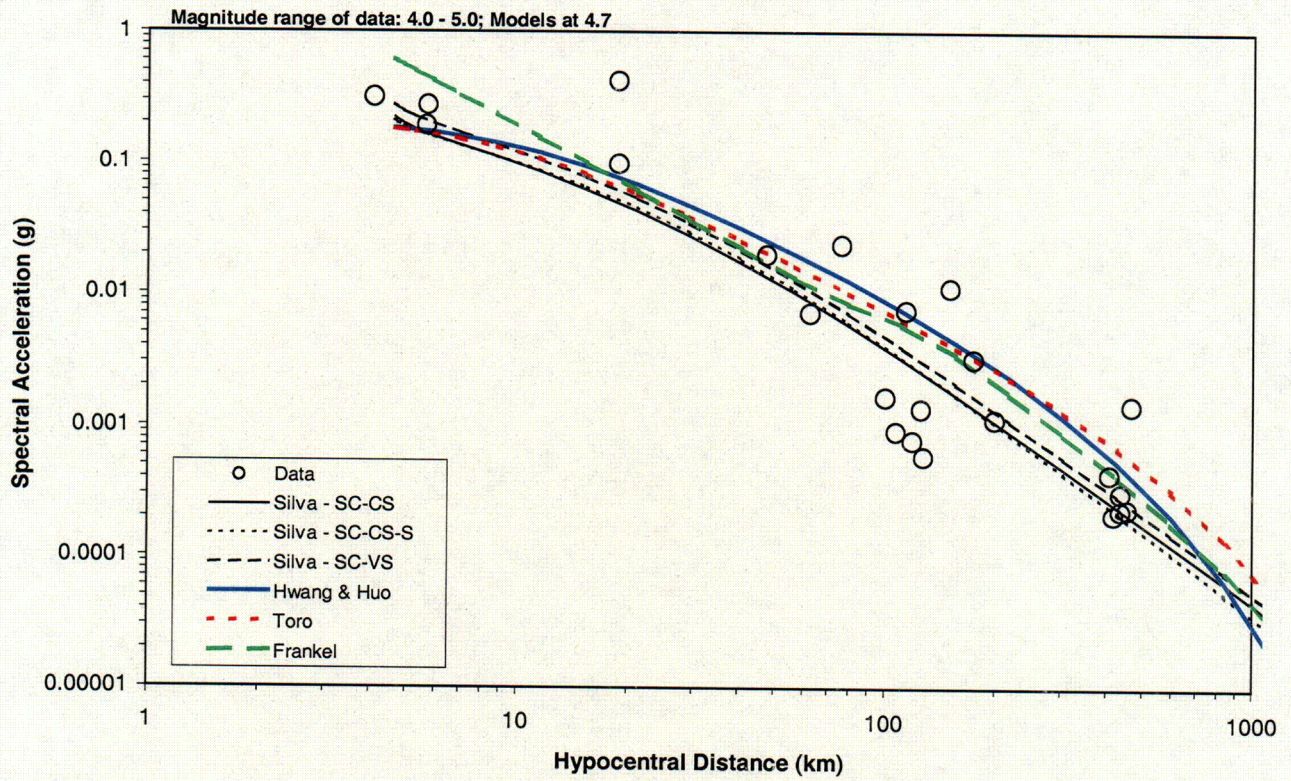
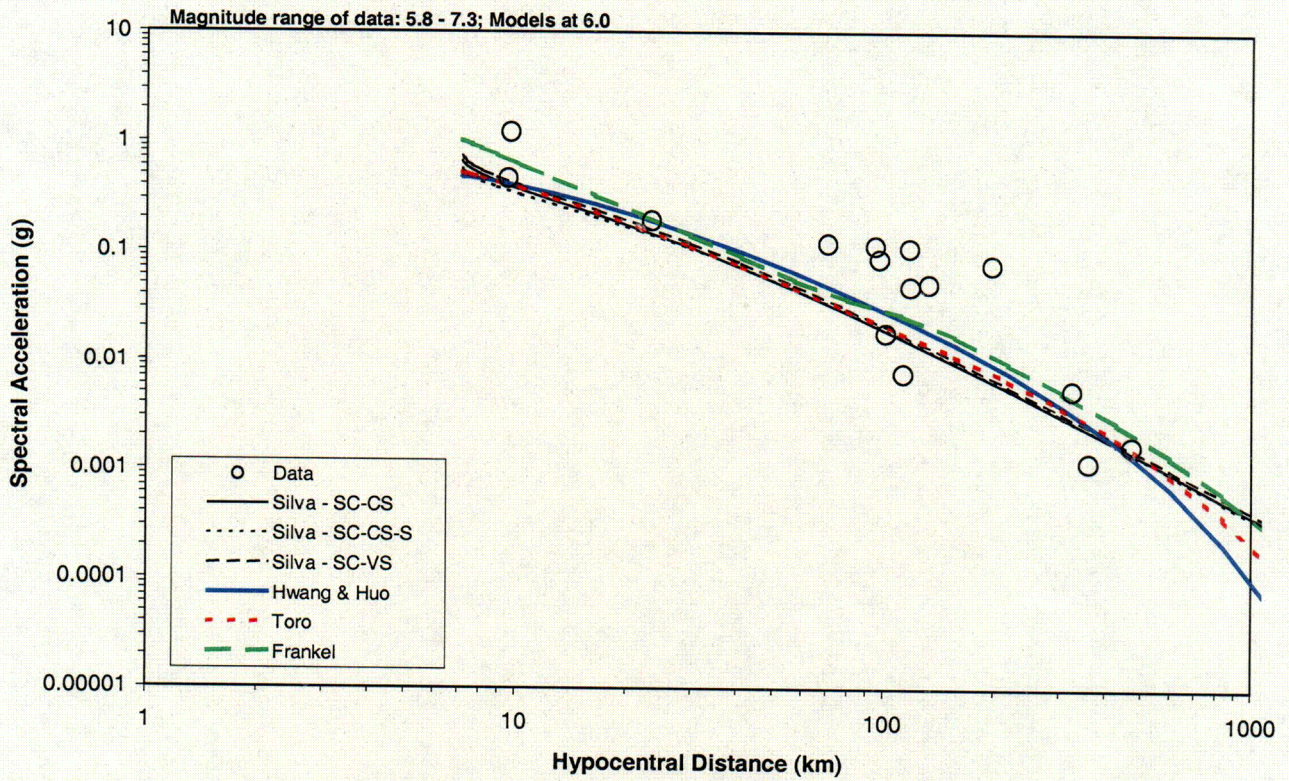


Figure 15  
Data Comparison Cluster 1: PGA



**Part 2 of DSER Open Item 2.5-1**

In RAI 2.5.2-2(b), the staff asked the applicant to provide additional information on the Silva et al. Cluster 1 attenuation relationships. In response, the applicant provided additional documentation on these attenuation relationships. The Silva et al. Cluster 1 relationships use an expression for the seismic attenuation parameter,  $Q$ , that is frequency dependent. This frequency-dependent  $Q$  value was derived from an inversion of the data from the 1988 Saguenay earthquake. This inversion solves for  $Q$ , as well as the local site attenuation parameter  $\kappa$  and the stress drop, which is the difference between the initial stress before and [sic] earthquake and the final stress. The staff was unable to determine how the recordings from a single earthquake can provide well-resolved values of both crustal  $Q$  and site  $\kappa$ . In addition, the  $Q$  value of 317 at 1 Hz is much lower than values found in other studies of eastern North American earthquakes. In addition, other studies have found less frequency dependence of  $Q$  in the east than in the west, which is contrary to the findings of Silva et al.

During telephone conversations on March 9 and 15, 2005, the NRC requested additional information related to this part of the open item to supplement Dominion's January 25, 2005 response [Dominion (2005)]. On March 17, 2005, the NRC sent a facsimile to Dominion [NRC (2005)] clarifying the additional information needed:

- (a) Discuss the expert's decision to not equally weight the attenuation models in view of the comments in the EPRI 2004 report on page 2-3 stating that the goal of the SSHAC approach is to represent "the legitimate range if technically supportable interpretations among the entire informed technical community." SSHAC recommends "simple integration" of the knowledge of the technical community at large whenever possible; in the "rare case" only, "when it becomes obvious that using equal weighting misrepresents the community-as-a-whole," should "explicit quantitative but unequal weights" be used (page 2-4 of the EPRI 2004 report).
- (b) Concerning the three Silva et al. (2002) attenuation models in Cluster 1, please address the following Staff concerns:
  - (1) As shown in Table 4-3 (EPRI 2004), the 1 Hz  $Q$  value used for the three Silva et al. (2002) models is much lower, while the exponent of the frequency is far higher in comparison to the other attenuation relationships.

- (2) The Q value used for the three Silva et al. (2002) models is determined from fitting the Saguenay earthquake as well as site-dependent kappa; this is an undetermined problem.
- (3) All three Silva et al. (2002) models, which receive a combined weight of 0.90, use the same geometrical spreading, Q function, and lack of Moho reflection. Yet these three models are treated as separate models. This unequal weighting essentially eliminates the other three Cluster 1 attenuation relationships, and therefore misrepresents the range of the informed technical community.
- (4) As a result of the above concern, the path epistemic uncertainty in terms of Q and path (Moho vs. no Moho reflections) is too low for Cluster 1. Specifically, the Q and path choice used by the three Silva et al. (2002) relationships is given a weight of 0.90. Other models in Cluster 1, which model the Q and path differently (include Moho reflections), are only given a combined weight of 0.06.

#### **Supplemental Response to Part 2 of DSER Open Item 2.5-1**

The NRC request for information involves both the overall process used in developing the EPRI CEUS ground motion model as well as specific aspects of particular constituent models. Because the ground motion project was sponsored by EPRI and can be used by others within the nuclear industry, Dominion determined that the appropriate response to this NRC request should be provided by EPRI. Enclosure 2 provides a copy of a March 25, 2005 letter from EPRI titled, "EPRI Response Pertaining to the Dominion Nuclear North Anna, LLC (Dominion) North Anna Early Site Permit Application DSER Open Item 2.5-1." This EPRI letter summarizes the scope of the EPRI CEUS Ground Motion Project, the evaluation process, and the feedback received from the Peer Review Panel.

Responses to the items identified in the NRC's March 17, 2005 facsimile are provided below, which supplement the EPRI response letter.

- (a) As described in Section 3.3.3 of NUREG/CR-6372 [SSHAC (1997)] and as explained on the March 9, 2005 conference call by Dr. Allin Cornell, a member of the Senior Seismic Hazard Analysis Committee (SSHAC) which prepared the SSHAC report, the SSHAC guidance on equal weighting applies to the weighting of experts in a panel and not to the weighting of proponent models. This is discussed on page 37 of the NUREG/CR-6372 Main Report, under "Outcome 2: Equal Weights." The SSHAC, in the last quote in Question 2, is providing guidance to the

Technical Facilitator Integrator (TFI) regarding the weighting of expert judgment in the facilitation process that is graphically displayed in Figure 3-1 of NUREG/CR-6372, "TFI Process Logic."

- (b)(1) & (2) The model functional form, basis for parameter selection, and the results developed in Silva et al. (2002) and its predecessor, Silva et al. (1997), are the responsibility of the lead author. Of particular relevance is the interdependence between model parameters, how the parameters were determined, model sensitivity to its parameters, and reasonable ranges in parameter values, based on expert judgement and expert interpretation of the scientific literature. It is unclear if a summary justification for the results of the Silva et al. (1997 and 2002) studies would resolve the items identified that seem, ultimately, to represent differences in expert judgement.

Differences in expert judgement are often difficult to reconcile. For this very reason, the SSHAC process was developed and accepted for use by the NRC. The EPRI 2003 ground motion model was developed by implementing a SSHAC Level 3 assessment process during which the EPRI Expert Panel identified the Silva, et al. relationships as ones that should be included in the assessment and evaluated. The EPRI Expert Panel considered specific parameterizations of individual ground motion relationships in determining whether or not a relationship should be included in the SSHAC Level 3 assessment process. All ground motion relationships identified as viable by the Expert Panel were evaluated using the same criteria following the SSHAC Level 3 process.

The SSHAC process does not guarantee that every scientist will agree with the assessments. It is rather intended to assure that the assessed results reflect the preponderance of current scientific views, which is the underpinning of safety decision-making.

- (b)(3) Cluster 1 corresponds to models based on the single-corner spectral model to develop ground motion attenuation relationships. In a cluster, each member model was considered an independent implementation of the cluster model type (e.g., single-corner spectral models). As discussed in EPRI (2004) alternative clustering approaches were considered by the Technical Integrator (TI) and discussed with the ground motion expert panel. One such clustering approach that considered additional seismological factors resulted in approximately 24 model classes. With only 13 candidate models available, this proved unworkable. The conclusion of these discussions favored the clustering approach that was

implemented. Further, at no time during discussions with the ground motion expert panel (during the first workshop when the ground motion models were presented and initial clustering ideas were discussed or later when the final clustering and model weights were reviewed by the panel members) was a concern raised about the multiple Silva et al. (2002) models included in Clusters 1 or 2.

As part of the evaluation process, a parametric approach was used to represent each cluster. The parametric representation of a cluster by the logarithmic mean and standard deviation (as a function of earthquake magnitude and distance), was not intended to retain the range of the models within a cluster. Ultimately, the EPRI (2003) ground motion model was defined in terms of a manageable, discrete set of median models with individual weights to represent the overall distribution of the technical community.

On review, the ground motion estimates of the Frankel, et al. (1996) are included in the range of the EPRI (2003) ground motion model estimates. Figure 4-16 in EPRI (2004) shows the median and the range of the EPRI (2003) median ground motion model estimates for each spectral frequency. A comparison of this range indicates estimates based on the Frankel et al. (1996) model are included in the range of the EPRI (2003) ground motion estimates.

(b)(4) The ground motion models in Cluster 1 considered a range of alternative stress drop models [see Table 4-2 of EPRI (2004)] and alternative Q and path models [see Table 4-3 of EPRI (2004), note that Table 4-3 also includes Atkinson and Boore's path model]. Collectively, these models represent alternative single-corner source spectrum models for the CEUS. In aggregate, these models provide a measure of the epistemic uncertainty in the median ground motion based on the single-corner source spectrum models (e.g., intra-cluster variability).

The statement in the NRC's March 17, 2005 request for information, "...the Q and path choice used by the three Silva et al. (2002) relationships is given a weight of 0.90" is not correct in that a weight is not assigned to the "Q and path choice" alone, as suggested. Weights were assigned to the alternative single-corner spectral models [which represent alternative estimates of stress drop, Q, path, site amplification, and near-surface attenuation (e.g.,  $\kappa$  or  $f_{max}$ )] based on the consistency of the median (mean log) ground motions estimated using the overall model with the data. Thus, the weights do not reflect a weight on the specific Q and

path model, but a weight on the overall ground motion “predictions” generated by the model.

As part of the CEUS model development an assessment was performed to estimate whether an additional component of epistemic uncertainty for path effects should be considered, beyond what was already represented by the intra-cluster variability of the median models. To assess this effect (considering path effects alone), calculations were performed in which a stress drop of 120 bars was used and the alternative path models in Table 4-3 of EPRI (2004) were considered. For purposes of this calculation, there was no objective basis to assign weights to the alternative path models. Consequently, the different models were equally weighted for purposes of estimating a logarithmic standard deviation. These results are shown in Figure 4-6 of EPRI (2004). In examining the results in Figure 4-6 to the variability in the Cluster 1 models shown in Figure 4-2 of EPRI (2004), it was judged these variabilities were similar, although the results in Figure 4-6 are higher, particularly at distances beyond 100 km. This assessment considers the fact that most of the models in Cluster 1 had already considered the variability in path effects as aleatory variability and thus it is ultimately included in the overall probabilistic hazard analysis.

The models in Cluster 1 considered the effects of changes in geometric spreading in a variety of ways. The Toro et al. (1997) model is based on the EPRI (1993) model in which specific effects of crustal reflections were included in the ground motion simulations [see Appendix 3A of EPRI (1993)]. The parameters that control the crustal reflections were randomized in the simulations, and the ultimate ground motion model equations smoothed through these results with a simpler form that incorporated only a change in slope at a distance of 100 km. The same effect was found by Somerville et al. (2001) in which wave propagation in the crust was specifically modeled in their simulations, but the final ground motion model equations smooth through these results with a change in slope, in this case at 50 km. Atkinson and Mereu (1992) also concluded that the bilinear form with a suitably chosen break point captures much of the behavior of their tri-linear geometric spreading model [which is used by Frankel et al. (1996)]. Silva et al. (2002) refer to the results of EPRI (1993) described above in justifying their use of a smooth bilinear geometric spreading model in their simulations. They then fit their simulations (which include randomized depths and Q) with a simple functional form and include the misfits of the simulations into their aleatory variability [which forms the basis for the aleatory variability model 4 of EPRI (2004)]. Atkinson and Boore (1995) have shown that using simple

ground motion estimation equations produces seismic hazard results that are close to those obtained from more complex simulation results based on the Atkinson and Mereu (1992) tri-linear geometric spreading model, even when there is no randomization of the path parameters.

Based on these arguments, it is concluded that the effects of complex geometric spreading have been incorporated into the models that form the basis for Cluster 1, even if the final functional form of the ground motion equations for the individual models do not have an explicit deterministic effect.

### **Part 3 of DSER Open Item 2.5-1**

In RAI 2.5.2-2(d), the staff asked the applicant to explain the weights given to each of the four clusters. In response to RAI 2.5.2-2, the applicant stated that the expert panel members, convened for the EPRI ground motion study, were asked to subjectively evaluate how well the alternative ground motion models relied on seismological principles. The staff considers the applicant's response to of RAI 2.5.2-2(d) to be somewhat indirect. The applicant has provided additional information, but the details still remain abstract in terms of specific "seismological principles." The response emphasizes the ranking of model clusters and the judgments involved in balancing data consistency and adherence to seismological principles. However, the applicant provided only abstract and very general references to these seismological principles. As a result, the staff was unable to evaluate the criteria or the weights applied to the four clusters.

### **Supplemental Response to Part 3**

During telephone conversations on March 9 and 15, 2005, the NRC stated that no further information on Part 3 of Open Item 2.5-1 was needed beyond Dominion's January 25, 2005 response [Dominion (2005)].

## References

- Atkinson, G. and R. Mereu (1992). "The shape of ground motion attenuation curves in southeastern Canada," *Bull. Seism. Soc. Am.*, 82, 2014-2031.
- Atkinson, G. M. and D. M. Boore (1995). "Ground-Motion Relations for Eastern North America," *Bulletin of the Seismological Society of America*: 85, 1, 17-30.
- Dominion (2005). Letter from Eugene S. Grecheck, Vice-President-Nuclear Support Services, Dominion, to U.S. Nuclear Regulatory Commission, Document Control Desk, "Dominion Nuclear North Anna, LLC, North Anna Early Site Permit Application, Response to Draft Safety Evaluation Report Open Item 2.5-1," January 25, 2005.
- EPRI (1993). "Guidelines for Determining Design Basis Ground Motions," Electric Power Research Institute, Technical Report TR-102293, November 1993.
- EPRI (2003). "CEUS Ground Motion Project – Model Development and Results," Electric Power Research Institute, Technical Report 1008910, August 2003.
- EPRI (2004). "CEUS Ground Motion Project Final Report," Electric Power Research Institute, Technical Report 1009684, submitted to the NRC by the January 25, 2005 Letter from Eugene S. Grecheck, Vice President-Nuclear Support Services, Dominion, to U.S. Nuclear Regulatory Commission, Document Control Desk, "Dominion Nuclear North Anna, LLC, North Anna Early Site Permit Application, Response to Draft Safety Evaluation Report Open Item 2.5-1."
- Frankel, A., Muller, C., Barnhard, T. et al. (1996), "National Seismic-Hazard Maps: Documentation June 1996," U.S. Geological Survey, Denver, CO: Open-File report 96-532.
- Hwang, H. and J. R. Huo (1997). "Attenuation Relations of Ground Motion for Rock and Soil Sites in Eastern United States," *Soil Dynamics and Earthquake Engineering*: 16, 363-372.
- NRC (1997). "Identification and Characterization of Seismic Sources and Determination of Safe Shutdown Earthquake Ground Motion," Regulatory Guide 1.165, U.S. Nuclear Regulatory Commission, Washington DC.
- NRC (2005). Facsimile, "Items still to be addressed for OPEN ITEM 2.5-1," March 17, 2005.

SSHAC (1997). Senior Seismic Hazard Analysis Committee, "Recommendations for Probabilistic Seismic Hazard Analysis: Guidance on Uncertainty and Use of Experts," NUREG/CR-6372, U.S. Nuclear Regulatory Commission, Washington, DC.

Silva, W., N. Abrahamson, G. Toro, and C. Costantino (1997). "Description and validation of the stochastic ground motion model," Report submitted to Brookhaven National Laboratory, Associated Universities, Inc., Upton, New York 11973, Contract No. 770573.

Silva, W.J., N. Gregor and R. Darragh (2002). "Development of Regional Hard Rock Attenuation Relations for Central and Eastern North America," Pacific Engineering and Analysis, El Cerrito, CA.

Somerville, P. G., N. Collins, N. A. Abrahamson, R. Graves and C. K. Saikia (2001). "Ground Motion Attenuation Relations for the Central and Eastern United States," Report to U.S. Geological Survey, NEHRP External Research Program, Award No. 99-HQ-GR-0098.

Toro, G. R., Abrahamson, N.A. and J.F. Schneider (1997). "Model of Strong Ground Motions from Earthquakes in Central and Eastern North America: Best Estimates and Uncertainties," Seismological Research Letters: 68, 41-57.

**Application Revision**

None.

**DSER Open Item 2.5-2 (DSER page 2-167)**

The staff focused its review of SSAR Section 2.5.2.5, "Seismic Wave Transmission Characteristics of the Site," on the applicant's incorporation of the seismic wave transmission characteristics of the material overlying the base rock at the site into the determination of the SSE. SSAR Section 2.5.4.7 provides a description of the transmission characteristics of the site material. According to the applicant's responses to RAIs 2.5.2-1(c) and 2.5.2-8, the applicant's SSE represents the ground motion at a depth well below the ground surface. However, 10 CFR 100.23(d)(1) states the following:

The Safe Shutdown Earthquake Ground Motion for the site is characterized by both horizontal and vertical free-field ground motion response spectra at the free ground surface.

As explained in more detail below, the staff has determined that the applicant's SSE does not represent the free-field ground motion at the free ground surface.

Figure 2.5.2-5, which reproduces SSAR Figure 2.5-62, shows that the shear wave velocity values for the ESP site reach a value of about 2500 feet per second (ft/s) at a depth of 60 feet.

This shear wave velocity value is well below that of the hard rock conditions ( $V_s = 9200$  ft/sec) assumed by the EPRI 2003 study for CEUS ground motion models. In addition, the applicant did not make shear wave velocity measurements at a depth greater than 65 feet. Thus, the hard rock shear wave velocity value of 9200 ft/s may not be reached at the ESP site until a considerable depth below the ground surface. According to SSAR Figure 2.5-62, from the ground surface to a depth of 30 feet, the shear wave velocity at the ESP site varies from 600 ft/s to about 1300 ft/s. The applicant needs to incorporate these lower shear wave velocities, as well as other subsurface material properties and their uncertainties, into the determination of the ESP site SSE. In addition, the applicant should provide the site amplification or transfer function for the staff to review. The staff needs this information to determine that the applicant has provided an SSE that meets the requirements of Appendix S to 10 CFR Part 50 and 10 CFR 100.23, which define the SSE as "free-field ground motion response spectra at the free ground surface." This is **Open Item 2.5-2**.

**Response**

As described in Dominion's February 18, 2005 letter (Reference 1), the current SSE spectrum in SSAR Section 2.5.2 is defined for "hard" rock conditions—rock that has a

shear wave velocity of 2.8 km/s or about 9,200 ft/sec [per Sections 3.2.4 and 5.1.4 of EPRI (2004) (Reference 2)]. In response to this open item, an analysis has been performed to modify the current hard rock SSE spectrum to meet the “free-field ground motion at the free ground surface” criteria of 10 CFR 100.23(d)(1) and Section I.1 of Standard Review Plan (SRP) Section 3.7.1 (Reference 3). The SSE ground motion has been estimated at a control point at the top of a hypothetical outcrop of Zone III-IV material. This is consistent with Section I.1 of SRP Section 3.7.1, which states, in part:

“...For sites composed of one or more thin soil layers overlying a competent material or in case of insufficient recorded ground-motion data, the control point is specified on an outcrop or a hypothetical outcrop at a location on the top of the competent material...”

The shear wave velocities for the Zone III-IV material range from 2,500 to 4,500 ft/sec, with a best estimate shear wave velocity of 3,300 ft/sec. See SSAR Table 2.5-45. A shear wave velocity of 3,300 ft/sec has been used in the control point SSE analysis. The elevation of the top surface of the Zone III-IV material varies across the site, as shown in SSAR Figures 2.5-57 and 2.5-58. The top of the Zone III-IV material has been chosen to be at a representative elevation of 250 ft in the control point SSE analysis. Site amplification factors or transfer functions have also been specified.

#### Description of Control Point SSE Analyses

In Dominion’s March 3, 2005 letter (Reference 4), a description of the control point SSE analyses was provided. Below is a further description of the various steps of the completed analyses.

##### a. Documentation of Site-Specific Rock Properties and Uncertainties

A shear wave velocity profile for the site was developed from data from four boreholes - three from the subsurface exploration for the existing Units 1 and 2 and the fourth from the subsurface investigation performed for the ESP. Shear wave velocity versus depth data for the three Units 1 and 2 boreholes are available in Reference 5. These data were obtained using a Birdwell “3D Velocity Recorder”. Velocity and density logs were made in boreholes B-20 and B-104, and Well #1 (W-1) by the Birdwell Division of Seismograph Service Corporation, with readings taken each 1 ft. Shear wave velocities from these tests are provided in Table 1. For the ESP subsurface investigation, down-hole seismic testing was conducted in boring B-802B. (B-802B is adjacent to B-802 and can be assumed to be identical to B-802.) The tabulated results of the ESP tests are provided in SSAR Section 2.5.4, Appendix B. Shear wave velocity measurements were made mainly at 5 ft depth intervals, but sometimes at 10 ft depth intervals. Table 1 contains the results of the ESP tests, linearly interpolated to 1 ft intervals.

The 1-ft interval shear wave velocity values in Table 1 for B-20, B-104, W-1, and B-802 are plotted against depth in Figure 1. As shown in Figure 1, starting at  $V_s = 3,300$  ft/sec at 21 ft depth, a visual "best-fit" line through the data reaches 9,200 ft/sec at around 160 ft depth.

Some limited additional laboratory and seismic data (SSAR Section 2.5.4, Appendix B and Reference 6) are available and were compared to the above borehole data. The "best-fit" line was judged to fit these additional data reasonably well.

In compiling these data and plotting them as a function of depth, it was noted that depth to top of rock over the site approximately follows the ground surface suggesting, as does the site geology, that the variation in lithology and shear wave velocity with depth is the consequence of weathering of the very hard gneiss bedrock. This allows depths to be associated with idealized elevations. Throughout this response, a zero-depth plant grade elevation of 271 feet is assumed and the depths listed in Table 1 may be converted to elevations by subtracting from 271.

Other material properties that must be defined for the rock column response analysis are density, Poisson's ratio, and the behavior of shear wave velocity and material damping as a function of strain.

SSAR Table 2.5-45 gives the strength of the Zone III-IV material as 4,000 psi, and the strength of the Zone IV material as 12,000 psi. This is the strength range for medium to very high strength concrete. The linearity of the stress-strain relationship is demonstrated well by the high quality unconfined compression tests on the ESP rock cores summarized in Table 2. As tabulated in Table 2, the maximum longitudinal strain is  $8 \times 10^{-1}$  percent for the Zone III-IV specimen and ranges from 3 to  $5 \times 10^{-1}$  percent for the five Zone IV specimens. All of these data confirm that the strong rocks of Zones III-IV and IV have essentially the same modulus throughout the strain range.

Other rock parameters needed for the SHAKE analysis were also obtained from SSAR Table 2.5-45, including: total unit weight = 163 pcf and Poisson's ratio = 0.33.

b. Generation of Alternative Randomized Rock Columns

Section 6A of EPRI (1993) (Reference 7) describes a stochastic model for shear-wave velocity profiles. This model was used in this analysis, with some modifications to account for the conditions at the North Anna ESP site. In addition to the site-specific material property characterizations outlined above, additional generic guidance about the correlation between shear wave velocity and its uncertainty as a function of depth and depth-wise correlation structure of the  $\ln(V_s)$  (the natural logarithm of the shear wave velocity) residuals from EPRI (1993), and uncertainty in damping consistent with

the variability observed in Costantino (1996) (Reference 8), were adopted. Finally, damping was taken as the same for all sub-layers within any given profile (that is, fully correlated between layers), but was allowed to vary between one artificial rock column and the next.

Fifty randomized shear wave velocity profiles were generated using the model parameters described above. Figure 2 shows the first 10 of these profiles for illustration. The balance of the profiles are of similar character.

c. Selection of Seed Time Histories and Match to the Current SSAR SSE

The horizontal hard rock SSE spectrum (9,200 ft/sec shear wave velocity) for the North Anna ESP site was established in consideration of two alternate approaches described in SSAR Section 2.5.2.6.7—a reference probability approach and a performance-based approach. The hard rock SSE horizontal spectrum shown in SSAR Figure 2.5-48 has been conservatively selected to envelop both approaches.

High frequency and low frequency spectra developed using the reference probability approach are shown in SSAR Figure 2.5-51. These spectra were developed using a mean reference probability of  $5 \times 10^{-5}$  per year and the procedure of RG 1.165.

The performance-based spectrum scales the mean  $10^{-4}$  annual probability of exceedance ground motion at any spectral frequency by a factor calculated to achieve a  $10^{-5}$  annual frequency of onset of significant inelastic deformation. This spectrum is shown in SSAR Figure 2.5-53.

The North Anna ESP site SSE spectrum has been conservatively defined to envelop, for any frequency, the high frequency reference probability spectrum, the low frequency reference probability spectrum, and the performance-based spectrum.

Both high frequency and low frequency time histories were developed for the evaluation of the effect of site-specific subsurface shear wave velocities between 9,200 ft/sec and 3,300 ft/sec control points. These time histories were made to match spectra that, in composite, matched the SSE spectrum but that, individually, are based on the high and low frequency reference probability response spectra shapes. Considering SSAR Figure 2.5-54A, for example, the low frequency time history was fit to a spectrum defined by the SSE spectrum for frequencies less than 1.5 Hz and by the  $5 \times 10^{-5}$  per year low frequency reference probability spectral values for higher frequencies. The high frequency time history was fit to a spectrum defined by the SSE spectrum for frequencies greater than 1.5 Hz and by the  $5 \times 10^{-5}$  per year high frequency reference probability spectral values for lower frequencies. A plot of the specific high and low frequency spectra that were matched is provided in Figure 3.

The average magnitude and distance ( $M\text{-bar}$  and  $D\text{-bar}$ ) values for the two scaled target spectra are given in SSAR Table 2.5-25. Based on these magnitude and distance values, two horizontal seed input time histories were selected from the database of Central and Eastern United States time histories given in NUREG/CR-6728 (Reference 9). The seed time histories selected were:

- CEUS modified San Ramon - Kodak, 180 degree horizontal component from the 1980 Livermore earthquake (high-frequency controlling earthquake) and
- CEUS modified Kashmar, Longitudinal component from the 1978 Tabas, Iran earthquake (low-frequency controlling earthquake).

Their 5%-damped response spectra were matched to the high- and low-frequency target spectra, respectively, satisfying the spectral matching criteria of NUREG/CR-6728 (Reference 9). Under these criteria, no spectral value may be either 30 percent greater or 10 percent less than the target spectrum, nor may a certain number of consecutive spectral acceleration values fall below the target spectrum. This last requirement is satisfied by scaling the spectrum-compatible time history up by a small scale factor.

Figure 4 shows the high-frequency spectrum-compatible time history that was developed, and Figure 5 shows the low-frequency spectrum-compatible time history. Figures 6 and 7 indicate the final fit of each of the high- and low-frequency time history response spectra to their respective high- and low-frequency target spectra.

d. SHAKE Analyses For Each Combination of the Two Spectrum-Compatible Time Histories and the 50 Randomized Rock Columns

A set of SHAKE2000 runs were performed on each of the 50 artificial rock profiles using the two input hard rock motions. The site was modeled by horizontal layers, each 7.5 ft thick, overlying a uniform half-space of hard bedrock subjected to the vertically propagating shear wave time histories.

The input time histories were applied on each artificial rock profile as an outcrop motion at the surface of the hard bedrock characterized with a shear wave velocity of 9,200 ft/sec. For each rock profile, 5% damping Acceleration Response Spectra (ARS) of the outcrop motion of Layers 1 and 10 of the rock column were calculated which represent the response of the site at depths of 0 ft and about 70 ft from the top of the rock (elevations 250 ft and about 180 ft). (The response at Elevation 180 ft was required for input to the revised liquefaction and slope stability analyses described later in parts g.

and h. of this response.) The level of strain of each rock profile was calculated for both input time histories to confirm that the strains in the rock strata are small enough to use strain independent stiffness and damping properties for the rock.

Maximum accelerations and acceleration time histories were computed for each rock profile using the time histories of the low and high frequency input motions. Horizontal maximum accelerations and response spectra for 5% damping were reported for the outcropping response of Layers 1 and 10 representing the seismic response of the rock strata at 0 ft and about 70 ft depth, respectively, below the Zone III-IV hypothetical rock outcrop control point. All spectra were calculated at 140 points equally-spaced in log-scale in the frequency range from 0.1 to 100 Hz (that is, in a period range of 0.01 to 10 seconds). The horizontal response spectra were calculated using a constant time step in the acceleration time history.

Log-averages of the results of all 50 artificial profiles 5% damping response spectra were calculated at each of the two elevations considered for each input time history.

Figure 8 shows the 5% critically damped acceleration response spectra obtained from the SHAKE analyses with low frequency and high frequency time histories for Layer 1. The log-average response spectra are plotted together with the individual spectra of each of the 50 rock profiles.

e. Examination of Strains Within the Randomized Rock Columns

The maximum strain of each rock layer of each rock profile was calculated with SHAKE using the time histories of the low and high frequency input motions. The mean strain profile and its standard deviation were computed for each input time history from the results of all 50 rock profiles.

The results show that the strains in the rock strata due to the input motions are small. The mean values of the maximum strain profiles do not exceed 0.29%. This confirms the use of the assumption of strain independent rock properties for the SHAKE analyses.

f. Specification of Frequency-Dependent Amplification Factors

For Layer 1, the 50 high-frequency response spectra of Figure 8 were log-averaged. To allow for this log-average spectrum to be subsequently compared to the hard rock SSE spectrum in SSAR Section 2.5.2, as detailed below, the NUREG/CR-6728 spectral matching criteria factor of 1.029 was divided back out from the log-average spectrum. Similarly, the 50 resultant low-frequency response spectra of Figure 8 were also log-averaged. To allow for this log-average spectrum to be subsequently compared to the

hard rock SSE spectrum in SSAR Section 2.5.2, the NUREG/CR-6728 factor of 1.010 was divided back out from the log-average spectrum. These two "de-scaled" spectra are shown in Figure 9 as thin jagged lines.

The response spectra coming from the SHAKE analyses were defined by a set of 140 values for frequencies from 0.1 to 100 Hz. The enveloped "de-scaled" log-average spectrum for Layer 1 was fit with a smooth fitting function using the commercial program Axum (Reference 10). Several different functional forms and powers available in Axum were tried, and a judgment was made to use a 16th-order polynomial Power fit, given in Table 3. Figure 9 shows the smooth fitting function for Layer 1 as a heavy smooth curve compared to the input 140-point layer response spectra. The resultant fitting function was used to obtain the response spectrum values for the same set of 21 frequencies (shown as open circles in Figure 9) that were used in SSAR Table 2.5-27. This 21-frequency set of response spectral ordinates defines the rock response spectrum for the corresponding Layer 1 horizon, that is, for the Zone III-IV hypothetical rock outcrop control point. Table 4 lists these values.

In order to develop the transfer functions between the hard rock SSE horizontal response spectrum given in SSAR Table 2.5-27 and Layer 1, each of the spectral values in Table 4 was divided by the corresponding spectral acceleration value in SSAR Table 2.5-27. Table 5 indicates the resulting transfer functions, defined at the same 21 frequency points considered in SSAR Section 2.5.2.

In order to define vertical response spectra for the Layer 1 horizontal rock spectra, the same set of V/H ratios used in SSAR Section 2.5.2 were applied. The ratios are a function of frequency and are simply multiplied by the corresponding horizontal response spectral value to give the corresponding vertical response spectrum. Figure 10 is a plot of both horizontal and vertical response spectra for Layer 1, that is, the Zone III-IV hypothetical rock outcrop control point. Table 6 lists the horizontal SSE spectral accelerations, V/H ratios, and vertical SSE spectral accelerations for this control point.

g. Determination of Hypothetical Rock Outcrop Motion for a Control Point at Elevation 180 Ft

The analysis described above focused on modification of the SSE spectra of SSAR Figure 2.5-48. This modification accounts for current best estimates of the shear wave velocity at the site from an idealized plant grade ground surface elevation of 271 ft to a depth at which the shear wave velocity reaches 9,200 ft/sec. Under this representation of the site subsurface, the control point at the top of the Zone III-IV material is considered to have an elevation of 250 ft, with a shear wave velocity of 3,300 ft/sec.

The analysis of material liquefaction potential and slope stability in SSAR Sections 2.5.4 and 2.5.5 used SHAKE analysis of a site rock-soil column specific to a site typical of the area occupied by the slope to the south of the existing units. For this analysis, the spectrum-compatible time histories developed to represent the high frequency and low frequency range of the horizontal SSE spectrum in SSAR Section 2.5.2 were input for Zone IV rock having the best-estimate shear wave velocity of 6,300 ft/sec. To re-evaluate the liquefaction potential and slope stability within, and at the surface of, the same rock-soil column, rock outcrop ground motions were developed where the shear wave velocity was about 6,300 ft/sec. This is at an elevation of about 180 ft using the "best-fit" line for the rock column for the control point SSE analysis described earlier. (The rock outcrop was actually taken at Elevation 182.5 ft in the SHAKE analysis.) These motions were then used as input at the base of the previously used rock-soil column. The material properties for this rock-soil column are defined in SSAR Section 2.5.4.7.1.

Horizontal response spectral values for the 180 ft elevation are given in Table 4 and shown in Figure 11 (as "Layer 10" values). Amplification factors between the 9,200 ft/sec and 6,300 ft/sec control point horizons are given in Table 5 (as "Transfer Function, Layer 10").

The spectrum-compatible time histories developed to represent the high frequency and low frequency range of the horizontal SSE spectrum in SSAR Section 2.5.2 were matched to the Layer 10 spectrum in a manner exactly analogous to the way the current SSAR SSE spectra were matched as described above.

h. Evaluations of Liquefaction Potential and Slope Stability

The SHAKE analysis was re-run using revised time histories based on the modified assumptions made in deriving the SSE as outlined immediately above. Computed peak ground surface accelerations increased by about 24% for the low frequency earthquake and 13% for the high frequency earthquake.

The liquefaction and slope stability analyses were re-run using these higher accelerations. As expected, the computed factors of safety against liquefaction and slope failure decreased. However, the decreases did not affect the conclusions about liquefaction and slope stability contained in SSAR Section 2.5.4, that is, (1) some of the Zone IIA saprolitic soils have a potential for liquefaction based on the low and high frequency ESP seismic parameters, and (2) based on the possibility of some liquefaction in the slope area and the marginal results obtained using Kramer's method, measures would be taken to ensure the safety of the slope and of the structures that may be located close to the bottom of the slope.

### References

1. Letter from Eugene S. Grecheck, Vice President-Nuclear Support Services, Dominion, to U.S. Nuclear Regulatory Commission, Document Control Desk, "Dominion Nuclear North Anna, LLC, North Anna Early Site Permit Application, Draft Safety Evaluation Report Open Item 2.5-2," February 18, 2005.
2. EPRI (2004). "CEUS Ground Motion Project Final Report," Electric Power Research Institute, Technical Report 1009684, submitted to the NRC by the January 25, 2005 Letter from Eugene S. Grecheck, Vice President-Nuclear Support Services, Dominion, to U.S. Nuclear Regulatory Commission, Document Control Desk, "Dominion Nuclear North Anna, LLC, North Anna Early Site Permit Application, Response to Draft Safety Evaluation Report Open Item 2.5-1."
3. NRC NUREG-0800, Standard Review Plan, Section 3.7.1, Seismic Design Parameters, Revision 2, August 1989
4. Letter from Eugene S. Grecheck, Vice President-Nuclear Support Services, Dominion, to U.S. Nuclear Regulatory Commission, Document Control Desk, "Dominion Nuclear North Anna, LLC, North Anna Early Site Permit Application, Responses to Draft Safety Evaluation Report Open Items," March 3, 2005.
5. Site Environmental Studies, Proposed North Anna Nuclear Power Station, Louisa County, Virginia, Virginia Electric Power Company Report (included in Units 1 and 2 PSAR as Appendix A), Dames and Moore, January 13, 1969. (Reference 7 of SSAR Section 2.5 References)
6. Weston Geophysical Research, Inc. "Velocity Measurements, North Anna Power Station, Virginia Electric and Power Company," for Stone and Webster Corporation, January 1970. (Contained as an addendum to the reply to Question 2.8 in the North Anna Units 1 & 2 PSAR Supplement Volumes.)

7. EPRI (1993). "Guidelines for Determining Design Basis Ground Motions, Vol. II: Appendices for Ground Motion Estimation," Electric Power Research Institute, TR-102293, Palo Alto, CA, November 1993.
8. Costantino, C.J. (1996). Recommendations for Uncertainty Estimates in Shear Modulus Reduction and Hysteretic Damping Relationships. Published as an appendix in Silva, W.J., N. Abrahamson, G. Toro and C. Costantino. (1997). "Description and validation of the stochastic ground motion model." Report Submitted to Brookhaven National Laboratory, Associated Universities, Inc. Upton, New York 11973, Contract No. 770573.
9. McGuire, R.K., W.J. Silva, and C.J. Costantino (2001). "Technical Basis for Revision of Regulatory Guidance on Design Ground Motions: Hazard and Risk-Consistent Ground Motion Spectra Guidelines," NUREG/CR-6728, October 2001.
10. MathSoft, Inc. (1997). "Axum 5.0C for Windows", computer program, version dated September 26, 1997.

**Table 1. Shear Wave Velocity Versus Depth for Four Boreholes.**

Depth, Ft	Shear Wave Velocity, Ft/sec				Depth, Ft	Shear Wave Velocity, Ft/sec			
	B-20	B-104	W-1	B-802		B-20	B-104	W-1	B-802
1	-	-	-	-	39	4050	4150	-	5716.2
2	-	-	-	-	40	4400	3400	-	5901.3
3	-	-	-	-	41	4750	2850	-	6086.4
4	-	-	-	-	42	5240	2650	-	6271.5
5	-	-	-	-	43	4820	2720	-	6365.8
6	-	-	-	-	44	4300	3300	-	6369.4
7	-	-	-	-	45	4020	3780	-	6373.0
8	-	-	-	-	46	3850	4100	5850	6376.6
9	-	-	-	-	47	3800	3850	5880	6380.2
10	-	-	-	-	48	3850	3800	5880	6280.9
11	-	-	-	-	49	3900	4280	5750	6078.7
12	-	-	-	-	50	4000	4900	5750	5876.5
13	-	-	-	3239.7	51	4050	5340	5900	5674.3
14	-	-	-	2849.1	52	4060	5340	6040	5472.1
15	-	-	-	2458.5	53	3950	5100	6020	5417.4
16	-	-	-	2067.9	54	3810	4700	5750	5510.2
17	-	-	-	1677.3	55	3750	4350	5500	5603.0
18	-	-	-	1861.6	56	3750	3950	4920	5695.8
19	-	-	-	2620.8	57	3850	3600	4500	5788.6
20	3100	5050	-	3380.0	58	3920	3680	4830	5844.8
21	3120	5800	-	4139.2	59	3900	3900	5290	5864.3
22	3130	5820	-	4898.4	60	3930	4200	5900	5883.8
23	3100	5300	-	5090.0	61	4050	4500	6520	5903.3
24	3040	5120	-	4714.0	62	4200	4850	6600	5922.8
25	3020	5200	-	4338.0	63	4460	4880	6420	5942.3
26	3200	5250	-	3962.0	64	4680	4790	6520	5961.8
27	3400	5200	-	3586.0	65	4740	4700	6620	5981.3
28	4350	5300	-	3509.5	66	4700	4770	6840	6000.8
29	6000	5700	-	3732.5	67	4850	5000	7020	6020.3
30	6620	5800	-	3955.5	68	4860	5300	6720	-
31	5300	5940	-	4178.5	69	4730	5220	6500	-
32	4600	5800	-	4401.5	70	4900	5140	6230	-
33	4000	5250	-	4605.6	71	5050	5000	6000	-
34	3600	4740	-	4790.9	72	5130	4830	5770	-
35	3570	4520	-	4975.8	73	4900	4750	6000	-
36	3600	4650	-	5160.9	74	4600	4830	6680	-
37	3630	5000	-	5346.0	75	4300	5100	6750	-
38	3800	4500	-	5531.1	76	4200	5350	6250	-

**Table 1. Shear Wave Velocity Versus Depth for Four Boreholes.**

Depth, Ft	Shear Wave Velocity, Ft/sec				Depth, Ft	Shear Wave Velocity, Ft/sec			
	B-20	B-104	W-1	B-802		B-20	B-104	W-1	B-802
77	4150	5550	5780	-	103	-	6700	7400	-
78	4200	5750	6000	-	104	-	7800	7430	-
79	-	5850	6430	-	105	-	7500	7470	-
80	-	5700	6860	-	106	-	7000	7500	-
81	-	5450	6560	-	107	-	6480	7700	-
82	-	5280	6520	-	108	-	6000	7680	-
83	-	5020	6660	-	109	-	5670	7650	-
84	-	4830	6650	-	110	-	5850	7500	-
85	-	4600	6800	-	111	-	6600	7200	-
86	-	4400	7000	-	112	-	7900	6850	-
87	-	4000	7060	-	113	-	8650	6300	-
88	-	3570	7040	-	114	-	8470	5980	-
89	-	3330	7010	-	115	-	8280	5980	-
90	-	3430	7050	-	116	-	8270	5890	-
91	-	3760	7210	-	117	-	8300	5800	-
92	-	4200	7460	-	118	-	8330	5900	-
93	-	4700	7440	-	119	-	7800	-	-
94	-	5200	7420	-	120	-	7050	-	-
95	-	5700	7400	-	121	-	6350	-	-
96	-	6350	7550	-	122	-	7000	-	-
97	-	6400	7500	-	123	-	7350	-	-
98	-	6950	7450	-	124	-	8200	-	-
99	-	6720	7680	-	125	-	8250	-	-
100	-	6350	7640	-	126	-	7880	-	-
101	-	6100	7600	-	127	-	7670	-	-
102	-	6150	7500	-	128	-	7750	-	-

<b>Table 2: Shear Wave Velocity from Elastic Modulus.</b>						
<b>Boring</b>	<b>Depth, Ft</b>	<b>Zone</b>	<b>E, ksi</b>	<b>Strain, %</b>	<b>G, ksi</b>	<b>V<sub>s</sub>, ft/sec</b>
B-801	49	IV	8,670	0.3	3,259	9,629
B-802	66.5	IV	4,613	0.3	1,734	7,024
B-803	71	IV	7,133	0.4	2,682	8,734
B-803	156	IV	7,173	0.4	2,697	8,758
B-804	50	IV	3,190	0.5	1,199	5,841
B-805	41.5	III-IV	336	0.8	126	1,896

**Table 3. Smooth Fitting Function Coefficients for  
Horizontal Spectral Acceleration (g).**

$$\text{Spectral Acceleration (g)} = c_0 * F^{**}[c_1 + c_2 * (\ln(F)) + c_3 * (\ln(F))^2 + c_4 * (\ln(F))^3 + c_5 * (\ln(F))^4 + c_6 * (\ln(F))^5 + c_7 * (\ln(F))^6 + c_8 * (\ln(F))^7 + c_9 * (\ln(F))^8 + c_{10} * (\ln(F))^9 + c_{11} * (\ln(F))^{10} + c_{12} * (\ln(F))^{11} + c_{13} * (\ln(F))^{12} + c_{14} * (\ln(F))^{13} + c_{15} * (\ln(F))^{14} + c_{16} * (\ln(F))^{15}]$$

where F is frequency

Coefficients	Layer 1	Layer 10
C <sub>0</sub>	6.77273E-02	6.77297E-02
C <sub>1</sub>	8.43103E-01	8.42544E-01
C <sub>2</sub>	5.71288E-01	5.68988E-01
C <sub>3</sub>	-3.58842E-02	-4.95737E-02
C <sub>4</sub>	-7.30875E-01	-7.37930E-01
C <sub>5</sub>	2.28462E-01	2.42281E-01
C <sub>6</sub>	3.69737E-01	3.76372E-01
C <sub>7</sub>	-1.62765E-01	-1.69782E-01
C <sub>8</sub>	-8.12240E-02	-8.38265E-02
C <sub>9</sub>	5.35173E-02	5.52992E-02
C <sub>10</sub>	3.32092E-03	3.71926E-03
C <sub>11</sub>	-7.97136E-03	-8.22307E-03
C <sub>12</sub>	1.38229E-03	1.36489E-03
C <sub>13</sub>	3.17926E-04	3.35538E-04
C <sub>14</sub>	-1.48631E-04	-1.49489E-04
C <sub>15</sub>	2.05928E-05	2.02092E-05
C <sub>16</sub>	-1.02359E-06	-9.83991E-07

<b>Frequency</b>	<b>Sa(g), Layer 1</b>	<b>Sa(g), Layer 10</b>
100	0.555	0.447
50	1.195	0.982
30	1.470	1.169
25	1.476	1.150
20	1.446	1.113
10	0.945	0.818
8	0.717	0.654
6	0.481	0.460
5	0.376	0.365
4	0.287	0.282
3	0.214	0.211
2.5	0.179	0.177
2	0.142	0.141
1	0.0677	0.0677
0.8	0.0576	0.0577
0.6	0.0488	0.0489
0.5	0.0429	0.0430
0.4	0.0343	0.0343
0.3	0.0233	0.0233
0.2	0.01298	0.01299
0.1	0.00382	0.00382

<b>Table 5. Selected Horizontal SSE Amplitudes and Transfer Functions for Layers 1 and 10.</b>			
<b>Frequency, Hz</b>	<b>Horizontal SSE Response Spectrum in SSAR Section 2.5.2</b>	<b>Transfer Function, Layer 1</b>	<b>Transfer Function, Layer 10</b>
100	0.374	1.483	1.196
50	0.780	1.532	1.259
30	0.924	1.591	1.265
25	0.930	1.588	1.237
20	0.869	1.664	1.282
10	0.578	1.635	1.416
8	0.499	1.436	1.310
6	0.405	1.189	1.136
5	0.351	1.073	1.041
4	0.266	1.080	1.060
3	0.200	1.065	1.052
2.5	0.175	1.021	1.012
2	0.145	0.982	0.977
1	0.0651	1.041	1.041
0.8	0.0581	0.993	0.993
0.6	0.0498	0.981	0.982
0.5	0.0450	0.954	0.955
0.4	0.0337	1.018	1.019
0.3	0.0229	1.015	1.015
0.2	0.0129	1.009	1.009
0.1	0.00412	0.927	0.926

<b>Table 6. Selected Zone III-IV Control Point Horizontal SSE Amplitudes, V/H Ratios from Reference 9, and Resulting Vertical SSE Amplitudes.</b>			
<b>Frequency, Hz</b>	<b>Selected Horizontal SSE Amplitudes, g</b>	<b>V/H Ratio</b>	<b>Selected Vertical SSE Amplitudes, g</b>
100	0.555	1.00	0.555
50	1.195	1.12	1.33
30	1.470	0.94	1.38
25	1.476	0.88	1.29
20	1.446	0.83	1.20
10	0.945	0.75	0.708
8	0.717	0.75	0.537
6	0.481	0.75	0.360
5	0.376	0.75	0.282
4	0.287	0.75	0.215
3	0.214	0.75	0.160
2.5	0.179	0.75	0.134
2	0.142	0.75	0.106
1	0.0677	0.75	0.0507
0.8	0.0576	0.75	0.0432
0.6	0.0488	0.75	0.0366
0.5	0.0429	0.75	0.0321
0.4	0.0343	0.75	0.0257
0.3	0.0233	0.75	0.0174
0.2	0.01298	0.75	0.00973
0.1	0.00382	0.75	0.00286

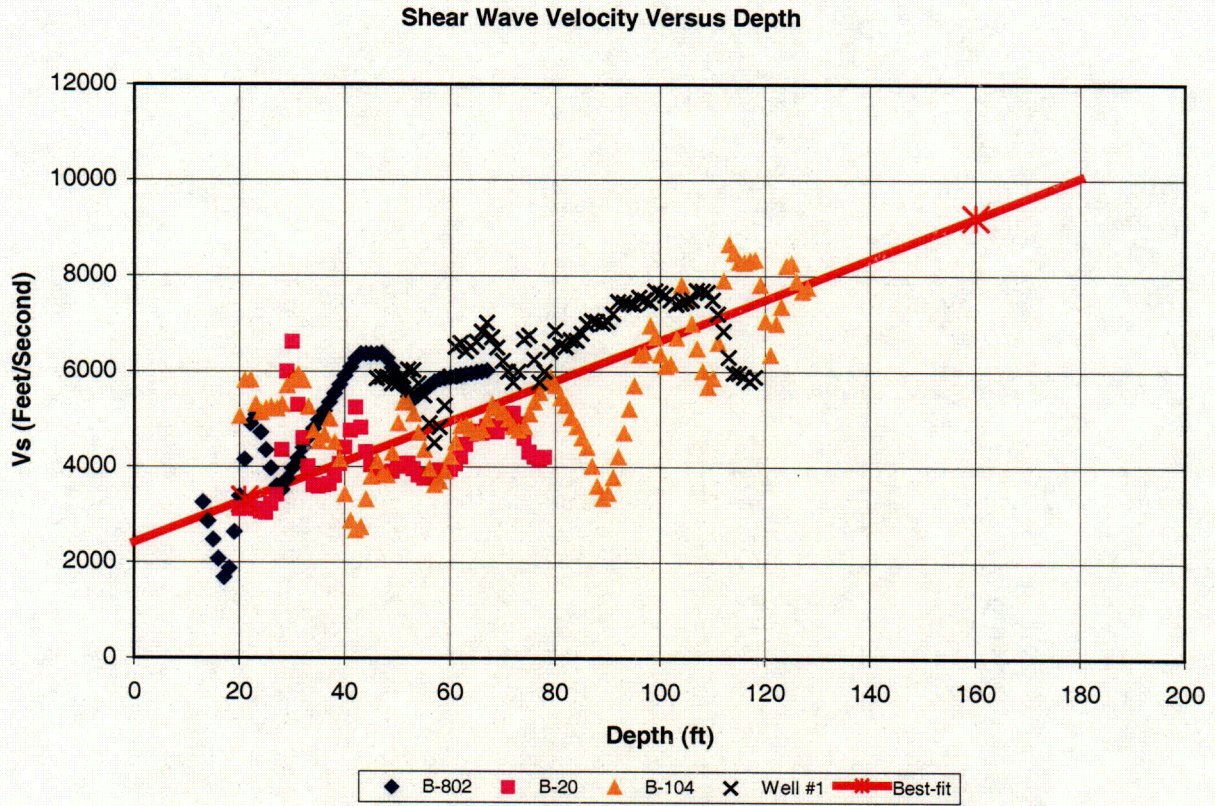
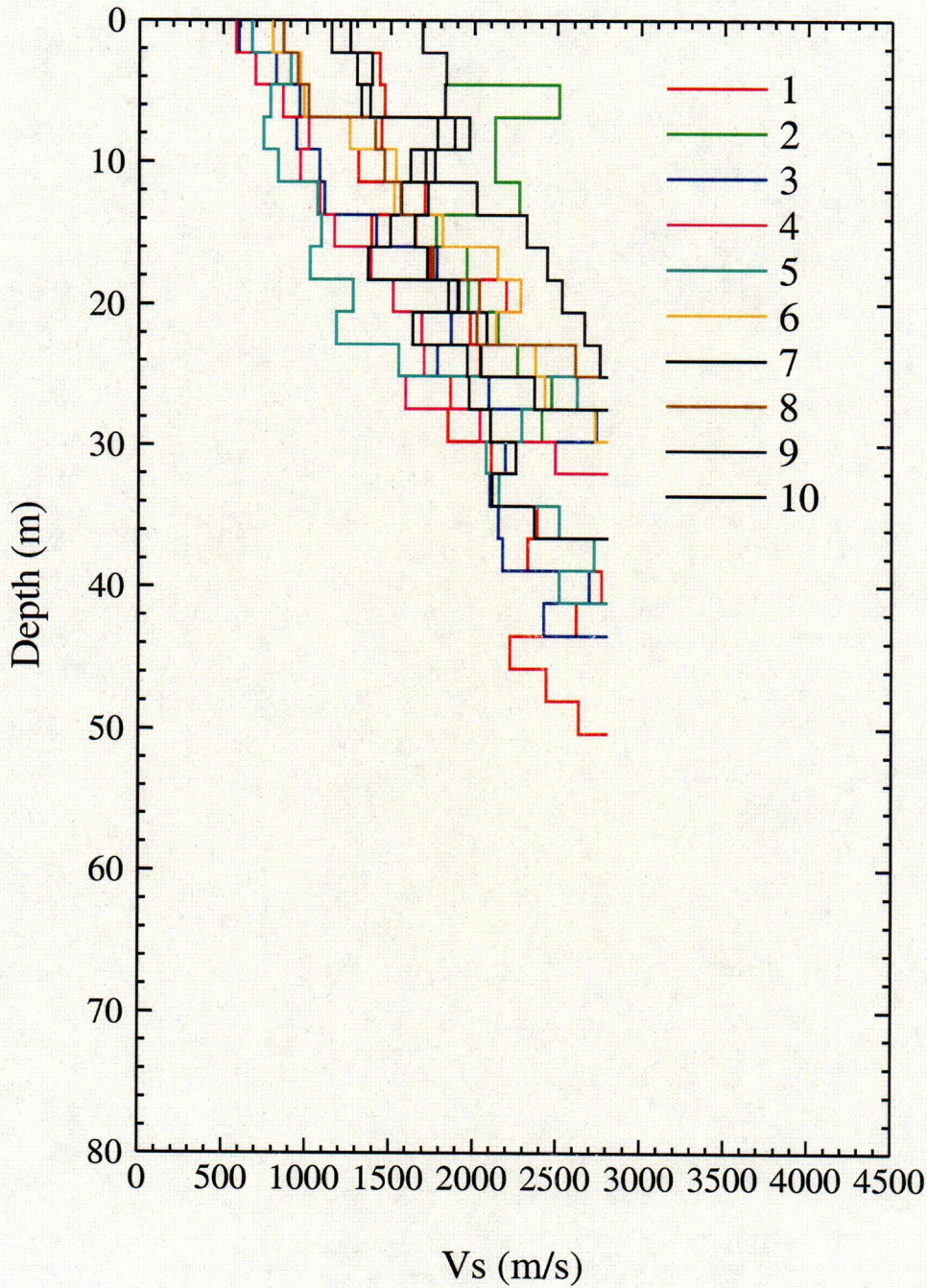


Figure 1. Shear wave data and "best fit" line.



**Figure 2.** Examples of North Anna randomized shear wave velocity profiles. Depth is depth below the hypothetical outcrop horizon at Elevation 250 ft (depth of 21 feet in Figure 1.)

Horizontal Spectra

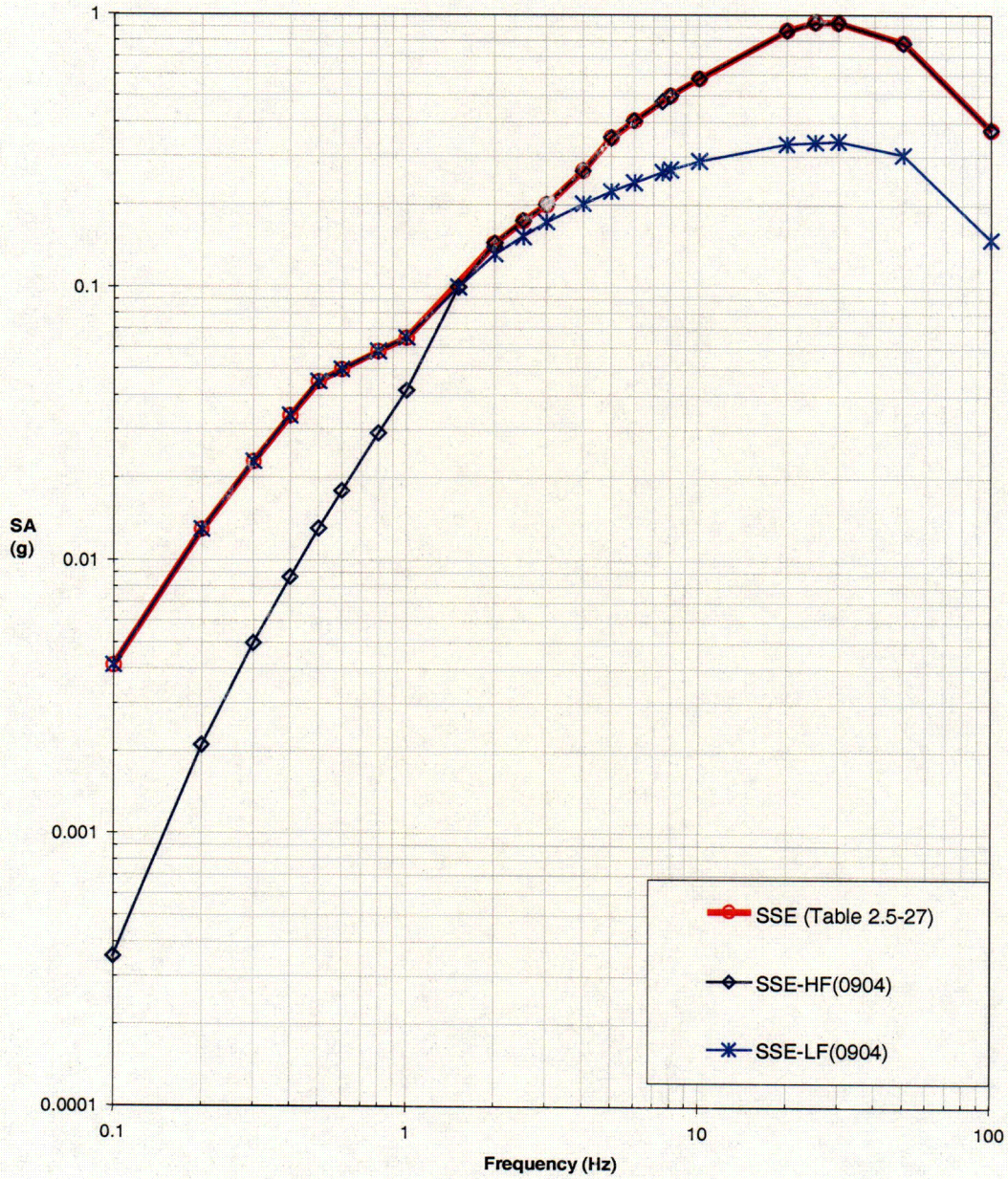


Figure 3. The horizontal SSAR Section 2.5.2 SSE spectrum partitioned to be represented by separate high- and low-frequency spectra, that envelope to comprise the SSE spectrum.

SSE0904 High Frequency: B-KOD180, Run7 scaled by 1.029

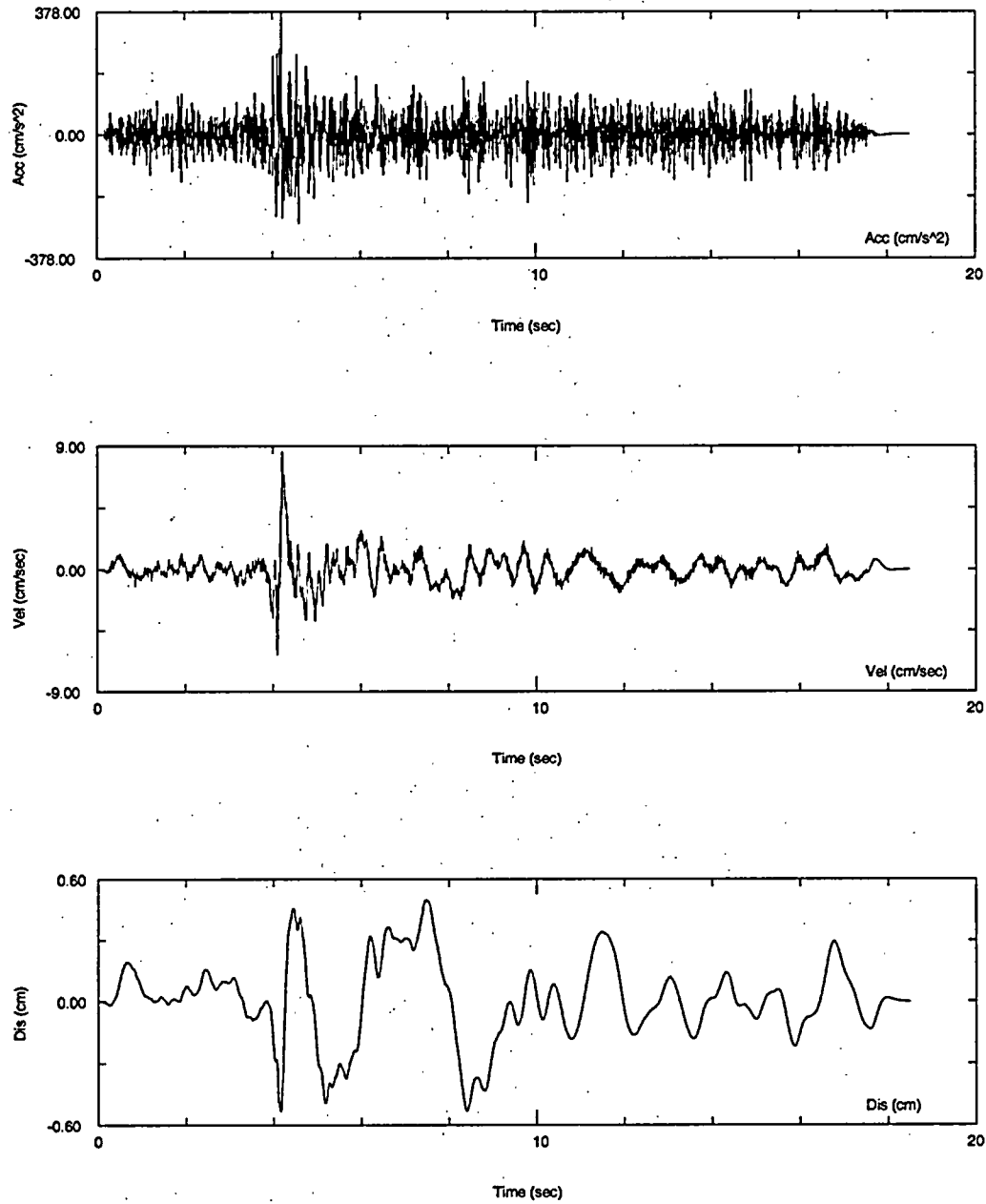


Figure 4. Time history developed to be spectrum-compatible with the high-frequency target spectrum (see Figure 3).

SSE0904 Low Frequency: KSH-L1, Run7 scaled by 1.010

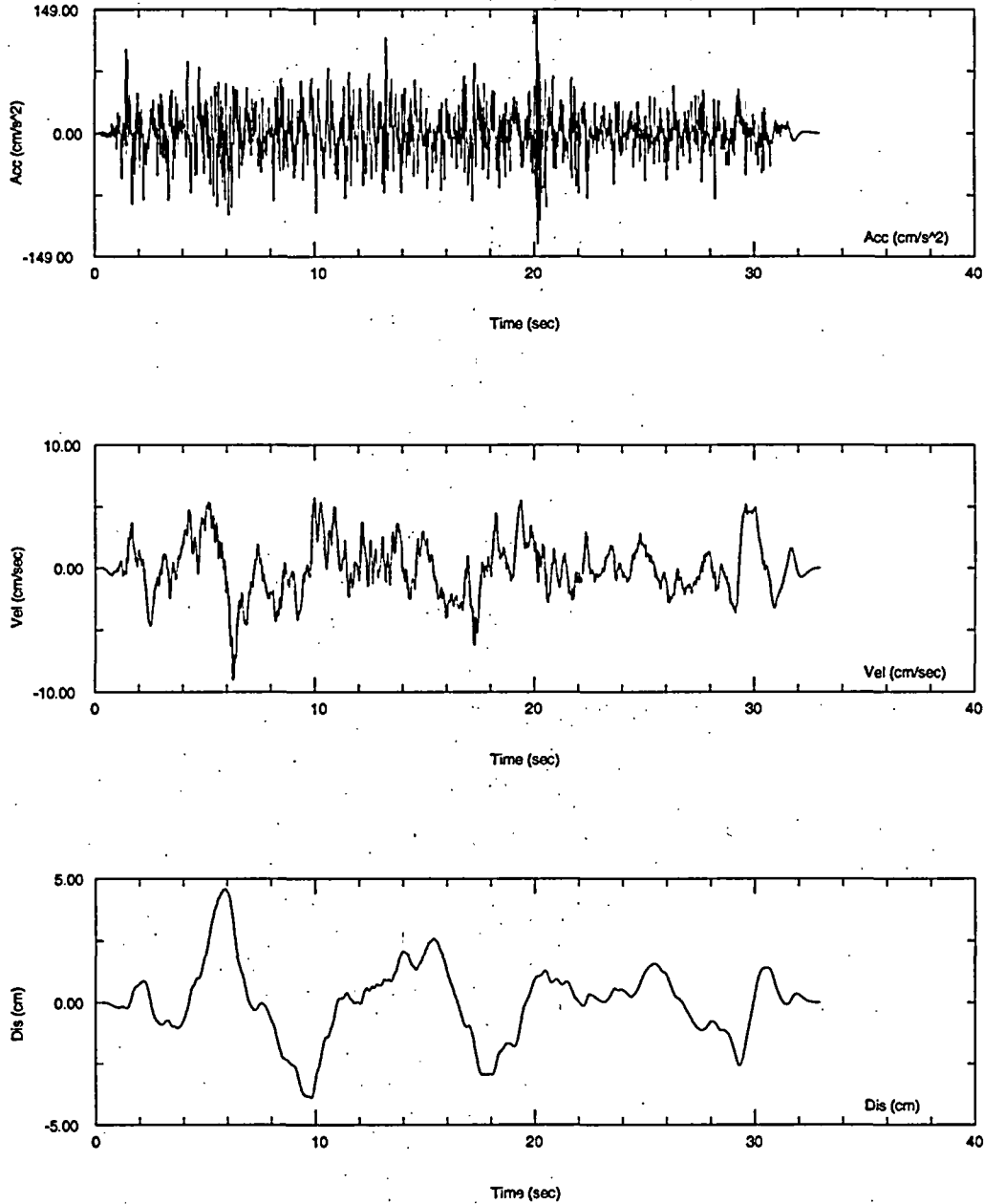
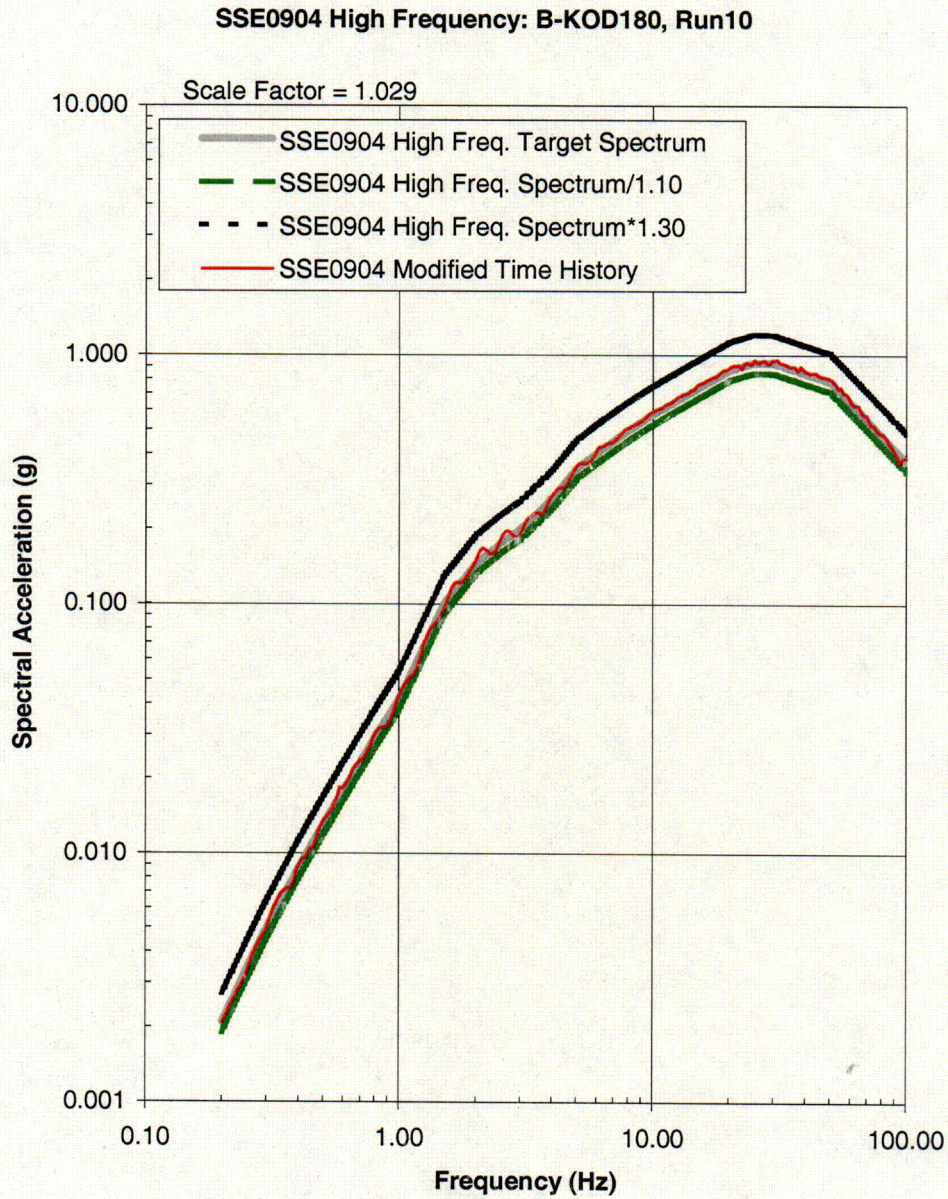
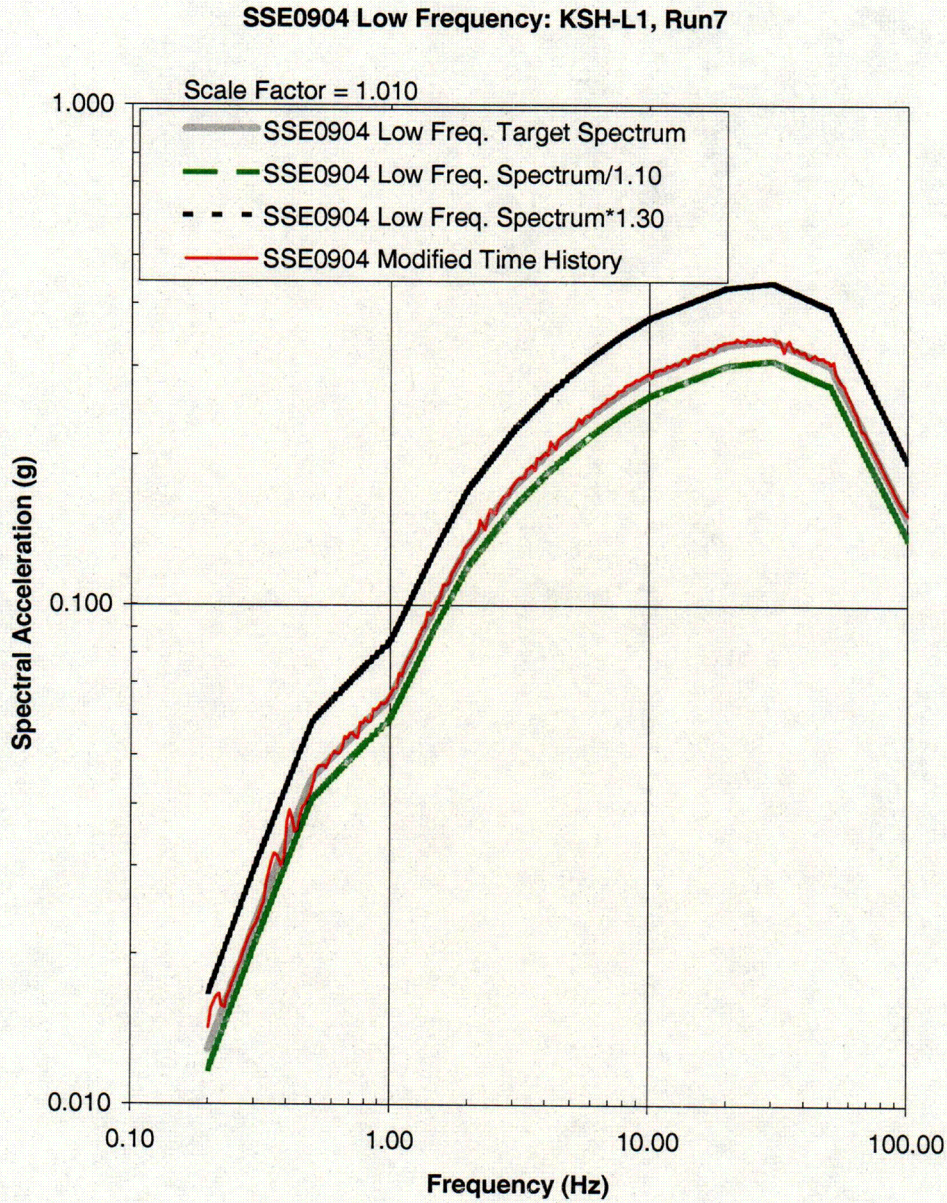


Figure 5. Time history developed to be spectrum-compatible with the low-frequency target spectrum (see Figure 3).



**Figure 6.** Comparison between the final scaled spectrum-compatible time history (thin red line) and the high frequency target spectra (heavy gray line). The upper (black) and lower (green) spectra bound the time history spectrum per NUREG/CR-6728 (Reference 9) criteria.

C15



**Figure 7.** Comparison between the final scaled spectrum-compatible time history (thin red line) and the low frequency target spectra (heavy gray line). The upper (black) and lower (green) spectra bound the time history spectrum per NUREG/CR-6728 (Reference 9) criteria.

016

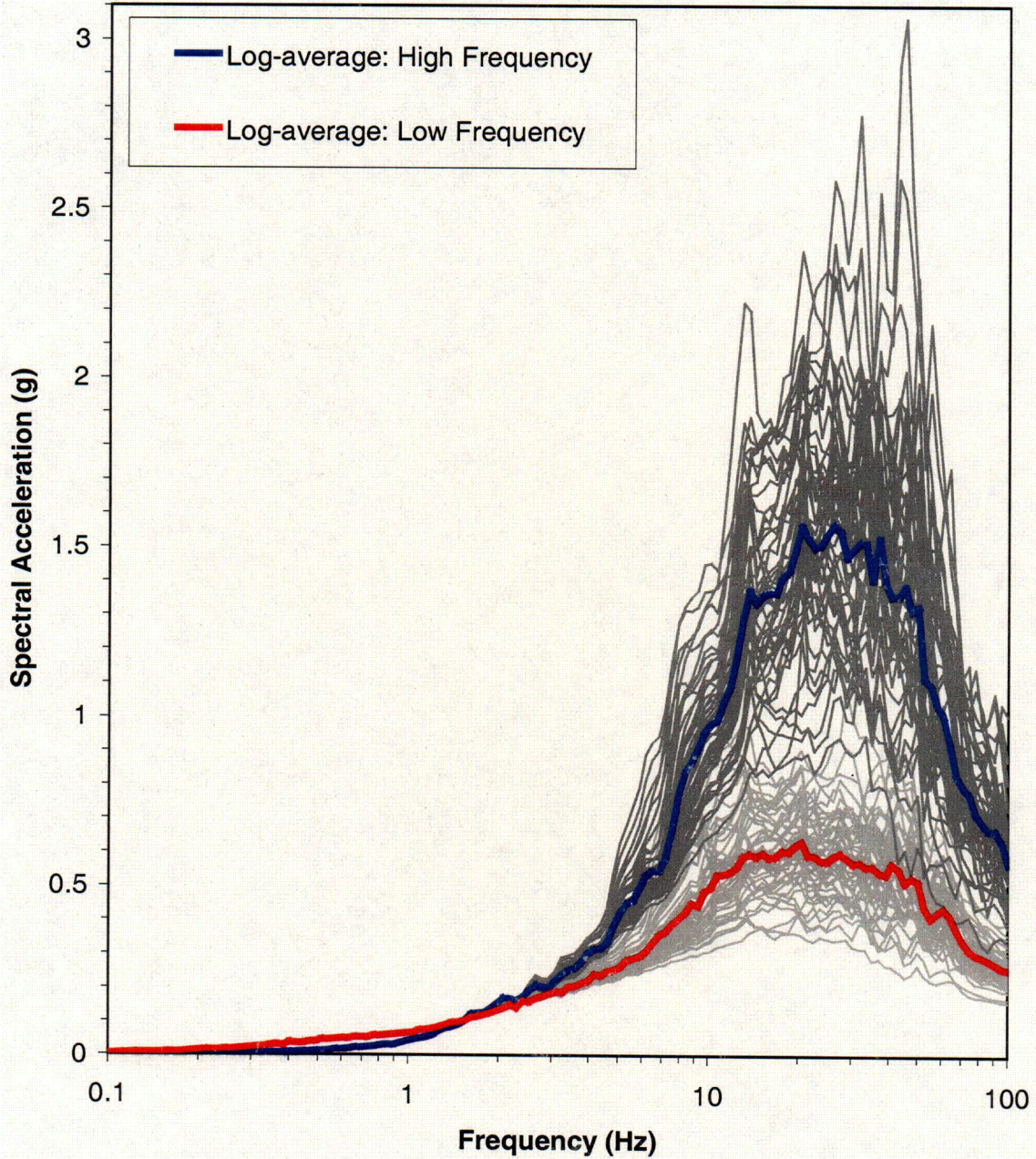


Figure 8. Response Zone III-IV control point (Elevation 250 ft., Layer 1) – 5% Critical Damping ARS – High Frequency [upper dark gray group] and Low Frequency [lower light gray group] time histories. Log-average of each set of 50 response spectra for the high and low frequency time histories indicated by the heavy blue and red lines, respectively.

C17

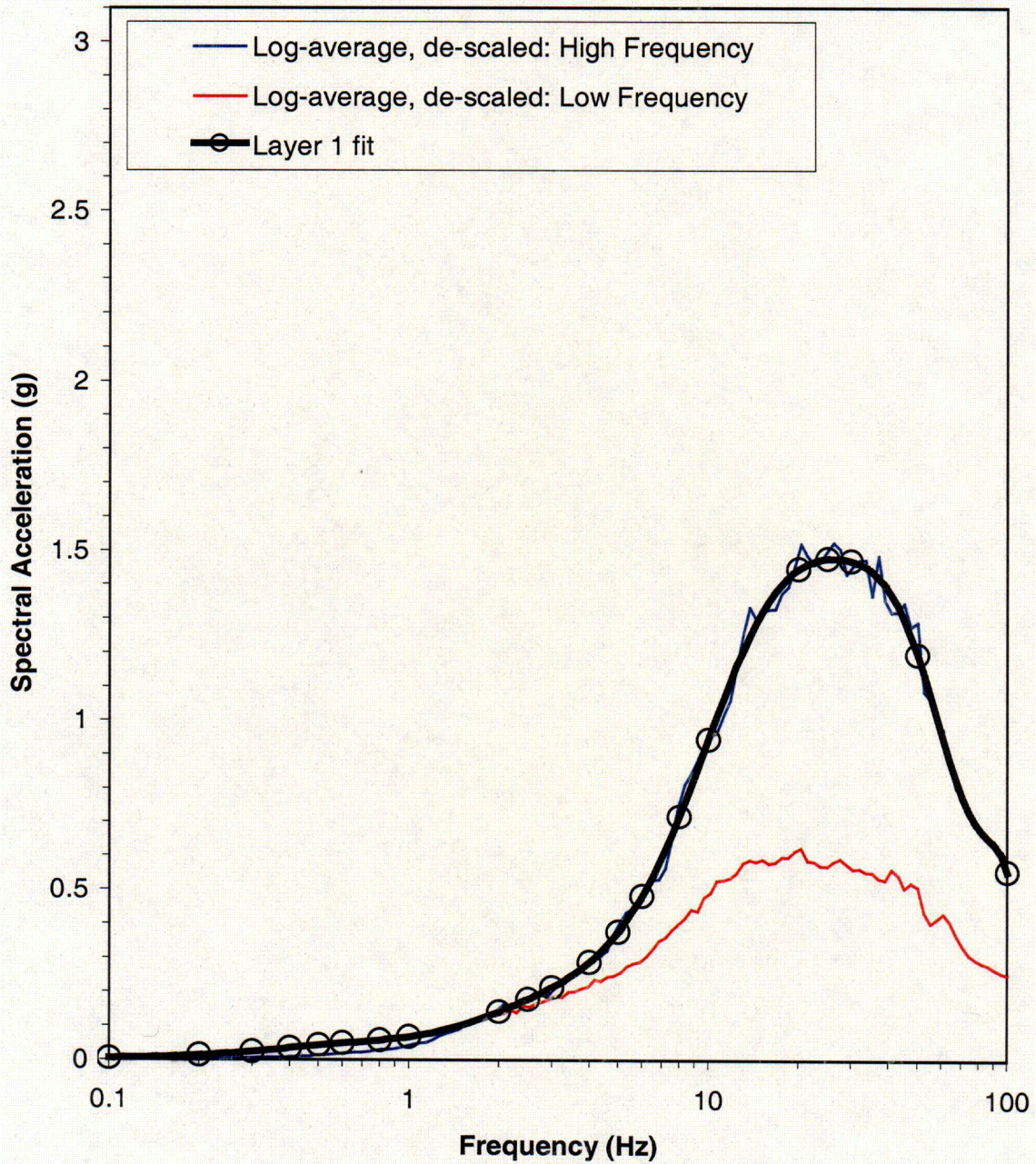


Figure 9. Smooth function fit [solid black line] to the envelope of the de-scaled high- and low-frequency log-average response spectra (Figure 8). Open circles indicate the set of 21 values that define the Zone III-IV control point SSE spectrum.

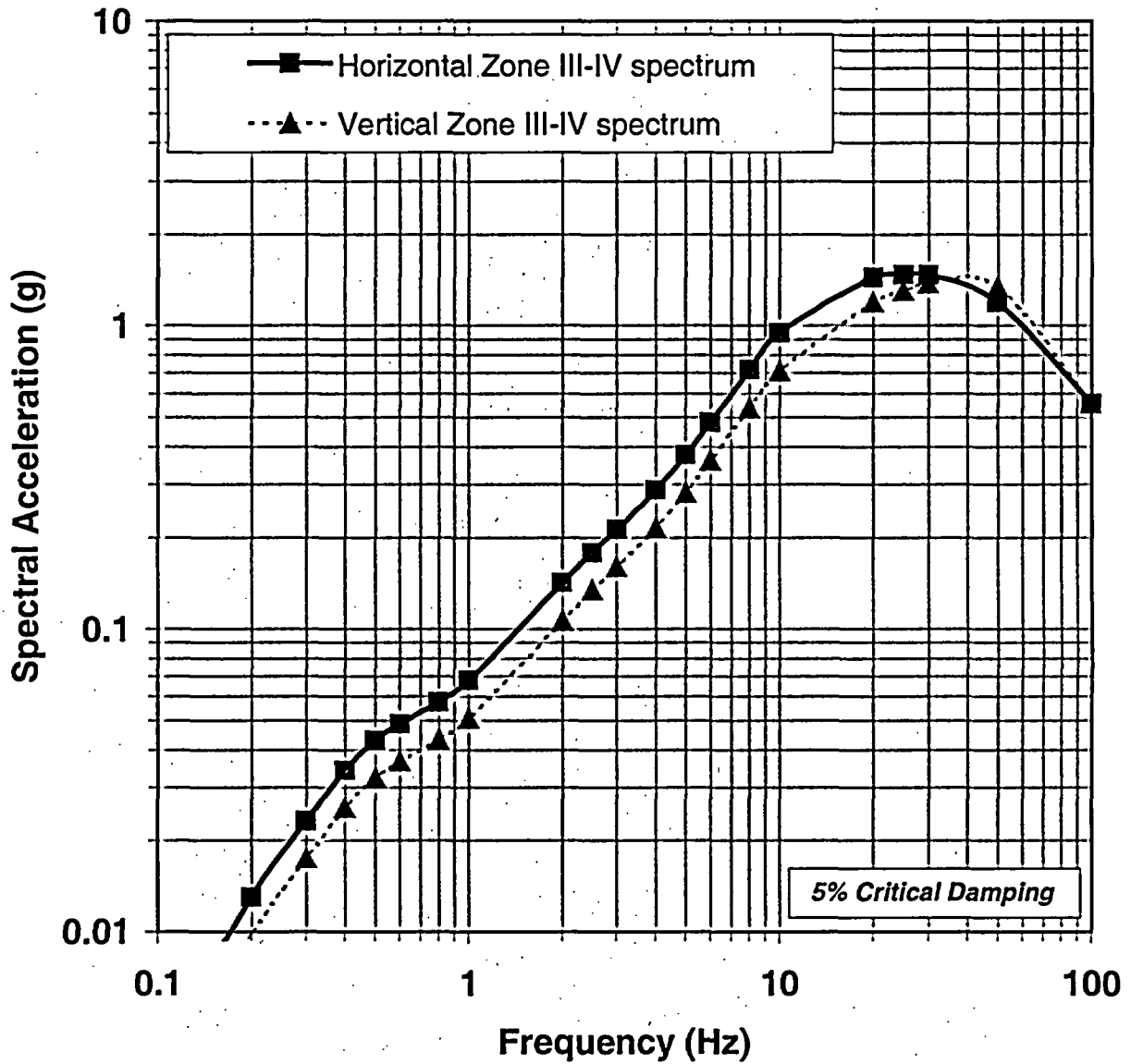


Figure 10. Selected horizontal and vertical response spectra for the hypothetical rock outcrop control point SSE at the top of Zone III-IV material (representative Elevation 250 ft, 3300 ft/sec shear wave velocity).

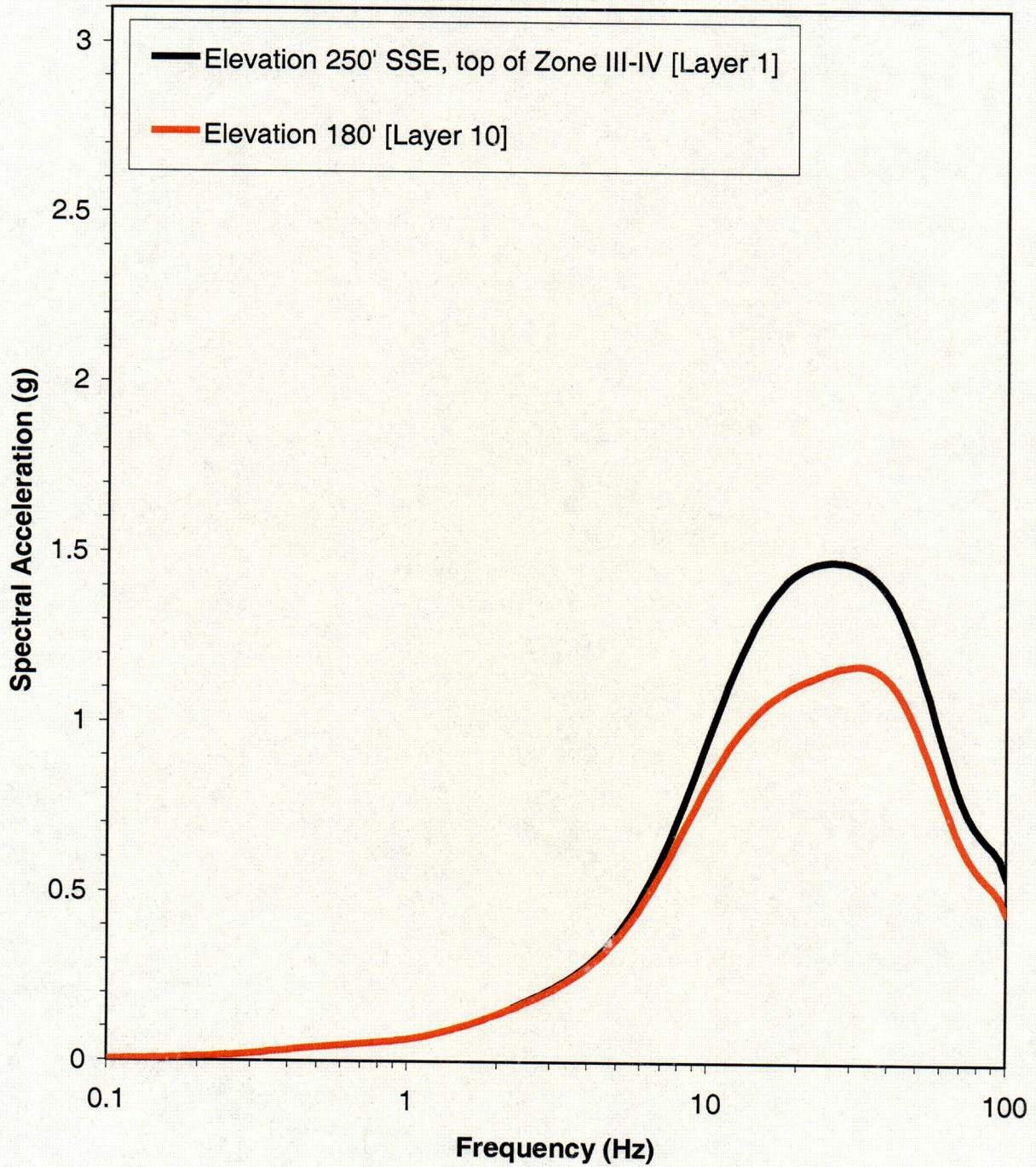


Figure 11. Smooth function fits to the envelopes of the de-scaled high- and low-frequency log-average response spectra) for Layers 1 and 10.

### **Application Revision**

The last paragraph of SSAR Section 2.5.2.5 will be revised to read as follows:

The seismic wave transmission characteristics of the site materials are described in Section 2.5.4.7. The description includes the shear wave velocity profile for the site and the variation of shear modulus and damping with strain for Zone II and III materials. As discussed in Section 2.5.4.7, Zone III-IV and IV rock materials behave elastically. Both generic and specific shear wave velocity profiles are described. The generic profile extends from plant grade at an elevation of 271 ft to depths at which the bedrock under the site is estimated to reach a velocity of about 9,200 ft/s. This generic profile is used to evaluate amplification of the 9,200 ft/s hard rock SSE ground motion to the top of competent rock, selected to be at the top of the Zone III-IV material (representative elevation of 250 ft), with a best-estimate shear wave velocity of about 3,300 ft/sec. A location-specific profile, differing from the generic profile in its uppermost 70 ft, is used to evaluate liquefaction potential and slope stability at a site typical of the area occupied by the slope to the south of the existing units. Sections 2.5.2.6 and 2.5.4.7 describe the site-specific acceleration-time history developed for the hard rock SSE and the results of rock and soil column amplification/attenuation analyses.

The first sentence of SSAR Section 2.5.2.6.7 will be revised to read as follows:

Figure 2.5-48 shows the hard rock (9,200 ft/sec control point) horizontal and vertical SSE ground motion spectra selected for the North Anna ESP site.

The first sentence of SSAR Section 2.5.2.6.7 c., Selection of Enveloping Horizontal SSE Spectrum, will be revised to read as follows:

Figure 2.5-54A shows four horizontal ground spectra—the mean  $5 \times 10^{-5}$  return period RG 1.165 high- and low-frequency scaled spectra (from Figure 2.5-51), the performance-based spectrum (from Figure 2.5-53), and the selected hard rock SSE spectrum (previously shown in Figure 2.5-48), which is the envelope of the other three spectra.

The last paragraph of SSAR Section 2.5.2.6.7 c. will be deleted and replaced with the following new paragraphs:

The spectra shown in Figures 2.5-48, Figure 2.5-51, Figure 2.5-53, Figure 2.5-54A, and Figure 2.5-54B represent scaled free-field hard rock control point ground motion spectra (9,200 ft/sec shear wave velocity) for 5 percent of critical damping. Figure 2.5-54B(1) shows the high-frequency spectrum-compatible

time history that was developed, and Figure 2.5-54B(2) shows the low-frequency spectrum-compatible time history. These spectra and time histories do not include any effects such as structure, embedment, or incoherence of seismic waves due to base mat size. Such effects would have to be determined on a design-specific basis as part of detailed engineering, and their effect would be to modify the selected SSE spectra shown in Figure 2.5-48 for appropriate design levels of SSCs of that specific design.

Section 2.5.4.7 describes currently available subsurface shear wave velocity and related material property information for the site. Based on the actual location of new units, additional subsurface information would be obtained during detailed engineering and described in the COL application, and would include borings to greater depths at these locations. Based on the currently available data, a generic site velocity profile has been developed. This best-estimate profile has been used to estimate the amplification of the 9,200-ft/sec hard rock ESP site SSE ground motion at a control point located on the top of competent Zone III-IV rock. As identified in Table 2.5-45, the shear wave velocities for the Zone III-IV material range from 2,500 to 4,500 ft/sec, with a best estimate wave velocity of 3,300 ft/sec. A shear wave velocity of 3,300 ft/sec has been used in the control point SSE analysis. The elevation of the top surface of the Zone III-IV material varies across the site, as shown in Figures 2.5-57 and 2.5-58. The top of the Zone III-IV material has been chosen to be at a representative elevation of 250 ft in the control point SSE analysis.

Both high frequency and low frequency time histories were developed for the evaluation of the effect of site-specific subsurface shear wave velocities between the 9,200 ft/sec and 3,300 ft/sec control points. These time histories were made to match spectra that, in composite, matched the SSE spectrum but that, individually, are based on the high and low frequency reference probability response spectra shapes. Considering Figure 2.5-54A, for example, the low frequency time history was fit to a spectrum defined by the SSE spectrum for frequencies less than 1.5 Hz and by the  $5 \times 10^{-5}$  per year low frequency reference probability spectral values for higher frequencies. The high frequency time history was fit to a spectrum defined by the SSE spectrum for frequencies greater than 1.5 Hz and by the  $5 \times 10^{-5}$  per year high frequency reference probability spectral values for lower frequencies.

The average magnitude and distance (M-bar and D-bar) values for the two scaled target spectra are given in Table 2.5-25. Based on these magnitude and distance values, two horizontal seed input time histories were selected from the database of Central and Eastern United States time histories given in Reference 171. The seed time histories selected were:

- CEUS modified San Ramon - Kodak, 180 degree horizontal component from the 1980 Livermore earthquake (high-frequency controlling earthquake) and
- CEUS modified Kashmar, Longitudinal component from the 1978 Tabas, Iran earthquake (low-frequency controlling earthquake).

Their 5%-damped response spectra were matched to the high- and low-frequency target spectra, respectively, satisfying the spectral matching criteria of Reference 171.

A stochastic model described in Reference 170, with some modifications to account for the conditions at the ESP site, was used to generate 50 randomizations of the generic ESP site rock column velocity profile between elevations with shear wave velocities of 9,200 ft/sec and 3,300 ft/sec. In addition to the site-specific material property characterizations outlined in Section 2.5.4.7, generic guidance about the correlation between shear wave velocity and its uncertainty as a function of depth and depth-wise correlation structure of the  $\ln(V_s)$  (the natural logarithm of the shear wave velocity) residuals from Reference 170, and uncertainty in damping consistent with the variability observed in Reference 197, were adopted. Finally, damping was taken as the same for all sub-layers within any given profile (that is, fully correlated between layers), but was allowed to vary between one artificial rock column and the next.

A set of SHAKE2000 runs were performed on each of the 50 artificial rock profiles using the two input hard rock motions. The site was modeled by horizontal layers, each 7.5 ft thick, overlying a uniform half-space of hard bedrock subjected to the vertically propagating shear wave time histories. The response spectra from the SHAKE analyses were defined at 140 frequencies from 0.1 to 100 Hz. The enveloped log-average spectrum for the Zone III-IV hypothetical rock outcrop control point at elevation 250 ft and shear wave velocity of 3,300 ft/sec was fit with a smooth fitting function. See Figure 2.5-54B(3). The resultant fitting function was used to obtain the response spectrum for the same set of 21 frequencies. This 21-frequency set of response spectral ordinates defines the rock response spectrum for the corresponding hypothetical rock outcrop control point on the top of Zone III-IV material. This spectrum is shown in Figure 2.5-48A.

SSAR Section 2.5.2.6.7 d., Development of Vertical SSE Spectra, will be revised to read as follows:

The applicable V/H ratios used to develop the selected vertical hard rock SSE spectrum (5 percent of critical damping) are listed in Table 2.5-27. The horizontal SSE spectral accelerations, V/H ratios, and vertical SSE spectral accelerations for the Zone III-IV hypothetical rock outcrop control point are listed in Table 2.5-27A. The vertical SSE spectra are calculated by multiplying the selected horizontal SSE spectral amplitude at each frequency by the applicable V/H ratio for that frequency. The selected horizontal and vertical spectra are plotted in Figure 2.5-48 for the hard rock SSE and in Figure 2.5-48A for the Zone III-IV hypothetical rock outcrop control point SSE.

SSAR Section 2.5.2.7 will be revised to read as follows:

A detailed analysis was not undertaken to establish the OBE ground motion. Rather, the simple decision was used to establish the OBE spectrum as one-third of the SSE spectrum in accordance with 10 CFR 50, Appendix S. Figure 2.5-55 plots the hard rock OBE spectra and the selected hard rock SSE spectra from Figure 2.5-48. Figure 2.5-55A plots the OBE spectra and the SSE spectra from Figure 2.5-48A for the control point SSE analysis at the top of Zone III-IV material. These spectra are based on 5 percent critical damping, as are all other spectra presented in Section 2.5.2.

The first and second paragraphs of SSAR Section 2.5.4.7.1 will be revised to read as follows:

Various measurements were made at the ESP site to obtain estimates of the shear wave velocity in the soil and rock. These are summarized in Section 2.5.4.4. The materials of interest here are the Zone IIA and Zone IIB saprolitic soils, the Zone III weathered rock, and the Zone III-IV slightly to moderately weathered rock.

In some locations, the top of Zone III-IV or Zone IV bedrock is found close to or even above planned plant grade. (This applies to most locations along the east-west subsurface profile in Figure 2.5-57.) In such cases, safety-related structures would be founded on bedrock or on a thin layer of lean concrete or compacted structural fill on the bedrock. In other locations, sound bedrock is relatively deep. (This applies to the northern and southern portions of the north-south subsurface profile in Figure 2.5-58.) In this case, some safety-related structures (excluding the reactors) may be founded on the Zone III weathered rock, Zone IIB saprolite, or Zone IIA saprolite. The shear wave velocity profiles shown on Figure 2.5-62

focus on this latter situation. Note that Figure 2.5-62 shows the top of Zone III-IV or Zone IV rock at 55 feet depth, i.e., there is 55 feet of weathered rock and soil above the competent rock. This 55-foot thick soil and weathered rock profile is typical of the area occupied by the slope to the south of the existing units. This slope is analyzed in Section 2.5.5. The soil thickness is generally greater in this profile than within the plant parameter envelope (PPE), where the best estimate of thickness, based on plant grade of El. 271 feet, is 21 feet. (This is referred to in Section 2.5.2.5 as the generic profile and is briefly described in the next paragraph.) The 55-foot profile will provide more seismic amplification than the thinner soil profile within the PPE, resulting in higher acceleration values and a correspondingly more conservative liquefaction analysis. In the soil column amplification/attenuation analysis in Section 2.5.4.7.4, the top of the Zone III-IV rock is assumed to be at 55-foot depth, and the top of the Zone IV rock is at 70-foot depth.

The generic profile extends from plant grade at an elevation of 271 ft to depths at which the bedrock under the site is estimated to reach a velocity of about 9,200 ft/sec. This generic profile is used in Section 2.5.2.6.7 to evaluate amplification of the 9,200 ft/s hard rock ESP site SSE ground motion to the top of competent rock within Zone III-IV, with a shear wave velocity of about 3,300 ft/sec, at an elevation of 250 ft.

The second to last paragraph and the first sentence of the last paragraph of SSAR Section 2.5.4.7.1 will be revised to read as follows:

As noted above, Zone III-IV is assumed to extend from 55 to 70 feet depth. Shear wave velocity for this rock is 3,300 ft/sec, derived from several values measured in the down-hole seismic test performed adjacent to boring B-802, and from elastic modulus values from unconfined compression tests (Section 2.5.4.2.5). The shear wave velocity of the Zone IV rock at 70 feet depth is taken as 6,300 fps, the best estimate value from Table 2.5-45.

The shear wave velocity design profiles shown in Figure 2.5-62, Profile (b), plus the shear wave velocity of the Zone III-IV rock from 55 to 70 feet depth is used in the seismic amplification/attenuation analysis.

SSAR Section 2.5.4.7.3 will be revised to read as follows:

Two single horizontal-component acceleration time histories were developed to be spectrum-compatible for use in the rock column amplification analysis of Section 2.5.2.6.7 and the soil column amplification analysis described in Section 2.5.4.7.4. These time histories represent the high frequency and low frequency range of the horizontal hard rock SSE spectrum of Figure 2.5-48. These two time histories are described in Section 2.5.2.6.7.

The first paragraph of SSAR Section 2.5.4.7.4 will be revised to read as follows:

The SHAKE2000 computer program was used to compute the site dynamic responses for the soil and rock profiles described in Section 2.5.4.7.1. The computation was performed in the frequency domain using the complex response method. The analysis used the acceleration-time histories described in Section 2.5.4.7.3. For the low frequency case, an earthquake with moment magnitude of 7.2 and an acceleration at bedrock level of 0.21g was used in the SHAKE2000 analysis, while for the high frequency case, an earthquake with moment magnitude of 5.4 and an acceleration at bedrock level of 0.43g was used.

The last paragraph of SSAR Section 2.5.4.7.4 will be revised to read as follows:

The zero period acceleration (ZPA) results for the SHAKE2000 analysis for the four soil profiles listed at the end of Section 2.5.4.7.1 are shown in Table 2.5-46 for both the low frequency and high frequency cases, with  $V_s$  values based on the best estimate shear wave velocity values given in Table 2.5-45. Values of  $G_{max}$  (proportional to the square of  $V_s$ ) were varied in the SHAKE analysis to determine the impact on the ZPA, using  $G_{max}$  values that were 67 percent and 150 percent of the best estimate  $G_{max}$  values derived from the  $V_s$  values in Table 2.5-46. For Profile 1, which is used in the liquefaction and slope stability analysis, the ZPA at the ground surface increased from 0.46g in Table 2.5-46 for the low frequency case to 0.57g using 150 percent  $G_{max}$ . For the high frequency case, the ZPA at the ground surface increased from 0.91g in Table 2.5-46 to 0.99g using 150 percent  $G_{max}$ . The ZPA results for Profile 1 using 150 percent  $G_{max}$  are also shown in Table 2.5-46. The 0.57g and 0.99g values were used for the peak ground acceleration in the liquefaction and slope stability analyses.

The second paragraph of SSAR Section 2.5.4.8.2 will be revised to read as follows:

The SSE at rock for the existing units has a maximum acceleration of 0.12g. This was amplified to 0.18g in the soil. The seismic margin maximum acceleration in soil (Reference 174) was 0.30g. The maximum ESP acceleration (using the high frequency earthquake) at Zone IV bedrock with a shear wave velocity of about 6,300 ft/sec is 0.43g, amplified at the unimproved soil surface to 0.99g, as discussed in Section 2.5.4.7.4 and shown in Table 2.5-46.

SSAR Section 2.5.4.8.4, parts a., b., and c., will be revised to read as follows:

a. Magnitude and Acceleration Values for ESP Liquefaction Analyses

As noted in Section 2.5.4.7.3, two earthquakes were used in the liquefaction analysis. The low frequency earthquake had a magnitude of 7.2 and an acceleration at Zone IV bedrock with a shear wave velocity of about 6,300 ft/sec of 0.21g. The high frequency earthquake had a magnitude of 5.4 and an acceleration at the same depth of 0.43g.

Table 2.5-46 shows the zero period acceleration values for the four soil/rock profiles described in Section 2.5.4.7.1. Since the Zone IIB saprolite and the Zone III weathered rock are non-liquefiable, Profiles 2 and 3 in Table 2.5-46 are not considered in the liquefaction analysis. In Profile 4, the Zone IIA saprolite is improved, i.e., this would be the profile for any safety-related structures founded on the Zone IIA saprolite. The soil would be improved sufficiently to ensure that the improved soil had a factor of safety against liquefaction equal to or greater than 1.1 (Section 2.5.4.8.2), at the SSE ground motion. In Profile 1, the Zone IIA saprolite (upper 30 feet) is not improved. Thus, Profile 1 is the only profile that is considered in the liquefaction analysis. As noted in Section 2.5.4.7.4, the ZPA at the ground surface increased from 0.46g to 0.57g for the low frequency case, and 0.91g to 0.99g for the high frequency case using 150 percent  $G_{max}$  (Table 2.5-46). The 0.57g and 0.99g values are used for the peak ground acceleration for the liquefaction analyses described in the following paragraphs.

b. Updated Seismic Margin Assessment

The seismic margin assessment described in Section 2.5.4.8.3 for the main plant area was modified in the ESP evaluation, maintaining the same assumptions as used in the original study but substituting the ESP design accelerations and moment magnitudes in soil of 0.57g and 7.2 (low frequency), and 0.99g and 5.4 (high frequency). Magnitude scaling factors of 1.13 and 2.5 were used in the analysis for the low and high frequency earthquakes, respectively. The resulting

FS values ranged from about 0.55 to 1.7, with average values generally close to but lower than 1.1.

c. Analysis of ESP Samples and CPT Results

Liquefaction analysis of each sample of Zone IIA saprolite obtained by SPT sampling during the ESP subsurface investigation was performed to determine the FS against liquefaction. The CPT results were also analyzed. The analysis conservatively ignored the age, overconsolidation, and mineralogy/fabric effects of the saprolite. Cohesive samples and/or samples above the groundwater table were considered non-susceptible to liquefaction.

The analysis followed the method proposed by Youd, et al. (Reference 178). This state-of-the-art liquefaction methodology is based on the evolution of the Seed and Idriss "Simplified Procedure" over the past 25 years. Magnitude scaling factors of 1.13 and 2.5 were used in the analysis for the moment magnitude 7.2 (low frequency) and 5.4 (high frequency) earthquakes, respectively. The  $K_s$  factor for high overburden pressures was incorporated into the analysis, using a relative density of 60 percent.

Using the peak ground accelerations and magnitude scaling factors for the low and high frequency earthquakes described above, the analysis of the SPT results gave FS values against liquefaction greater than 1.1 for those samples that were liquefiable, except for 3 samples. For the eight CPTs performed, the liquefaction analysis showed 5-foot thick zones in two CPTs and a 22-foot thick zone in another CPT where the FS against liquefaction was less than 1.1.

SSAR Section 2.5.4.8.5, bullets 5, 6, and 7, will be revised to read as follows:

- A seismic margin liquefaction analysis of the main plant area, modified to use the ESP seismic parameters ( $M = 7.2$  with 0.57g peak ground acceleration for low frequency and  $M = 5.4$  with 0.99g peak ground acceleration for high frequency), and ignored structure, fabric, and mineralogy effects, gave average FS values that were generally close to, but lower than, 1.1.
- A state-of-the-art liquefaction analysis of the ESP SPT samples using the low and high frequency ESP seismic parameters gave FS values greater than 1.1 for all except three SPT results analyzed.
- A state-of-the-art liquefaction analysis of the ESP CPT measurements using the low and high frequency ESP seismic parameters indicated an approximately 22-

foot thick zone and two 5-foot thick zones where the FS against liquefaction was less than 1.1.

The last paragraph of SSAR Section 2.5.5.2.3, part a., will be revised to read as follows:

The input to the analysis and the results are shown in Figure 2.5-69. The computed factor of safety is about 1.75. This value is above the minimum 1.5 factor of safety required.

The second paragraph of SSAR Section 2.5.5.2.3, part b., will be revised to read as follows:

The pseudo-static analysis was run using SLOPE/W. For the high frequency earthquake, the peak horizontal acceleration used was 0.65g. This is the average peak acceleration in the top 55 feet of unimproved soil shown in Table 2.5-46 for 150 percent  $G_{max}$ . (The maximum horizontal acceleration is 0.99g at the ground surface.) The vertical acceleration used was 0.325g. The computed factor of safety was significantly less than the required 1.1. For the low frequency earthquake, the equivalent peak horizontal acceleration used was 0.26g with a vertical acceleration of 0.13g. The computed factor of safety was slightly less than 1.1.

The fourth and fifth paragraphs of SSAR Section 2.5.5.2.3, part b., will be replaced with the following four new paragraphs:

The liquefaction analysis of the Zone IIA saprolite indicated some of the material has a potential for liquefaction. However, its age, fabric and interlocking angular grain structure, along with the significant portion of low plasticity clay minerals present in the material, have been demonstrated to give the grain structure a low susceptibility to pore pressure build-up or liquefaction (Section 2.5.4.8). This material would not lose a significant proportion of its shear strength during shaking. Thus, for the low frequency earthquake, with a design Magnitude  $M = 7.2$ , the pseudo-static analysis should be limited to a horizontal acceleration of only 0.15g.

Although the 0.99g computed peak ground acceleration from the high frequency earthquake at North Anna is greater than the 0.75g referenced by Seed, the highest accelerations are in the top 5 feet of the soil – the average acceleration in the soil is closer to 0.62g below the top 5 feet. In addition, the design high frequency earthquake has a relatively low energy (Magnitude 5.4), which is significant when estimating its potential impact on slope stability. Thus, at North

Anna, a pseudo-static design using an inertia force of 0.1g will be adequate for the high frequency earthquake.

The pseudo-static analysis was again run using SLOPE/W. This time the horizontal accelerations used were 0.1g and 0.15g, with zero vertical acceleration. The computed factors of safety were greater than 1.1. The input to the analysis and the results for the 0.1g case are shown in Figure 2.5-70.

Other researchers have also recommended substantially reducing the peak acceleration when applying the pseudo-static analysis. Kramer (Reference 188) recommends using an acceleration of 50 percent of the peak acceleration. Using the average peak acceleration for the high frequency earthquake in the top 55 feet of 0.65g, the horizontal input using Kramer's recommendation would be 0.325g and the vertical input would be 0.1625g. This level of input provides a factor of safety against slope failure just above 0.9. Although this is somewhat less than the required factor of safety of 1.1, it is considered marginal based on the high level of seismic acceleration being applied and the relatively low energy level of the design earthquake. For the low frequency earthquake, where the average peak acceleration in the top 55 feet is about 0.26g, the horizontal input using Kramer's recommendations would be 0.13g and the vertical input would be about 0.065g. This results in a factor of safety of greater than the required 1.1.

The following new reference will be added to SSAR Section 2.5 References:

197. Costantino, C.J. (1996). Recommendations for Uncertainty Estimates in Shear Modulus Reduction and Hysteretic Damping Relationships. Published as an appendix in Silva, W.J., N. Abrahamson, G. Toro and C. Costantino. (1997). "Description and validation of the stochastic ground motion model." Report Submitted to Brookhaven National Laboratory, Associated Universities, Inc. Upton, New York 11973, Contract No. 770573.

New SSAR Table 2.5-27A will be added as follows:

**Table 2.5-27A      Selected Zone III-IV Control Point Horizontal SSE Amplitudes, V/H Ratios from Reference 171, and Resulting Vertical SSE Amplitudes**

<b>Frequency, Hz</b>	<b>Selected Horizontal SSE Amplitudes, g</b>	<b>V/H Ratio</b>	<b>Selected Vertical SSE Amplitudes, g</b>
100	0.555	1.00	0.555
50	1.195	1.12	1.33
30	1.470	0.94	1.38
25	1.476	0.88	1.29
20	1.446	0.83	1.20
10	0.945	0.75	0.708
8	0.717	0.75	0.537
6	0.481	0.75	0.360
5	0.376	0.75	0.282
4	0.287	0.75	0.215
3	0.214	0.75	0.160
2.5	0.179	0.75	0.134
2	0.142	0.75	0.106
1	0.0677	0.75	0.0507
0.8	0.0576	0.75	0.0432
0.6	0.0488	0.75	0.0366
0.5	0.0429	0.75	0.0321
0.4	0.0343	0.75	0.0257
0.3	0.0233	0.75	0.0174
0.2	0.01298	0.75	0.00973
0.1	0.00382	0.75	0.00286

The shear and compression wave velocity descriptions in SSAR Table 2.5-45 will be revised to read as follows:

Stratum	IIA		IIB	III	III-IV	IV
	Coarse-grained	Fine-grained	Saprolite w/10 to 50% Core Stone	Moderately to Highly Weathered Quartz Gneiss w/Biotite	Slightly to Moderately Weathered Quartz Gneiss w/Biotite	Fresh to Slightly Weathered Quartz Gneiss w/Biotite
Description	Saprolite	Saprolite				
<b>Shear and compression wave velocity</b>						
Shear wave velocity range, ft/sec	600 to 1350		No range available	1500 to 2500	2500 to 4500	4000 to 8000
Shear wave velocity best estimate, ft/sec	950		1600	2000	3300	6300
Compression wave velocity best estimate, ft/sec	2100		3500	4500	7400	14,000

SSAR Table 2.5-46 will be replaced with the following new table:

**Table 2.5-46 ZPA Results from SHAKE Analysis**

Depth, ft	V <sub>s</sub> , ft/sec	Profile 1		Profile 2	Profile 3	V <sub>s</sub> , ft/sec	Profile 4
		G <sub>max</sub>	150% G <sub>max</sub>				
<b>Low Frequency Case</b>							
0.0	700	0.458g	0.567g	- a	-	1275	0.415g
2.5	700	0.394g	0.503g	-	-	1275	0.396g
5.0	700	0.328g	0.357g	-	-	1275	0.338g
7.5	700	0.314g	0.329g	-	-	1275	0.247g
10.0	700/950	0.255g	0.283g	-	-	1275/1380	0.245g
12.5	950	0.286g	0.268g	-	-	1380	0.239g
15.0	950	0.272g	0.273g	-	-	1380	0.224g
17.5	950	0.323g	0.228g	-	-	1380	0.212g
20.0	950/1200	0.300g	0.269g	-	-	1380/1500	0.199g
22.5	1200	0.265g	0.294g	-	-	1500	0.205g
25.0	1200	0.310g	0.281g	-	-	1500	0.239g
27.5	1200	0.302g	0.252g	-	-	1500	0.241g
30.0	1200/1600	0.219g	0.268g	0.463g	-	1500/1600	0.275g
35.0	1600	0.223g	0.286g	0.361g	-	1600	0.300g
40.0	1600/2000	0.229g	0.185g	0.359g	0.393g	1600/2000	0.224g
45.0	2000	0.223g	0.180g	0.335g	0.353g	2000	0.232g
50.0	2000	0.180g	0.164g	0.301g	0.250g	2000	0.193g
55.0	2000/3300	0.181g	0.162g	0.212g	0.213g	2000/3300	0.174g
60.0	3300	0.175g	0.158g	0.184g	0.227g	3300	0.169g
65.0	3300	0.157g	0.159g	0.171g	0.229g	3300	0.171g
70.0	3300	0.151g	0.158g	0.151g	0.214g	3300	0.163g
Outcrop	6300	0.213g	0.213g	0.213g	0.213g	6300	0.213g
<b>High Frequency Case</b>							
0.0	700	0.906g	0.989g	- a	-	1275	0.918g
2.5	700	0.792g	0.860g	-	-	1275	0.872g
5.0	700	0.612g	0.752g	-	-	1275	0.748g
7.5	700	0.654g	0.669g	-	-	1275	0.698g
10.0	700/950	0.703g	0.810g	-	-	1275/1380	0.605g
12.5	950	0.698g	0.762g	-	-	1380	0.474g
15.0	950	0.632g	0.776g	-	-	1380	0.486g
17.5	950	0.627g	0.753g	-	-	1380	0.557g

**Table 2.5-46 ZPA Results from SHAKE Analysis**

Depth, ft	V <sub>s</sub> , ft/sec	Profile 1		Profile 2	Profile 3	V <sub>s</sub> , ft/sec	Profile 4
		G <sub>max</sub>	150% G <sub>max</sub>				
20.0	950/1200	0.558g	0.744g	-	-	1380/1500	0.619g
22.5	1200	0.511g	0.834g	-	-	1500	0.648g
25.0	1200	0.590g	0.826g	-	-	1500	0.695g
27.5	1200	0.658g	0.722g	-	-	1500	0.726g
30.0	1200/1600	0.630g	0.607g	1.034g	-	1500/1600	0.667g
35.0	1600	0.674g	0.532g	0.902g	-	1600	0.746g
40.0	1600/2000	0.652g	0.535g	0.680g	0.989g	1600/2000	0.506g
45.0	2000	0.535g	0.493g	0.572g	0.853g	2000	0.428g
50.0	2000	0.425g	0.416g	0.498g	0.542g	2000	0.389g
55.0	2000/3300	0.321g	0.435g	0.411g	0.414g	2000/3300	0.346g
60.0	3300	0.312g	0.423g	0.400g	0.371g	3300	0.336g
65.0	3300	0.291g	0.384g	0.378g	0.358g	3300	0.303g
70.0	3300	0.286g	0.366g	0.451g	0.339g	3300	0.343g
Outcrop	6300	0.431g	0.431g	0.431g	0.431g	6300	0.431g

a. Dash denotes soil not present.

The titles of the following SSAR figures will be revised to read as follows:

- Figure 2.5-48 Selected Horizontal and Vertical Hard Rock SSE Spectra for the North Anna ESP Site
- Figure 2.5-51 Low-Frequency, High-Frequency, and Envelope Horizontal Hard Rock SSE Spectra for RG 1.165 Reference Probability Approach Using  $5 \times 10^{-5}$
- Figure 2.5-53 Performance-Based Horizontal Hard Rock SSE Spectrum, and Mean  $10^{-4}$  Horizontal Uniform Hazard Spectrum
- Figure 2.5-54A Comparison of Performance-Based Spectrum, Mean  $5 \times 10^{-5}$  Scaled Spectra, and Selected Hard Rock SSE Spectrum (Which Envelops the Other Three)
- Figure 2.5-54B Comparison of Mean  $5 \times 10^{-5}$  RG 1.165 Envelope, 1989 EPRI (Reference 115), 1989 LLNL (Extrapolated from Reference 129), and Selected Hard Rock SSE Spectra

New SSAR Figures 2.5-48A, 2.5-54B(1), 2.5-54B(2), 2.5-54B(3), and 2.5-55A will be added as shown on the following pages.

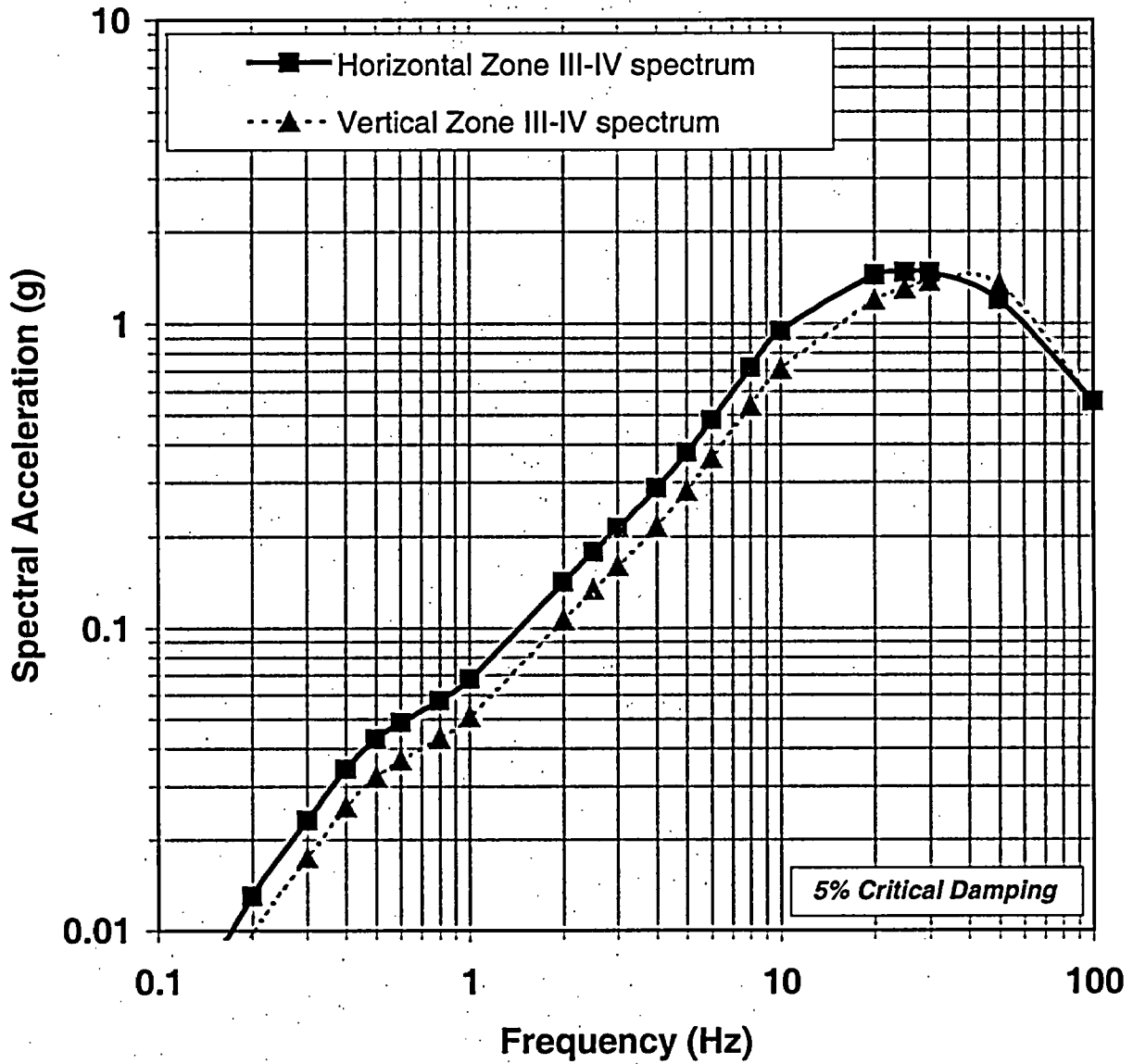
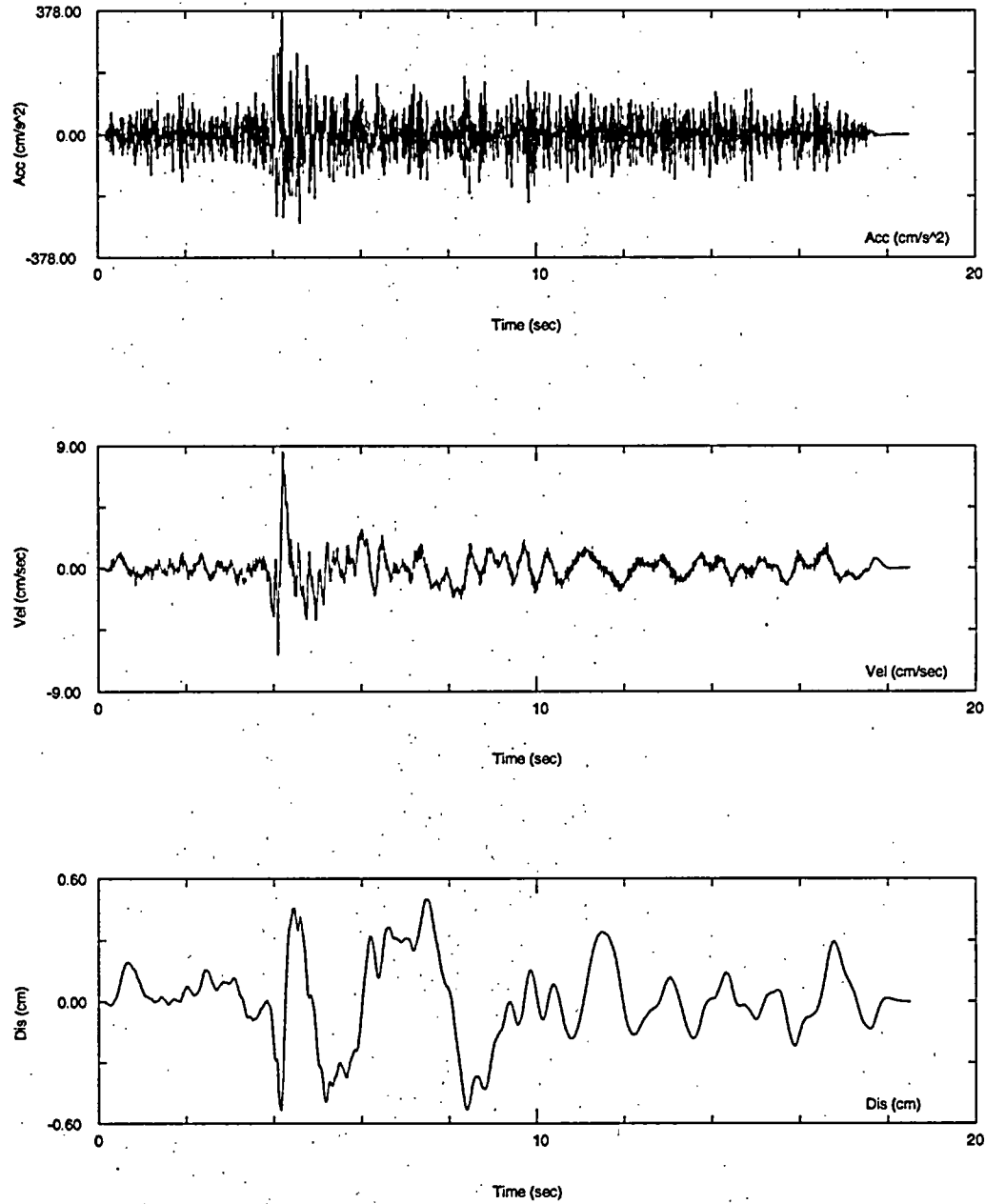
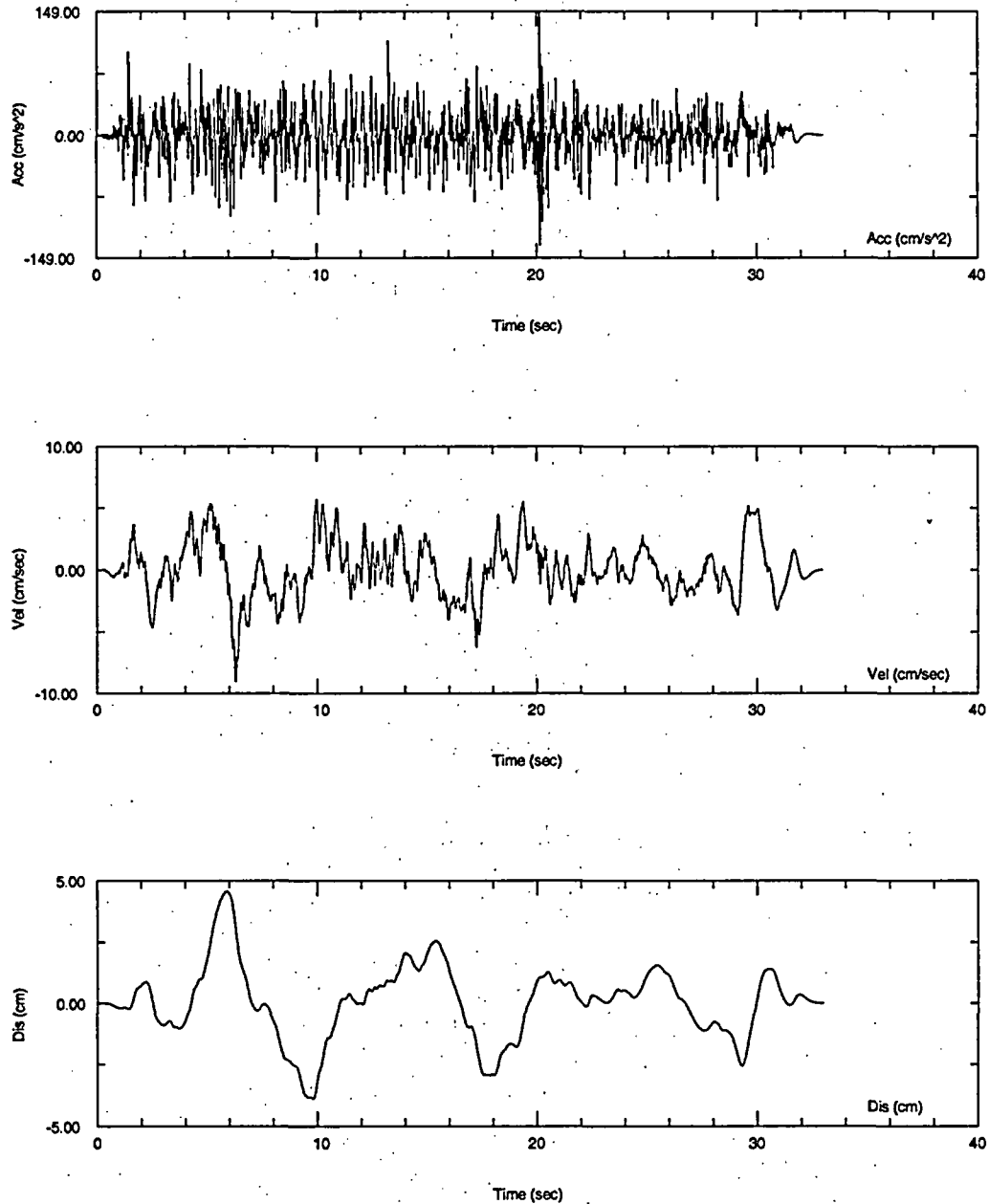


Figure 2.5-48A Selected Horizontal and Vertical Response Spectra for the Hypothetical Rock Outcrop Control Point SSE at the Top of Zone III-IV Material (Representative Elevation 250 ft, 3300 ft/sec Shear Wave Velocity)



**Figure 2.5-54B(1) Time History Developed to be Spectrum-Compatible with the High-Frequency Target Spectrum for the Hard Rock SSE**



**Figure 2.5-54B(2) Time History Developed to be Spectrum-Compatible with the Low-Frequency Target Spectrum for the Hard Rock SSE**

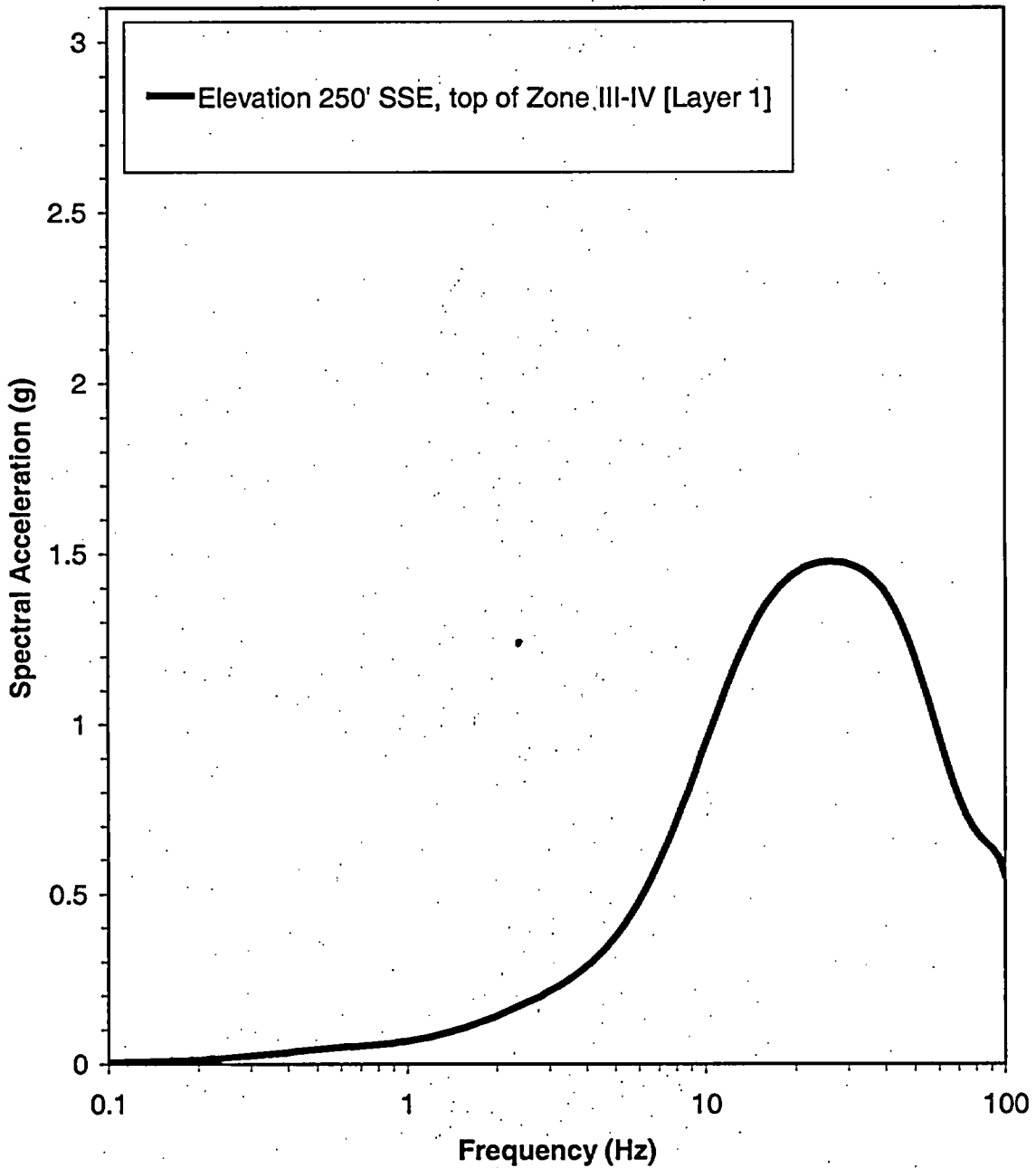


**Figure 2.5-54B(3) Smooth Fitting Function Through the SHAKE Analysis Response Spectrum Results for the Hypothetical Rock Outcrop Control Point at the Top of Zone III-IV Material (Representative Elevation 250 ft, 3300 ft/sec Shear Wave Velocity)**

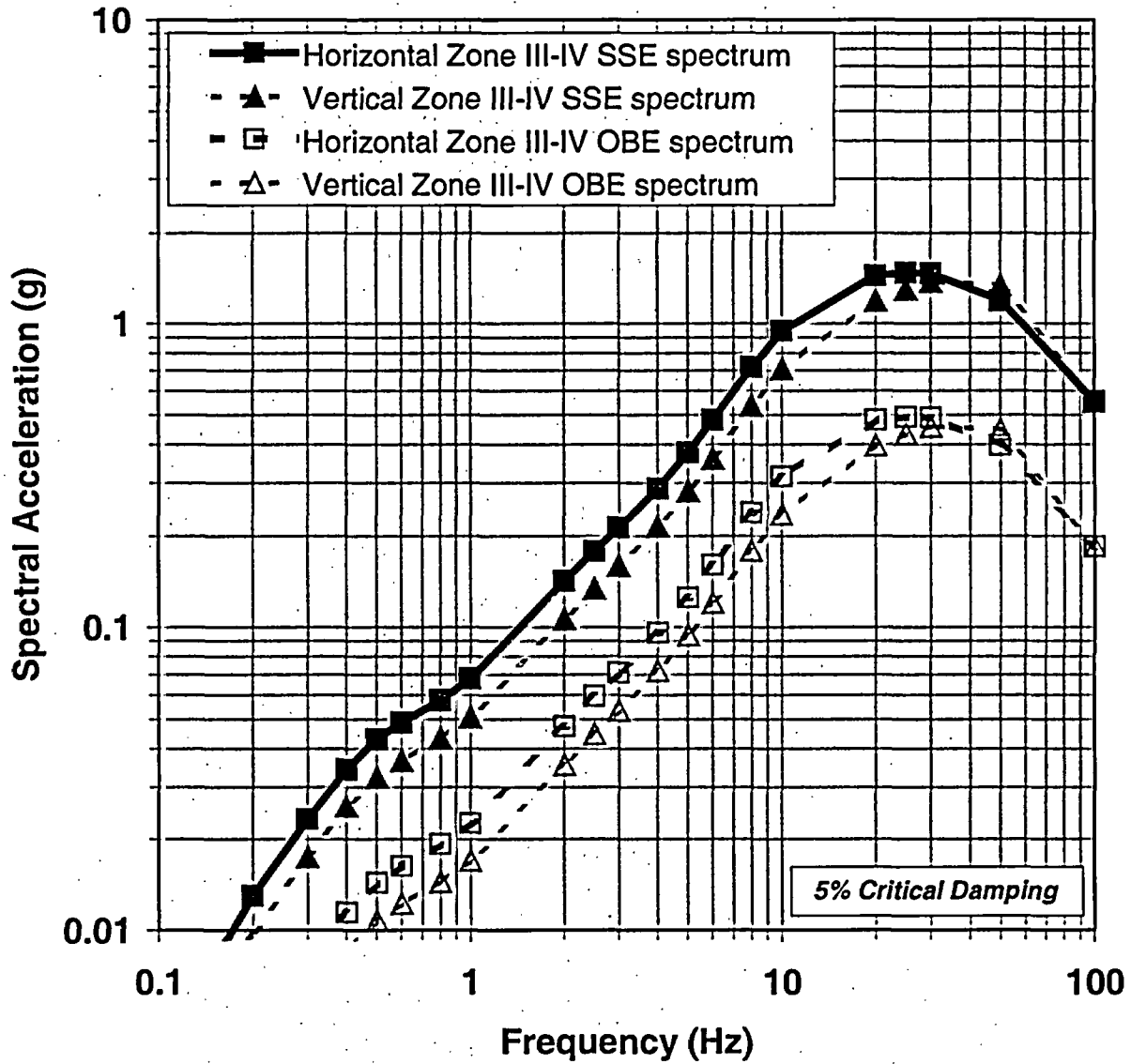


Figure 2.5-55A Selected Horizontal and Vertical OBE and SSE Spectra for the Hypothetical Rock Outcrop Control Point at the Top of Zone III-IV Material (Representative Elevation 250 ft, 3300 ft/sec Shear Wave Velocity)

Serial No. 05-194  
Docket No. 52-008  
Responses to DSER Open Items

**Enclosure 2**

**“EPRI Response Pertaining to the  
Dominion Nuclear North Anna, LLC (Dominion)  
North Anna Early Site Permit Application DSER Open Item 2.5-1,”  
Letter from Edmund T. Rumble,  
Electric Power Research Institute,  
March 25, 2005**

March 25, 2005

Mr. Mike Bourgeois  
Entergy Nuclear, Inc.  
1340 Echelon Parkway  
Jackson, MS 39213

Mr. Thomas Mundy  
Exelon Generation Company, LLC  
200 Exelon Way, KSA3-E  
Kennett Square, PA 19348

Mr. Marvin Smith  
Dominion Generation  
5000 Dominion Blvd.  
Glen Allen, VA 23060

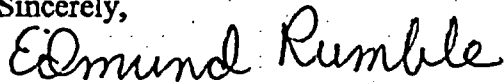
Gentlemen:

**Subject: EPRI Response Pertaining to the Dominion Nuclear North Anna, LLC (Dominion)  
North Anna Early Site Permit Application DSER Open Item 2.5-1**

The Draft Safety Evaluation Report for Dominion's North Anna Early Site Permit Application includes Open Item 2.5-1 that addresses the CEUS Ground Motion Project described in, "CEUS Ground Motion Project Final Report," EPRI Technical Report 1009684, December 2004.

The purpose of this letter is to transmit the enclosed document, "EPRI 2003 CEUS Ground Motion Model Development." This document provides a description of the attributes of the approach used to develop the EPRI 2003 CEUS Ground Motion Model to provide objectivity, credibility and confidence that it is appropriate for use in probabilistic seismic hazard analysis for Early Site Permit Applications.

Sincerely,



Edmund T. Rumble

Enclosure: EPRI 2003 CEUS Ground Motion Model Development

c: L. Sandell, EPRI

## EPRI 2003 CEUS Ground Motion Model Development March 2005

### Background

In Part 1 of DSER Open Item 2.5-1 for the North Anna Early Site Permit Application, the staff asked the applicant to provide additional details on the 2003 EPRI CEUS ground motion evaluation that it used for the ESP PSHA, specifically details about intra-cluster weighting that was based on comparison of the models to data in the strong motion database. In Part 2 of DSER Open Item 2.5-1, the staff asked the applicant to provide additional information on the Silva et al. Cluster 1 attenuation relationships. In Part 3 of DSER Open Item 2.5-1, the staff asked the applicant to provide additional information about the inter-cluster weights.

### Scope

This document is a summary of activities that were implemented for development of the EPRI 2003 CEUS Ground Motion Model. The document includes a summary of the scope of the project, the evaluation process and the feedback received from the Peer Review Panel. The purpose of this summary is to support responses to Open Item 2.5-1. More detailed information is available in the CEUS Ground Motion Project Final Report (EPRI, 2004).

### Application of SSHAC Guidance

The objective of the CEUS Ground Motion Project was to develop a CEUS ground motion model for use in PSHAs that quantifies the epistemic uncertainty and aleatory variability based on an assessment of viable existing proponent ground motion attenuation models following the guidance of the SSHAC (1997). For purposes of this project, "viable existing proponent ground motion attenuation models" refers specifically to available functional relationships with defined coefficients or look-up tables that span the range of earthquake magnitudes and epicentral distances of interest. The resultant EPRI 2003 model represents the diversity of views of the informed technical community. Development of the model following the SSHAC guidance was: (1) based on evaluations of viable models using available strong-motion data and information about the modeling approach and parameterization and (2) provided for assessment of uncertainties.

The SSHAC noted: *the most important and fundamental fact that must be understood about a PSHA is that the objective of estimating annual frequencies of exceedance of earthquake-caused ground motions can be attained only with significant uncertainty.* Despite significant recent research, major gaps remain in our understanding of the mechanisms that cause earthquakes and the processes of transmission of the seismic energy from source to site. The limited information that does exist is often, and legitimately, interpreted quite differently by different experts, resulting in important uncertainties in the numerical results of a PSHA.

A basic principle defined by the SSHAC is: *the underlying basis for the inputs related to any of these issues must be the composite distribution of views represented in the appropriate scientific community.* Expert judgment is used to evaluate the informed scientific community's state of knowledge. The SSHAC process provides guidance for

performing the assessment using a representative set of experts. Regardless of the level of an assessment the SSHAC goal remains the same: *to represent the center, the body, and the range of technical interpretations that the larger informed technical community would have if they were to conduct the study.*

The CEUS Ground Motion Project Final Report (EPRI, 2004) summarizes the SSHAC methodology in Section 2.2.1. Key aspects of its application to this project described in Section 2.2.2 include the staffing of the Technical Integrator, Ground Motion Expert Panel and Peer Review Panel. SSHAC guidance was followed in inviting available experts, establishing clear roles for participants, and executing the assessment process to ensure the center, body and range of technical interpretations the larger informed technical community were represented. The technical core of the project included eleven highly respected and experienced PSHA and ground motion practitioners with diverse backgrounds and viewpoints (see list of participants in Table 1).

**Table 1**  
**List of Project Participants**

<b>Role</b>	<b>Participants</b>
Technical Integrator <sup>1</sup>	Martin W. McCann, Jr. James E. Marrone Robert R. Youngs
Peer Review Panel	C. Allin Cornell J. Carl Stepp
Ground Motion Expert Panel	Gail Atkinson Kenneth Campbell Richard Lee Walter Silva Paul Somerville Gabriel Toro

<sup>1</sup>Norm Abrahamson assisted the TI during the early phases of the project

The roles of the participants were clearly defined at the outset of the project. The technical approach (discussed below) utilized available strong-motion data in a manner that was systematic, logical, transparent and repeatable. Subjective aspects of the process were clearly organized, managed and documented. In summary, the CEUS Ground Motion Project was carried in full compliance with the SSHAC Guidance.

#### **Basic Principles and Approach for Model Development**

The development plan for the new CEUS ground motion model was prepared by the Technical Integrator (TI) with review and guidance provided by the Peer Review Panel (EPRI, 2004). The plan identified the participatory groups (i.e., Technical Integrator, Ground Motion Expert Panel and Peer Review Panel) and their responsibilities, the project scope, and schedule.

In defining the project scope, the basic principles and approach to be followed for model development were established such that:

- A SSHAC Level 3 analysis be performed;
- Clear responsibilities be defined for the project participants;
- Existing ground motion models be the basis for the model development; and
- Peer review be participatory.

In establishing that a Level 3 evaluation be conducted, the defined process went beyond the general guidance for participation provided by the SSHAC for this level of analysis. The SSHAC characterizes a Level 3 analysis as one in which a meeting of experts is convened to address the technical issues associated with (in this case) ground motion modeling. Convening the experts is intended to provide a forum for experts to interact and to ultimately provide the TI with information that supports the integration and evaluation process. It is this forum that gives the experts the opportunity to present their models, discuss and evaluate their basis and to debate technical issues associated with individual models, parameter estimates, etc.

This project expanded the scope of the Level 3 analysis to include ongoing participation of the ground motion experts. The increased Level 3 scope carried out as part of this project provided for the Ground Motion Expert Panel to:

- Participate in a workshop in which proponents (model authors) of ground motion models present their models to the other experts, the TI and the Peer Review Panel;
- Participate in 2 additional workshops to contribute insights and guidance to the development of the TI evaluation process;
- Review and comment on the TI evaluation process (e.g., progress reports); and
- Comment on the project draft report.

This expanded scope for this Level 3 analysis provided for extensive involvement of the ground motion experts throughout the course of the evaluation process.

As described in (EPRI, 2004), the SSHAC Level 3 process: *brings together proponents and resource experts for debate and interaction; the TI focuses debate and evaluates alternative interpretations.* As one in a series of workshops, the first project workshop was focused on this SSHAC objective of bringing the experts together. This workshop was the vehicle that brought experts and model proponents together to review and discuss alternative models with their peer group. It was during this workshop that the scientific basis for ground motion models were presented by the model proponents and discussed by the other experts. Participants in the workshop were the EPRI project manager, the Ground Motion Expert Panel, the TI, and the Peer Review Panel. Others were invited including knowledgeable NRC staff and potentially available model proponents, but were unable to attend. However, almost all of the 13 CEUS ground motion models identified for this project were represented.

Because of the expanded participation of the ground motion experts in this Level 3 assessment, the first workshop was also an opportunity for the experts to provide guidance for the development of the TI evaluation process, for the development of

criteria for evaluating the viable ground motion models and ultimately for the assessments that supported the development of the EPRI 2003 ground motion model.

### **TI Evaluation Process**

The evaluation process used to develop the EPRI 2003 ground motion model is described in Section 3 of the project report (EPRI, 2004). This section highlights features of the process and its implementation.

Given the set of viable ground motion models (as identified by the ground motion experts and the TI) and the responsibility to estimate the composite distribution of the informed technical community, the TI had to establish an evaluation process for developing the composite distribution. The evaluation process was required in order to:

- Objectively evaluate the viable ground motion models;
- Identify and model the sources of epistemic uncertainty in the median ground motion and aleatory variability; and
- Derive the composite distribution of the informed technical community.

The development of the evaluation process was initiated during the first workshop and continued during workshops 2 and 3 as well.

The initial discussions during the first workshop on building an evaluation process focused on two areas. The first was the recommendation by the Ground Motion Expert Panel that the consistency of the 13 viable ground motion models with the existing strong-motion database be an evaluation and assessment criterion. The second recommendation for evaluating and assessing the viable models was a criterion based on a model's 'theoretical' foundation and development (e.g., basis in seismological principles, expression of aleatory and epistemic uncertainty, etc.). As part of this discussion, the ground motion experts developed a list of attributes for model evaluation and assessment using this criterion. This was followed by each model proponent presenting an evaluation case for their model and a rating. This proponent evaluation accomplished a number of items:

- Provided initial insight for model clustering;
- Identified criteria the ground motion experts believed were important in the evaluation of candidate ground motion models;
- Gave the ground motion experts (in particular the model proponents) the opportunity to evaluate their model; and
- Gave the other panel members the opportunity to discuss/question a proponent's evaluations.

As discussed in (EPRI, 2004), the TI pursued the implementation of an objective evaluation process that: *did not rely solely on subjective assessments such as the assignment of subjectively determined probability weights (e.g., by the TI) to viable ground motion attenuation models. While such assessments are a part of a Level 4*

*evaluation, the TI believed an approach that was objective as possible should be developed and implemented.*

The TI noted that within the set of viable ground motion models there is a large degree of dependency between many of the models to the extent that subsets of them should be considered a representation of epistemic uncertainty in a single modeling type. This observation was manifested in the Ground Motion Expert Panel discussions and their grouping of models by model type.

The discussions at the first workshop and the concerns with respect to model dependency led to the development of a process for grouping the 13 viable models. The process of defining distinct ground motion model clusters also had the advantage that it allowed for an evaluation among the clusters. That is, the merits of different clusters (ground motion modeling approaches) as opposed to a consideration of individual models could be assessed. In this context, the clusters could be assigned relative weights based on an evaluation of their scientific merits.

The TI evaluation process was implemented in three parts. The first was the evaluation of models within groups or clusters. The second was the assessment of the epistemic uncertainty in the median ground motion within a cluster. The third part of the process was the evaluation and weighting of the different clusters.

A number of alternative approaches for grouping ground motion models were considered. These alternatives were discussed at each of the project workshops. At the highest level, three classes of models were defined: spectral models (with 9 members), hybrid models (3 members), and finite source/Green's function modeling (1 member). Following consideration of a number of cluster approaches, one was selected as the most straightforward and acceptable to the Ground Motion Expert Panel, given the set of viable models. Four clusters were defined; single-corner spectral models, double-corner spectral models, hybrid models and finite source/Green's function modeling. More detailed clustering alternatives considered other seismological factors, such as separation of source and path effects, but these proved to lack resolving power, given the current set of viable models.

As discussed above, a strong focus of the TI was to develop an objective evaluation process. Under ideal circumstances, an objective evaluation would be carried out through a comparison of models to data or other objective information (e.g., physical experiments). The Ground Motion Expert Panel recommended this approach be pursued for the evaluation of individual proponent models. This approach was adopted by the TI to evaluate the proponent models within each cluster and also to evaluate the different clusters. The consistency of the models with data was used as a means to weigh each model within a cluster. These weights were then used to represent each cluster (model type) in terms of its logarithmic mean and standard deviation for each ground motion measure (defined as a function of earthquake magnitude and distance).

There are a number of advantages to the data-based weighting criterion used to evaluate the proponent models in each cluster. First, the use of the strong-motion data follows the

recommendation of the Ground Motion Expert Panel to assess the consistency of proponent models with the data. Second, a data-based approach is clear and objective. Third, all of the models within a cluster contribute to some degree to the estimate of the cluster median and variability.

The second part of the TI evaluation process involved the evaluation of the epistemic uncertainty within each cluster. Here, the TI developed a simple uncertainty model to augment the within cluster variability to account for uncertainties not represented by the set of models with the cluster.

The final step in the TI evaluation process assessed the alternative model clusters (model types). This assessment was conducted in two parts. The first part compared the clusters in terms of their consistency with the strong-motion data (similar to the evaluation of the models within each cluster). The second part evaluated the extent to which seismological principles were used and uncertainties were evaluated for each cluster and their member models. The comparison of the model prediction with the data is a clear and objective evaluation. The second part of this assessment involves a subjective assessment, based on input from the Ground Motion Expert Panel (as provided in the workshops and the written survey results) by the TI.

The development of the evaluation process was carried out by and was the responsibility of the TI. As discussed above, the Level 3 SSHAC process implemented in this project provided for the ongoing participation of the Ground Motion Expert Panel and the Peer Review Panel. The dialogue with the Ground Motion Expert Panel included:

- Project workshops (the subject of these workshops was discussed above);
- Written survey, (see Appendix D, EPRI, 2004);
- Review of progress report and a follow-on telephone interview; and
- Review of the project draft report.

The participation of the peer review is summarized below.

#### **Peer Review**

As recommended by SSHAC a participatory peer review was carried out as part of the project (SSHAC, 1997). The responsibility of the Peer Review was defined to: *provide review and oversight of the implementation of the Level 3 elicitation and evaluation process* (EPRI, 2004).

The Peer Review Panel participation included:

- Providing review and guidance during the development of the project plan;
- Attending all project workshops with the Ground Motion Expert Panel;
- Meeting with the TI immediately following each workshop to review the proceedings and to offer guidance for the work ahead;
- Providing written feedback to the TI following each workshop;
- Review of the final draft of the project report; and

- A summary letter to the TI regarding the implementation of the Level 3 process.

In their letter the Peer Review Panel states:

*The model is state-of-practice in the use of multiple current models in the field as well as in the incorporation of epistemic uncertainty in estimates both of the median ground motion and of the standard deviation reflecting random variability of ground motion about the median. The resulting product consequently fully satisfies all the modern requirements for a model of the ground motion component of a probabilistic seismic hazard assessment.*

The Peer Review Panel concludes by stating:

*In summary: 1) the Review Panel considers the SSHAC Level 3 assessment approach to be appropriate for the development of the EPRI 03 Ground Motion Model; and 2) we consider the Project Team's implementation of the approach to have been thorough and complete. We therefore consider the EPRI 03 Model to represent current state of knowledge for application in probabilistic seismic hazard analyses for nuclear plant seismic regulation.*

The Appendix contains a copy of the Peer Review Panel letter to the TI at the conclusion of the project.

#### References

EPRI, *CEUS Ground Motion Project Final Report*: Dominion Energy, Glen Allen, VA, Entergy Nuclear, Jackson MS and Exelon Generation Company, Kennett Square, PA: Palo Alto, CA, EPRI 1009684, 2004.

Senior Seismic Hazard Analysis Committee (SSHAC), *Recommendations for Probabilistic Seismic Hazard Analysis: Guidance on Uncertainty and Use of Experts*, NUREG/CR-6372, Volume 1, Washington, D.C., U.S. Nuclear Regulatory Commission, 1997.

**Appendix**

**EPRI 2003 CEUS Ground Motion Project Peer Review Panel Letter**

January 24, 2005

Martin W. McCann, Jr.  
Jack R. Benjamin and Associates  
530 Oak Grove Avenue, Suite 101  
Menlo Park, CA 94025

James E. Marrone  
Bechtel Corporation  
50 Beal Street, MS 50/2/C101  
San Francisco, CA 94105

Robert R. Youngs  
Geomatrix Consultants  
2101 Webster Street, 12<sup>th</sup> Floor  
Oakland, CA 94612-3027

Gentlemen:

Reference: ***CEUS Ground Motion Project: Model Development and Results***

The Peer Review Panel for the *CEUS Ground Motion Project: Model Development and Results* takes pleasure in providing this letter, which conveys the Panel's overall appraisal of this important implementation of the SSHAC Level 3 elicitation procedure. The Panel's review was greatly facilitated by having reviewed the Project plan and by participating in all phases of the implementation procedure. The participatory nature of the review encouraged the Panel to perform in-depth evaluations of the Project implementation process and permitted the Project Team to effectively incorporate the Panel's recommendations at the appropriate stage. The Panel believes that the participatory review process permitted its recommendations to be fully accommodated and reflected in subsequent stages of the implementation process. The Panel expresses its appreciation to EPRI's Project Management for implementing this very effective project implementation and review process and to members of the Project Team for their responsive implementation of our recommendations. Our additional comments and overall appraisal of this important work are given in the following paragraphs.

The major objective of the project was to develop a ground motion model for representative hard rock site conditions in the central and eastern United States that incorporates uncertainty representing the current state of knowledge of the informed technical community. The Project Team successfully accomplished this objective by implementing a SSHAC Level 3 assessment methodology. The SSHAC Methodology has received broad professional review and acceptance by earthquake engineering and

strong motion seismology practitioners and it has been reviewed by the U. S. Nuclear Regulatory Commission for generic application in probabilistic seismic hazard analyses for nuclear power generating plants. The Review Panel considers the SSHAC Level 3 assessment approach to be appropriate for developing the CEUS Ground Motion Model; it gives the EPRI 03 Model the requisite scientific acceptability for application in nuclear plant seismic regulation.

A SSHAC Level 3 assessment requires the Project Team (called the Technical Integrator in the SSHAC Report) to compile current data and current ground motion modeling approaches and to perform assessments, which become the technical basis for a composite ground motion model that incorporates the technical community's epistemic uncertainty. A key component of SSHAC Level 3 is the assessment of that community's epistemic uncertainty through extensive interactions with a panel of ground motion modeling experts that is representative of the entire scientific community. For the EPRI Project the Ground Motion Expert Panel was constituted of six individual experts all of whom are actively engaged in the development of ground motion models for application in the central and eastern United States. The Expert Panel identified credible ground models and provided evaluations of the relative effectiveness of each considering available strong ground motion recordings in central and eastern North America and the degree to which each incorporates seismological principles governing generation of earthquake ground motion and seismic wave propagation. The Project Team incorporated these evaluations in their assessments using an innovative approach of grouping the models in classes based on similarity of modeling approaches for the purpose of assessing epistemic uncertainty. Although the model class grouping approach is a somewhat more complex method of assessing uncertainty than simple weights on models, the Review Panel believes it constitutes an advancement in the assessment of epistemic uncertainty in ground motion modeling and leads to improved confidence in the EPRI 03 Ground Motion Model.

The final project report presents a state-of-practice model for making estimates of earthquake induced ground motion in the central and eastern United States. The model is state-of-practice in the use of multiple current models in the field as well as in the incorporation of epistemic uncertainty in estimates both of the median ground motion and of the standard deviation reflecting random variability of ground motion about the median. The resulting product consequently fully satisfies all the modern requirements for a model of the ground motion component of a probabilistic seismic hazard assessment.

In summary: 1) the Review Panel considers the SSHAC Level 3 assessment approach to be appropriate for the development of the EPRI 03 Ground Motion Model; and 2) we consider the Project Team's implementation of the approach to have been thorough and complete. We therefore consider the EPRI 03 Model to represent current state of knowledge for application in probabilistic seismic hazard analyses for nuclear plant seismic regulation. Although we do not identify specific cautions with respect to use of the model, we recommend that it be submitted in a suitable format to the Nuclear

Martin W. McCann  
James E. Marrone  
Robert R. Youngs

January 24, 2005

Regulatory Commission for review for generic application. We believe this action would assure stable application of the model in future nuclear plant licensing applications and, importantly, would provide stability in the regulatory review process.

Respectfully submitted,

  
J. Carl Stepp  
Earthquake Hazards Solutions

  
C. Allin Cornell  
Consultant